Federal Ministry of Education and Research

UNIVERSITE D'ABOMEY - CALAVI (UAC)

INSTITUT NATIONAL DE L'EAU

WASCAL

West African Science Service Center on Climate Change and Adapted Land Use

Registered under N°: ……/UAC/VR-AARU/SA

A DISSERTATION

Submitted

In partial fulfillment of the requirements for the degree of

DOCTOR of Philosophy (PhD) of the University of Abomey-Calavi (Benin Republic)

In the framework of the

Graduate Research Program on Climate Change and Water Resources (GRP-CCWR)

By

Fati Aziz

======

MODELLING THE IMPACT OF CLIMATE AND LAND USE/LAND COVER CHANGE ON STREAMFLOW AND SEDIMENT YIELD IN THE BLACK VOLTA RIVER BASIN

Supervisors:

1. **Emmanuel Obuobie**, Dr., Senior Research Scientist, Water Research Institute, Accra – Ghana.
2. **Jaehak Jeong**, Associate Professor, Spatial Science Laboratory, Texas A&M University, United States of America.
3. **Abel A. Afouda**, Professor, Laboratoire d'Hydrologie Appliquée Faculté des Sciences de l'Université de Abomey Calavi - Benin Republic.
4. M**ouhamadou Bamba Sylla**, Dr., West Africa Science Service Centre on Climate Change and Adapted Land Use, Ouagadougou, Burkina Faso.

Dedication:

To my dad, Abdel-Aziz Farouk and mum, Memuna Musah

Alhamdulillah, we made it!!!

ACKNOWLEDGEMENTS

This PhD work is realized in the framework of the West African Science Service Center on Climate Change and AAdapted Land use (WASCAL) and funded by the **German Ministry of Education and Research (BMBF) in collaboration with the Benin Ministry of High Education and Scientific Research** (MESRS).

Alhamdulillah.

I'm extremely grateful to my main supervisor Dr. Emmanuel Obuobie for his massive support and guidance throughout this research. I couldn't have asked for more. Thank you very much. To my other supervisors Dr. Jaehak Jeong, Prof. Abel Afouda and Dr. Mouhamadou Bamba Sylla, thank you for your assistance.

My special thanks go to the German Federal Ministry of Education and Research (BMBF) for providing the funds for this research through the West African Science Service Centre on Climate Change and Adapted Land Use (WASCAL).

I would like to express my appreciation to Mr. Aaron Bundi Aduna, Basin Officer of the White Volta River Basin, Ghana, for his immeasurable help and support during fieldwork. I will forever remain indebted to you, Sir.

I would like to thank Dr. Raghavan Srinivasan, Director of the Spatial Science Laboratory, Texas A&M University, USA for providing me office space and expert advice during my sojourn at the University. Many thanks go to Dr. Prasad Daggupati of the Spatial Science Laboratory, Texas A&M University for supervising the thesis during my research stay at Texas A&M University. Thanks to Dr. Yihun Dile and Dr. James Kiniry for their assistance in the research.

My appreciation goes to Mr. Samuel Guug and Mr. Kwasie, for the great help during sampling and for holding the fort whenever I was engaged in other aspects of the research. Many thanks go to Mr. Ben and all my field workers who worked tirelessly to ensure the realization of this research. Monica, you made fieldwork interesting, I'm grateful.

My sincere gratitude goes to Dr. Benjamin Kofi Nyarko, a Senior Lecturer at the University of Cape Coast - Ghana and Coordinator of the WASCAL Doctoral program on Climate Change and Agriculture, for providing me with office space and a GIS tutor at the University of Cape Coast. Special gratitude to Mr. Osman Adams for opening for me the doors to the Geographic Information Systems (GIS) world.

I would like to thank Professor Ousmane Seidou, of the University of Ottawa, Canada, for providing the CORDEX downscaling tool used in the climate downscaling aspect of this research.

Many thanks to Mr. Collins Kissi and Mr. Appiah of Water Research Institute, Ghana for guiding me throughout my field and laboratory work. My gratitude goes to Dr. Barnabas Amisigo, Dr. Emmanuel Bekoe, Mr. Abdul-Razak Iddrisu, Mr. and Mrs. Gown, Mr. Peter Baako, Mr. Mahmud Mohammed and Madam Sahada, for taking special interest in the progress of my work.

Special thanks go to the Banguras, the Bibilazus, the Affuls, Emma, Isaac, Sintayehu and Fikirte for making life and work comfortable and fun during my PhD working visit to the Spatial Science Laboratory at the Texas A&M University, USA.

To all friends who supported and encouraged me throughout this research, thank you for being there for me.

Thank you to my wonderful parents and siblings, for the love and support. I'm also grateful to the entire Cofie family, for their encouragement.

I will forever be grateful to my husband, Mr. Abdul Razak Mohammed Cofie for his massive support throughout the research and for being the greatest "backing vocalist" ever.

ABSTRACT

This study investigated the impacts of climate change and the sensitivity of land use/land cover (LULC) changes on river flow and sediment yield in the Black Volta River Basin (BVRB) using a modelling approach, with the aim of providing water resources and basin managers with science-based evidence of impacts of global change at basin level to inform sustainable planning and management of water resources in the basin.

Climate change impact and sensitivity of LULC change on streamflow and sediment yield in the studied basin were assessed using the Soil and Water Assessment Tool (SWAT) model. Sensitivity analysis, calibration, validation and uncertainty analysis of the SWAT model were performed in SUFI-2 algorithm of SWAT-CUP. Calibration and validation were done at monthly time step for river flow and total sediment yield at Bui and Chache, respectively. Due to lack of long term data of good quality, calibration of flow was limited to 6 years (1995-2000) while that of total sediment yield was from 2000 to 2004 (5 years). Validation of flow was for 5 years (2002-2006) and for sediment, 3 years (2005-2007). The calibrated SWAT model was driven with three RCM/GCM pairs (RCA4/MPI-ESM-LR, RACMO22T/ICHEC-EC-EARTH and RCA4/CanESM2) of downscaled rainfall and temperature data analyzed in this study. The model was also driven with the ensemble mean values of the RCM/GCM pairs. The RCM/GCM data were obtained from the CORDEX archives and consisted of data forced by two IPCC emission scenarios- Representative Concentration Pathways (RCPs) 4.5 and 8.5 for two future time slices: 2051-2075 - representing the late 21st century (the 2060s) and 2076-2100 - representing the end of the 21st century (the 2080s). The period 1984- 2010 was set as the baseline. The sensitivity of streamflow and sediment yield to changes in LULC in the BVRB was assessed based on the basin's LULC maps of 1990 and 2000.

The SWAT model results showed that the curve number (CN2) and canopy storage (CANMX) were, respectively, the most and least sensitive model parameters, with respect to streamflow. The model performance in reproducing monthly streamflow and sediment yield of the basin during calibration was rated as "good". The Nash-Sutcliffe efficiency (NSE), coefficient of determination (R^2), percent bias (PBIAS) and root mean square error (RSR) values for streamflow calibration were 0.85, 0.86, 8.1% and 0.38 respectively. Sediment calibration results yielded NSE of 0.68, R^2

of 0.74, PBIAS of 27.5% and RSR of 0.59. In general, the model validation results were "satisfactory" for both flow and sediment yield. The NSE, R^2, PBIAS and RSR values for streamflow validation were 0.60, 0.62, 20.1% and 0.64 respectively while that for sediment yield were 0.66, 0.74, 39.1% and 0.59 respectively. The p- and r-factor values for the model calibration and validation indicated that low levels of uncertainties existed in the model results.

The projected precipitation over the basin by the ensemble members of the models showed a mixed pattern of positive and negative trends. However, both the positive and negative future trends in the rainfall were statistically non-significant. Analyses of the average annual, intra-annual and seasonal precipitation indicated high uncertainty regarding the direction of the future rainfall. Mean annual precipitation change for the late 21st century ranged between -16% and +6% under the RCP4.5 scenario and between -27% and +14% under the RCP8.5 scenario. The end of the 21st century projections showed changes in mean precipitation amounts ranging between -23% and +2% and between -33% and +13% under the RCP4.5 and RCP8.5 scenarios, respectively. With regards to temperature, average annual projections by the ensemble runs showed increases over the basin under both RCP scenarios and for both time periods. Warming over the basin is projected to be higher under the RCP8.5 scenario than under the RCP4.5 scenario, with the end of 21st century period being warmer than the late 21st century. Average annual mean temperature increase across the model run ranged between 2.2oC and 2.6oC under the RCP4.5 scenario and between 3.5oC and 3.7oC under the RCP8.5 scenario for the end of the 21st century.

Analysis of dry - (November to March) and wet - (August to October) period streamflow and sediment yield showed mainly increases for the 2060s and 2080s under both scenarios. The model runs also projected increases in mean annual streamflow and sediment yield for the basin. The change in streamflow is projected to range between +40% and +42%, and between +100% and +143% for sediment yield during the late 21st century under the RCP4.5 scenario. For the end of the 21st century, the projected change ranges between -6% and +78% while sediment yield is between +100% and +216%. Under the high emission RCP8.5 scenario, streamflow is projected to range between +48% and up to +148% across the models. For sediment yield the projected change ranges from +249% to +335%. The end of century projections of flow is between +69% and +243% while total sediment ranges between +358% and 412% across models. Analysis of the trends in the future annual flow and sediment yield indicated that the increasing trends observed are statistically significant at the 5% level of significance.

Sensitivity analysis of streamflow in the basin based on a 10-year land use/land cover change showed statistically insignificant changes.

Key words: Climate change, land use/land cover change, streamflow, sediment yield.

SYTNTHESIS

La Volta Noire est un fleuve très important pour les trois pays riverains qui le partagent. Les changements climatiques et d'utilisation des terres sont les facteurs parmi tant d'autres qui affectent les bénéfices tirés de cette ressource en eau. Afin de contribuer à une gestion durable du bassin versant de la Volta Noire, ce travail étudie l'impact des changements climatiques sur l'écoulement fluvial et la production de sédiments dans ce bassin versant. Cette étude évalue aussi la sensitivité de l'écoulement de ce fleuve aux changements de climat et d'utilisation des terres.

Le modèle hydrologique SWAT a été utilisé pour l'analyse des changements climatiques sur l'écoulement fluvial et la production sédimentaire dans le bassin versant à cause de sa haute versatilité. Le programme SUFI-2 de SWAT- CUP a été utilisé pour la calibration et la validation du modèle hydrologique SWAT pour les sous-bassins Bui et Chache respectivement pour l'analyse de débit et de production de sédiments. En outre, les données journalières de précipitations, de température minimale et maximale pour 11 stations climatiques et couvrant les périodes 1985-2005 (simulation de contrôle) et 2051-2100 (simulations pour le futur) ont été réduites à l'échelle locale et corrigées avant d'être utilisées comme données d'entrée dans le modèle hydrologique pour simuler les débits et productions sédimentaires futurs. Les données sont constituées de projections de 2 modèles de circulation régionaux alimentés par 3 modèles de circulation généraux (RACMO22T/ ICHEC-EC-EARTH, RCA4/CanESM2 et RCA4/MPI-ESM-LR) pour deux (2) des familles de scénarios de IPCC qui sont RCP4.5 et RCP 8.5 La sensitivité de l'écoulement fluvial et de la production sédimentaire aux changements d'utilisation/couverture des terres a été évaluée en alimentant le model SWAT avec les cartes d'utilisation et de couverture des terres de 1990 et 2000 établies pour le bassin de la Volta Noire.

Les valeurs des critères de validation tels que « NSE », « R^2 », « RSR » et « PBIAS » ont montré la bonne performance du modèle SWAT à simuler les débits mensuels et la production de sédiments dans le bassin versant de la Volta Noire. Cependant, les valeurs de « P-factor » et « R-factor » obtenues durant la calibration et la validation du modèle montrent un degré d'incertitudes dans les simulations du modèle. En comparaison avec la période de calibration pour le débit d'écoulement et la production de sédiments, la période de validation a les meilleures mesures d'incertitudes. Le degré d'incertitude était meilleur pour la simulation du débit d'écoulement que pour la production de sédiments.

Les projections de précipitations sur le bassin versant obtenues par simulation d'un ensemble de modèles montrent des évolutions positives et négatives. Cependant, ces 2 types d'évolution de précipitations sont statistiquement non significatifs. L'analyse de la moyenne des précipitations annuelles, inter annuelles et saisonnières indiquent une grande incertitude concernant l'évolution des précipitations futures. Les variations des moyennes des pluies annuelles pour les dernières années du XXI siècle se situent entre -16 % et +6 % sous le scenario « RCP4.5 » et entre -27% et +14% sous le scenario « RCP8.5 ». Les projections de la fin du XXIe siècle montrent variations dans les volumes de précipitations moyennes comprises entre -23% et +2% et entre -33% et +13% sous respectivement les scenarios « RCP4.5 » et « RCP8.5 ». Concernant les températures, les projections de moyennes annuelles faites par les ensembles de simulations montrent une augmentation dans le bassin versant sous les deux scénarios et pour les deux périodes considérées. Par ailleurs, le réchauffement est plus grand sous le scenario « RCP8.5 » que pour le scenario « RCP4.5 » avec la fin du XXIe siècle plus chaude que les dernières années du XXIe siècle. La moyenne des températures annuelles connait des hausses comprises entre 2.2ºC et 2.6ºC sous le scenario « RCP4.5 » et 3.5ºC et 3.7ºC sous le scenario « RCP8.5 » pour la fin du XXIe siècle.

L'analyse des débits et des productions sédimentaires pour les périodes sèches (Novembre-Mars) et humides (Aout-Octobre) montrent des hausses pour 2060s et 2080s sous les deux scenarios (Figures A1, A2, A3 and A4). Les simulations montrent aussi des augmentations de moyennes annuelles de débit et de productions sédimentaires au sein du bassin versant. Les projections de variations de débits sont comprises entre + 40% et 42%, et entre 100% et 143% pour la production sédimentaire pendant les dernières années du XXIe siècle. Sous le scénario « RCP4.5 ». Pour la fin du XXIe siècle, les projections de variation sont comprises entre -6% et +75% pour le débit et +100% et 216% pour la production sédimentaire. Sous le scenario d'émission élevée « RCP8.5 », les variations de débits sont comprises entre 48% et 148% tandis qu'ils sont compris entre 249% et 335% pour la production sédimentaire. Les projections de variation pour la fin du siècle sont comprises entre 69% et 243% pour le débit et 358% et 412% pour la production sédimentaire à travers les modèles. L'analyse des évolutions futures de débits et productions sédimentaire annuels indiquent que les augmentations observées sont statistiquement signifiantes avec un niveau de confiance de 5%.

L’analyse des débits simulés a montré que les écoulements fluviaux dans le bassin de la Volta Noire ne seraient pas très sensitifs au changement d’utilisation/couverture des terres, particulièrement pour les changements en savanes et terres cultivées.

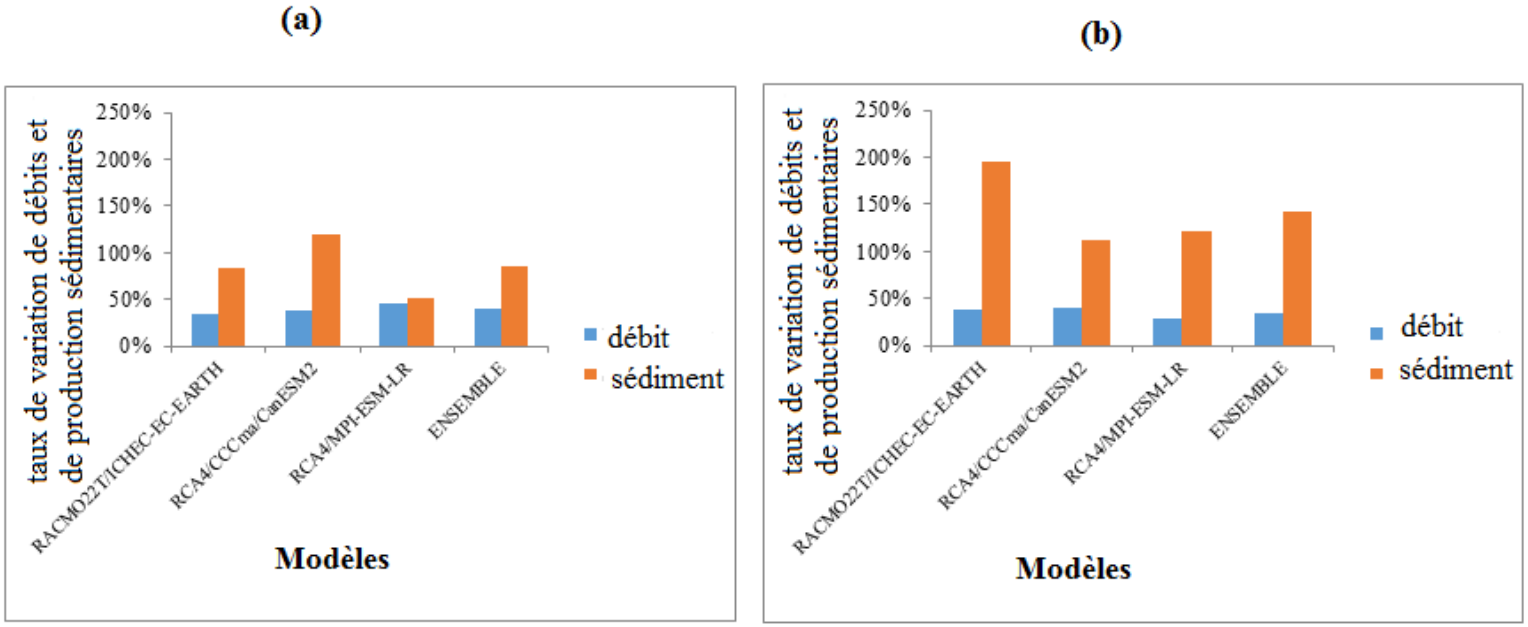

Figure A1: taux de variation de débits moyens saisonniers et de production sédimentaires pour la fin du XXI siècle (2060s) sous le scenario RCP4.5 : (a) pendant la saison sèche (Janvier-Mars) et (b) pendant la saison humide (Août- Octobre)

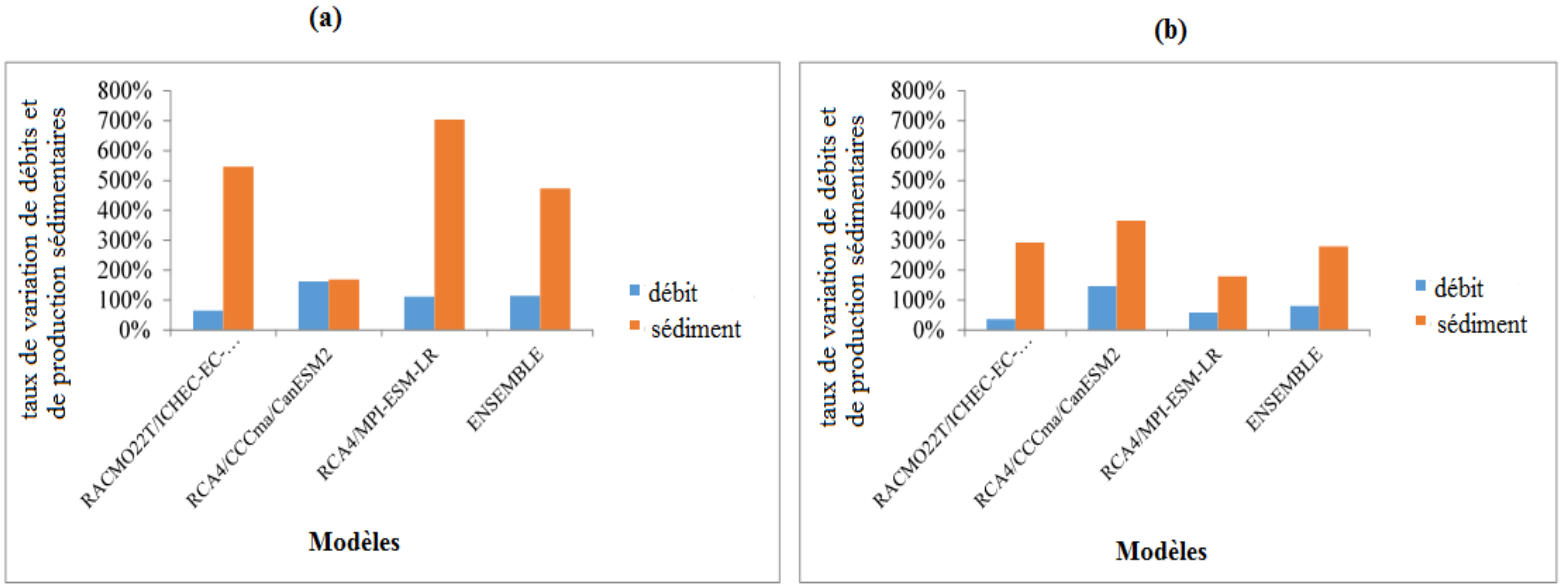

Figure A2: taux de variation de débits moyens saisonniers et de production sédimentaires pour la fin du XXI siècle (2060s) sous le scenario RCP8.5 : (a) pendant la saison sèche (Janvier-Mars) et (b) pendant la saison humide (Août- Octobre)

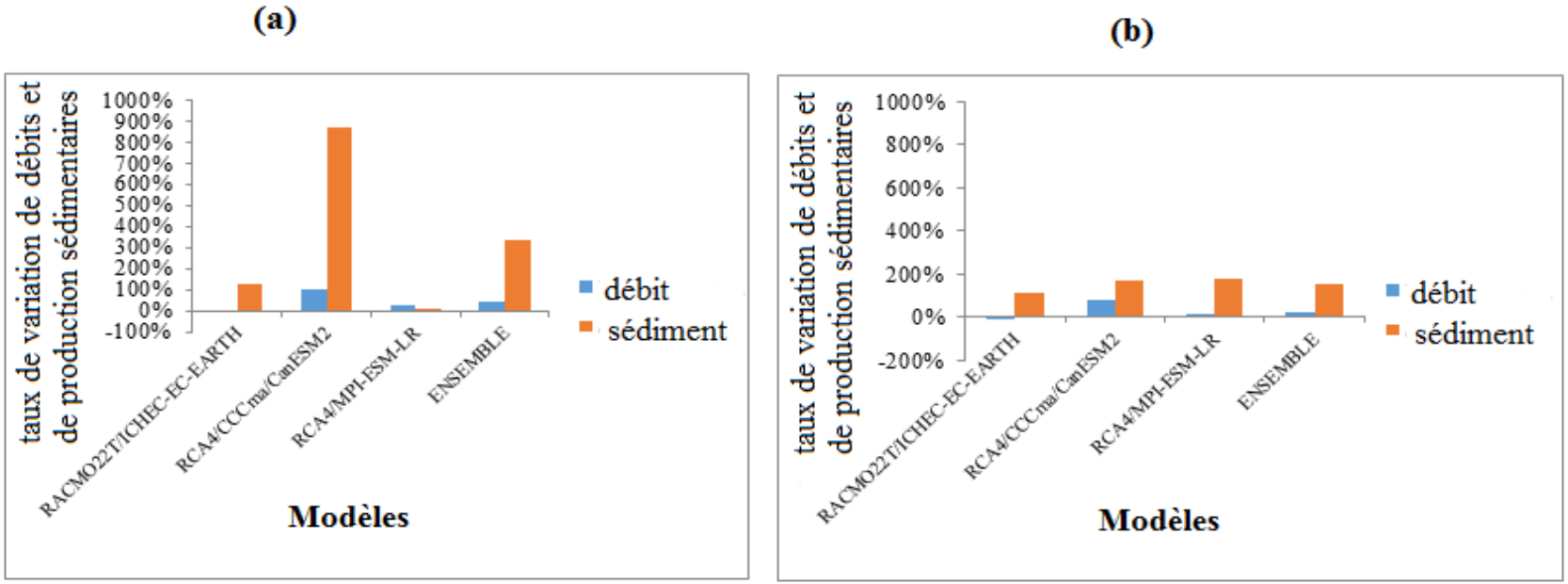

Figure A3: taux de variation de débits moyens saisonniers et de production sédimentaires pour la fin du XXI siècle (2080s) sous le scenario RCP4.5 : (a) pendant la saison sèche (Janvier-Mars) et (b) pendant la saison humide (Août- Octobre)

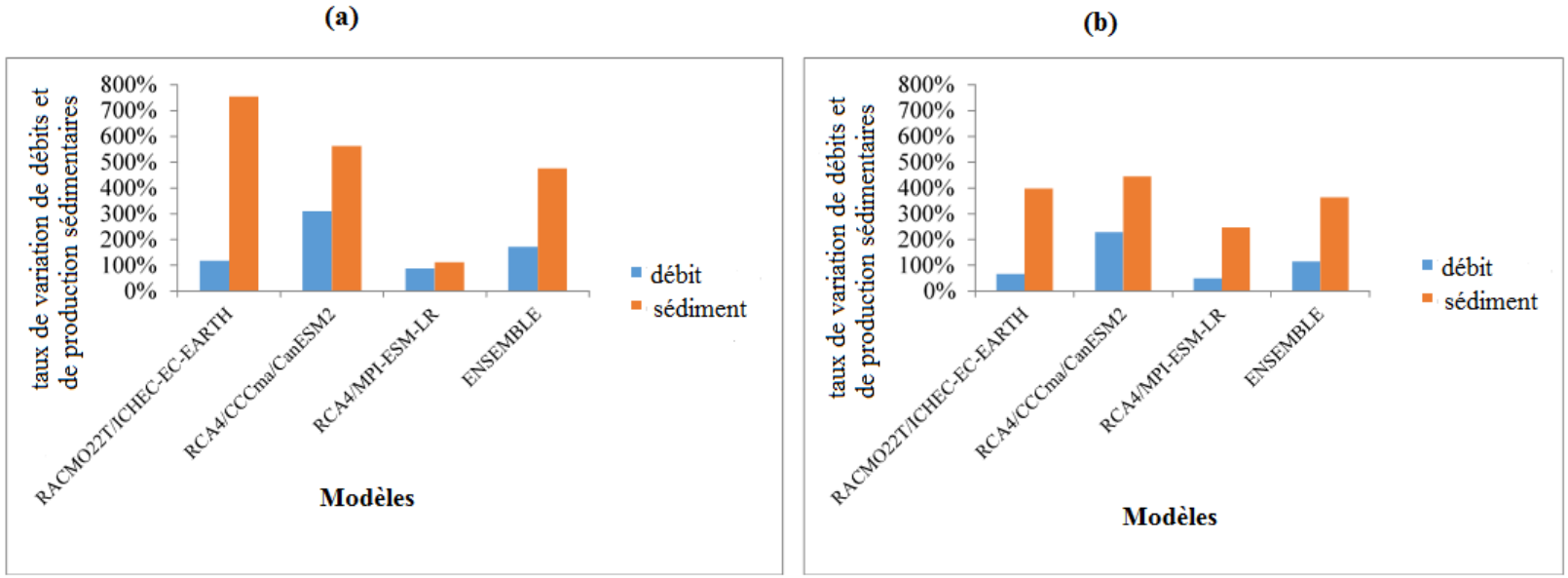

Figure A4: taux de variation de débits moyens saisonniers et de production sédimentaires pour la fin du XXI siècle (2080s) sous le scenario RCP8.5 : (a) pendant la saison sèche (Janvier-Mars) et (b) pendant la saison humide (Août- Octobre)

TABLE OF CONTENTS

LIST OF ACRONYMS

BVRB	Black Volta River Basin
CC	Climate Change
CFSR	Climate Forecast System Reanalysis
CMIP5	Coupled Model Intercomparison Project Phase 5
CORDEX	Coordinated Regional Climate Downscaling Experiment
CREAMS	Chemicals, Runoff, and Erosion from Agricultural Management Systems
DEM	Digital Elevation Model
EPIC	Erosion Predictability Impact Calculator
GCM	Global Climate Model
GIS	Geographic Information System
GLEAMS	Groundwater Loading Effects on Agricultural Management Systems
GLUE	Generalized Likelihood Uncertainty Estimation
HRU	Hydrologic Response Unit
IPCC	Intergovernmental Panel on Climate Change
LULC	Land use/land cover
MCMC	Markov Chain Monte Carlo
MDG	Millennium Development Goal
MUSLE	Modified Universal Soil Loss Equation
NGO	Non-governmental Organization
NSE	Nash-Sutcliffe-Efficiency
Parasol	Parameter Solution
PBIAS	Percent Bias
PET	Potential Evapotranspiration
R^2	Coefficient of determination
RCM	Regional Climate Model
RCP	Representative Concentration Pathway
RMSE	Root Mean Square Error
RSR	RMSE-observations standard deviation ratio
SCS	Soil Conservation System
SRTM	Shuttle Radar Topographic Mission
SUFI-2	Sequential Uncertainty Fitting, version 2
SWAT	Soil and Water Assessment Tool
SWAT-CUP	Soil and Water Assessment Tool- Calibration and Uncertainty Programs
UN	United Nations
UNEP	United Nations Environment Programme
USDA	US Department of Agriculture
USDA-ARS	United States Department of Agriculture-Agricultural Research Service
USLE	Universal Soil Loss Equation
VRB	Volta River Basin
WMO	World Meteorological Organization

LIST OF FIGURES

LIST OF TABLES

1. GENERAL INTRODUCTION

This chapter provides a general introduction of the research and presents research background, problem statement, objectives, hypothesis and significance of the study. The chapter also reviews literature on the subject matter. Definitions and concepts of key terminology of the research have been defined and explained in this chapter. Further, the effects of soil erosion and sedimentation as well as climate and land/use land cover (LULC) change in West Africa and the Volta basin are discussed. The chapter also highlights possible conflicts that may arise from sharing the river basin in the absence of proper management.

1.1. Context and Problem Statement

Water resources are indispensable in every living system, playing a key role in various economic and social developments. Water is also important in addressing issues of hunger, health and poverty. Its availability and accessibility has huge effects on patterns of economic growth for many regions of the world, especially the African region (Odada, 2006).

Rapid population growths, expansion of irrigated agriculture and industrialization have increased the demand for water related goods and services worldwide, putting the resource at risk. Climate change is undeniably occurring and poses additional risks to water resources. The Intergovernmental Panel on Climate Change (IPCC, 2007) reports that global average surface air and ocean temperatures are increasing at rates unequivocal to any other period on record. Changes in climate affect rainfall and temperature which causes changes in the hydrology of river basins, alters streamflow and modifies the transport characteristics of sediments (Tu, 2009). In West Africa, climate change impacts coupled with the anticipated reduction in precipitation and an increase in potential evaporation rates over the entire Volta River Basin threaten to increase the challenges associated with insufficient water resources in the basin region (Kasei, 2009). Studies

by Obuobie (2008) and Awotwi et al. (2015) revealed that the White Volta Basin is sensitive to changes in climate, with increases in temperature and precipitation resulting in increases in annual surface runoff, annual baseflow and evapotranspiration.

Land-use/land-cover (LULC) is another important factor that affects water resources (Stonestrom et al., 2009). Studies by Elfert and Bormann (2010), Ghaffari et al. (2010) and Li et al. (2009) for example, have shown that LULC change affects hydrological processes. Land-use/land-cover is linked directly with the hydrological cycle and influences the partitioning of rainfall into runoff, evapotranspiration, infiltration (Foley et al., 2005) and sediment yield (Walling, 1994). To this end, changes in LULC constitute an important human interference that affects the quality and quantity of water resources (Dwarakish and Ganasri, 2015). Climate change and range of human activities (e.g. land-use/land-cover change) within a catchment area affect the sediment load of rivers.

Lahmer et al. (2001) have shown that although the hydrological effects of land use/land cover and climate variation/change happen at all spatial scales, studies conducted at smaller scales, (e.g. regional level) tend to be more beneficial for the provision of key information for local developments. This study investigated the impacts of climate change on streamflow and sediment yield in the Black River Volta Basin. It also assessed the sensitivity of LULC change on the streamflow.

The water resources of the Black Volta River Basin support important economic activities such as agriculture, hydro-power generation and domestic water supply in Ghana, Burkina Faso and Cote D'lvoire. The hydrological benefits of the basin could however be threatened by global change (Kasei, 2009). It is established that climate variability and/change can cause changes in peak-flows

and volume of water in rivers (Prowse et al., 2006), whereas changes in land use can cause changes in flood frequency, infiltration, groundwater recharge, base flow, runoff and annual mean discharge (Brath et al., 2006; Costa et al., 2003; Crooks and Davies; Lin, et al., 2007).

A number of drought events affected the water resources of the studied basin in the 1980s and 1990s (IIED, 1992 *cited in* Kasei, 2009) and were worsened by increases in hydrologic seasonality (Kasei, 2009). The exacerbation of seasonal precipitation together with climate change and land use/land cover change may have some more profound effects on the water resources.

1.2. Literature Review

1.2.1. Climate Change

Climate Change denotes changes in climate over a period of time (decades or more) caused by either natural variability or human activity. According to the United Nations Framework Convention on Climate Change (UNFCCC), climate change is "a change of climate which is attributed directly or indirectly to human activity that alters the composition of the global atmosphere and which is in addition to natural climate variability observed over comparable time periods" (IPCC, 2007b).

1.2.2. Land use

Land use refers to how mankind use land and land resources, for example for agricultural purposes, mining and urban development. The FAO (1997a) defines land use as the human action, which alters land cover.

1.2.3. Land cover

Land cover is the physical undisturbed state of the surface of the land. It includes categories like forests, roads, cropland and urban areas. Land cover has also been defined by several other authors

(Di Gregorio and Jansen, 1998; Jansen and Di Gregorio, 1998) as the observed (bio) physical cover on the surface of the earth.

1.2.4. Land use/land cover change

Land use/land cover (LULC) change can be classified into two; conversion and modification (Butt and Olson, 2002). Land use/land cover conversion occurs when there is a complete change from one cover/use to another. In such a situation, one land cover type completely replaces another, and changes its classification e.g. conversion of forest land to urban settlement. In the case of land use/land cover modification there is a slight change which alters the characteristics of the land cover. In this instance even though the land cover is modified the original is retained giving rise to the maintenance of the original classification e.g. fragmented forest or overgrazed grassland. According to Butt and Olson (2002), key LULC changes include desertification, wetland drainage, deforestation and agricultural extensification. Land use/land cover changes are caused by both natural and human driving forces (Meyer and Turner, 1994). Human beings however, play a key role in contributing to land use/land cover change. At the same time they are equally affected by the changes (Lambin and Geist, 2006).

1.2.5. Soil erosion and sediment yield

Sediment yield is the amount of sediment supplied at the outlet of a catchment at a specific time (Patra, 2001) and result from erosion and deposition processes within a basin (Jain and Das, 2010). It is the sum of sediments generated by overland flow, gully, and stream channel erosion in a catchment (Duru, 2015). Transport of sediment in the channel network is a function of degradation and aggradation (Neitsch et al., 2005).

Runoff transport capacity is the main factor which controls sediment yield (Mutchler et al., 1988). As such, whenever runoff transport capacity is insufficient to sustain transport, the bulk of the sediment gets deposited at intermediate locations (Julien, 2010). Only a small fraction of eroded sediment within a drainage basin usually finds its way to the outlet. Sediment yield from catchments are usually slightly lower than the rates of soil erosion measured from plots of hillslope (Edwards, 1993 and Wasson et al., 1996). This shows that most sediments move only short distances (Parsons and Stromberg 1998) and then gets deposited. Varying proportions of the eroded materials are deposited between the source and the outlet, with a large proportion usually remaining in lakes or reservoirs.

In the Volta River Basin, erosion occurring upstream of the basin causes sediments to fill river channels and reservoirs, thereby reducing the quality of the water in the process. A major source of degradation of the water resource is thus the transport of sediment among the riparian countries of the Basin (Barry et al., 2005). Sedimentation also affects the storage capacity and life span of reservoirs and dams in the Volta Basin (Mul et al., 2015) and may lead to floods and hamper the fight against food insecurity in the region.

According to Nagle (2000), materials which make up sediment yield are of three different types: dissolved load (soluble materials carried as chemical ions); suspended load (made up of clay and silt held up by the turbulent flow), and bed load (includes larger particles moved by saltation, rolling and sliding). The quantity of sediments transported by streams usually contain between 70 and 99% suspended load (Babiński, 2005). The rest of the sediment materials are transported by saltation or intra-sediment movement (Yves, 2008). Sediment yield in a catchment reflects soil type, land cover/use, hydrology, topography, runoff, drainage network, sediment characteristics and geologic formation (Stand and Pemberton, 1982 *cited in* Duru, 2015).

1.2.6. Climate Change and evidence of global warming in West Africa

There is an overwhelming scientific agreement that humans are contributing to global warming. The Intergovernmental Panel on Climate Change (IPCC) has since its establishment provided evidence to the scientific community in support of the warming of the climate system. The IPCC is a scientific international body set up by the World Meteorological Organization (WMO) and by the United Nations Environment Programme (UNEP) in 1988 to assess the science related to Climate Change. In their Fifth Assessment Report, the IPCC highlights that successively warming trends have been recorded over the Earth's surface in the last three decades than any preceding decade since 1850 (IPCC, 2014a). For major parts of Africa, warming could go beyond 2 °C by 2050 and rise by as much as 2.6–4.8 °C by the end of the century under both medium and high emission scenarios (IPCC, 2013). Temperatures in West Africa are expected to rise by between 3 °C and 6 °C by the end of the 21 century under a range of scenarios. Unlike temperature, projections for rainfall in West Africa are less certain. Many global models however project a wetter main rainy season with a slight delay in the onset of the rainy season by the end of the 21 century (CDKN, 2014). Although Africa's contribution to greenhouse gas emissions has not been as much as the emissions by other regions of the world, the costs it faces, for example in terms of health issues, will continue to be huge due to the low adaptive capacity (Boko et al., 2007). Due to the projected mean changes in precipitation, temperature and increases in the frequency of extreme events (Rosenzweig et al., 2002) climate change is expected to amplify the pressure on water availability, affect food security and impact on human health significantly in the Africa region (IPCC 2013, IPCC 2014b).

1.2.7. Land use/land cover change in West Africa and the Volta Basin

The West African land cover has seen some changes in the past forty years as a result of increase in population, increases in the use of land for agriculture and economic development as well as the spread of settlement (Braimoh and Vlek 2005; Abbas et al., 2010; Ouedraogo et al., 2010). Quantification of land cover change within the Volta Basin for the years 1990, 2000 and 2007/8 showed that 64%, of the Volta Basin area (400,000 km^2) remained the same over the 18 years (1990-2008). Thirteen per cent (13%) got transformed from natural vegetation to agricultural areas and 8% from "natural, mostly woody savanna", to "natural herbaceous or bare surface". Three per cent (3%) of the total area got modified (Liebe et al., 2010).

1.2.8. Climate Change effects on water-related disasters in the Volta Basin

The Volta Basin has experienced loss of lives, severe damage and large economic and societal losses resulting from unexpected weather conditions in the region over the past 40 years. Extreme weather or climate event, popularly termed extreme event, is one of the key manifestations of climate change in a region or an area. It occurs when the "value of a weather or climate variable exceed (or go below) a threshold value near the upper (or lower) ends ('tails') of the range of observed values of the variable" (IPCC, 2012). The high spatial and temporal variability of rainfall intensities and amount within and between the countries that share the Volta River has greatly exacerbated local water shortages and competition in the basin. In the past few decades, the region has recorded significant increases in the frequency of heavy rainfall events and a common occurrence of droughts (Oyebande and Odunuga, 2010), resulting in several instances of water-related disasters. In 2007, for instance, a massive rainfall in the Basin caused severe flooding which resulted in the death of 56 people in Ghana (OCHA, 2007).

1.2.9. Water uses in the Volta Basin

The water resources of the Volta basin are used mainly for hydro-power generation, agriculture and domestic water supply. Ghana, which is located downstream of the Volta basin relies heavily on the Volta river for hydro-power production as opposed to Burkina Faso, which has invested in water infrastructure upstream of the basin mostly for irrigated agriculture. The trade-off between upstream irrigation and downstream hydropower production can lead to conflicts between countries if water infrastructure investments in the Volta basin are not optimized for mutual benefits. Most often than not, Ghana blames upstream Burkina Faso when there is too much or too little water downstream as is usually the case between riparian countries. For instance, the 2007 flood in Northern Ghana which caused severe economic losses was linked to the spilling of water from the Bagre dam in Burkina Faso (Armah et al., 2010).

1.2.10. Downscaling

Simulation of time series of climate variables with regards to rising greenhouse gas concentrations in the atmosphere is carried out using mathematical modelling in Global Climate Models (GCMs). These GCMs use IPCC emission scenarios to project future climate conditions. Most GCMs have spatial resolution of about 250km and represent the various earth systems (atmosphere, ocean and land surface) but are too coarse for direct use in impact assessments (Storch et al., 1993; Xu, 1999). Due to their coarse spatial resolution, GCMs are unable to satisfactorily represent land surface heterogeneity (for example vegetation and complex topography) at regional or local scale. According to Wilby et al. (2002), failure to capture these important local geographic characteristics may lead to weak projections. In West Africa, unsuitable grid box of GCMs coupled with the large spread among GCM projections (Hoerling et. al., 2006; Giannini et al., 2008) which has made unclear the response of the West African Monsoon (WAM) rainfall to anthropogenic climate

change (Douville et al., 2006; Christensen et al. 2007) play a major role in limiting climate change projections (Diallo et al., 2012) over the region. To overcome the issue of scale and obtain meteorological variables (especially precipitation and temperature) at regional and local scales for impact assessment, statistical or dynamical downscaling techniques (IPCC, 2001) are employed. According to Hayhoe (2010), even simple downscaling techniques yield better estimations in comparison to direct output from GCM simulation. Generally, there are two forms of climate downscaling: dynamic and statistical downscaling.

1.2.10.1. Dynamic downscaling

Dynamic downscaling uses Regional Climate Models (RCMs) nested into a GCM. RCMs have high spatial resolutions ranging from 20 to 50 km and have been found to simulate precipitation extremes better than GCMs (Frei et al., 2003; Huntingford et al., 2003). Studies by several authors (e.g. Nikulin et al. 2012; Endris et al. 2013; Kim et al. 2013; Panitz et al. 2014) have confirmed that RCMs are able to capture broad precipitation characteristics with some biases specific to the individual models, seasons and sub regions. A major weakness from using this downscaling technique, however, is the possible introduction of systemic biases from the global models to the overall regional climate simulation results since RCMs use GCMs as starting boundary conditions (IPCC, 2007b).

Various studies (e.g. Vizy and Cook 2002; Afiesimama, 2006; Gaetani et al. 2010; Sylla et al. 2010a; Sylla et al. 2011) have been conducted to highlight the importance of RCMs as valuable tools for improving our understanding of the WAM dynamics. To help improve the characterization of the WAM at different time-scales, coordinated frameworks such as the West African Monsoon Modelling and Evaluation (WAMME) initiative (Druyan et al. 2010; Xue et al.

2010), the African Multidisciplinary Monsoon Analysis (AMMA) (Redelsperger et al., 2006; Ruti et al. 2010) and the Ensemble-based prediction of Climate Change and their Impacts (ENSEMBLES) (Paeth et al., 2011) have been implemented. More recently, the Coordinated Regional Downscaling Experiment (CORDEX) (Giorgi et al. 2009; Jones et al. 2011) has been established using different RCMs.

1.2.10.2. Statistical downscaling

Statistical downscaling methods involve the derivation of empirical relationships between measured small scale local variables (predictands) and large-scale (GCM) variables (predictors) (Goodess et al., 2005; Boyer et al., 2010). Three important premises govern statistical downscaling techniques. First of all, the predictands are functions of synoptic forcing. Secondly, the transfer function stays valid under period outside the period of fitting. Thirdly, the predictors incorporate fully the climate change signal (Wilby et al., 2004). The statistical downscaling methodology can be grouped into three: regression methods (eg. von Storch et al., 1993), weather generators (Katz, 1996) and weather typing (e.g. Hay et al., 1991). Statistical downscaling techniques have a number of limitations. For example, in the weather generators (Wilby et al., 2004) a main limitation arises from the establishment of relationship between the large historical datasets with GCM during calibration. In this regard, the future relationship will change if the future weather and climatic conditions change with respect to time (Kumar, 2014) and will be entirely different from that used for the calibration process. In comparison to dynamical downscaling, statistical downscaling is less expensive and uses less computational resources.

1.2.11. Climate scenarios

Climate scenarios are assumptions made to access the impact of climate change patterns on the future. The Intergovernmental Panel on Climate Change (IPCC), the international body for

assessing the science related to climate change has since 1992 published different sets of climate scenarios to describe plausible trajectories of future climate. The scenarios represent many of the major driving forces of anthropogenic climate change and include processes, impacts (physical, ecological, and socioeconomic), and potential responses for climate change policy (Moss et al., 2010) to improve understanding of the future. The Representative Concentration Pathways (RCPs) are the latest iteration of the scenario process, superseding the second generation of projections, the Special Report on Emissions Scenarios (SRES). The RCPs include four greenhouse gas concentration trajectories RCP2.6, RCP4.5, RCP6.0, and RCP8.5 (Table 1.1) and derive their names from a possible range of radiative forcing values in the year 2100 relative to pre-industrial values (+2.6, +4.5, +6.0, and +8.5 W/m2, respectively) (van Vuuren et al, 2011a; Moss et al, 2010; Rogelji et al, 2012).

Representative Concentration Pathway (RCP) 2.6 scenario is compared to pre-industrial conditions and hence designed to meet the 2°C global average warming target with a peak in the radiative forcing at approximately 3 W/m^2 (~400 ppm CO_2) before the year 2100. This peak is followed by a decline to 2.6 W/m^2 (~330 ppm CO_2) by the end of the 21st century (van Vuuren et al., 2011b). RCP4.5 scenario includes long-term, global emissions of greenhouse gases, short-lived species, and land-use-land cover which stabilize radiative forcing at 4.5 W/m^2 (~650 ppm CO2) in the year 2100. The third scenario, RCP 6.0 is a medium-end scenario in which greenhouse gas emissions increase gradually, stabilizing radiative forcing at 6.0 W/m^2 (~670 ppm CO2) in the year 2100 (Moss et al., 2010; van Vuuren et al., 2011c). Compared to the total set of Representative Concentration Pathways (RCPs), RCP8.5 assumes the highest greenhouse gas emissions (business as usual) scenario, with a high rate of radiative forcing increase which peaks at 8.5 W/m^2 (~940 ppm CO_2) in year 2100 (Riahi et al., 2011). The RCP scenarios have the primary purpose of

providing time-dependent projections of atmospheric greenhouse gas (GHG) concentrations (IPCC, 2007a) and are neither projections nor predictions but representations of alternative, possible ways in which the future may unfold depending on how much greenhouse gasses are emitted in the years to come. They were released in the year 2000 and have been used in the latest IPCC report - Assessment Report Five (AR5) in 2014**.**

Table 1.1: Characteristics of the IPCC Representative Concentration Pathways (Moss et al., 2010)

Name	Radiative Forcing	Concentration (ppm)	Emissions Pathway
RCP8.5	>8.5 W/m^2 in 2100	>1370 eq-CO_2 in 2100	Rising
RCP6.0	~6W/m^2 at the stabilization level after 2100	~850 eq-CO_2 at the stabilization level after 2100	Stabilization without overshoot
RCP4.5	~4.5W/m^2 at the stabilization level after 2100	~660 eq-CO_2 at the stabilization level after 2100	Stabilization without overshoot
RCP2.6	Peak at ~3/Wm^2 before 2100 then decrease	Peak at ~490 eq-CO_2 before 2100 then decrease	Peak and decline

1.2.12. The Coordinated Regional Downscaling experiment (CORDEX)

The Coordinated Regional Downscaling experiment (CORDEX) is an initiative founded by the World Climate Research Program of the World Meteorological Organization with the aim of fostering international collaboration to produce an ensemble of high-resolution historical and future climate projections at regional scales to be used as inputs for impact and adaptation studies (Giorgi et al. 2009; Jones et al. 2011). By downscaling different Global Climate Models (GCMs) participating in the Coupled Model Intercomparison Project Phase 5 (CMIP5) (Taylor et al. 2012) in combination with RCPs (Moss et al., 2008, 2010), the CORDEX project has produced projected future climate data for several regions in the world. Specifically, each climate model output from

the CORDEX project is made up of an ensemble of RCM runs each one of them based on the output of one CMIP5 multi-model ensemble (Taylor et al. 2012), plus evaluation runs driven by ERA-Interim reanalysis data. The dataset includes precipitation, solar shortwave radiation and minimum and maximum temperature. These datasets are made up of control runs and projections based mostly on the emission scenarios RCP4.5 and RCP8.5. A few of the datasets are also available for RCP2.6. For the Africa domain, the RCM simulations are at a grid resolution of 0.44°x 0.44° (Figure 1.1), approximately 50 km. Further details about the CORDEX simulations for Africa can be found in Jones et al. (2011) and Nikulin et al (2013). Studies conducted over the entire African continent (e.g. Nikulin et al., 2012; Panitz et al., 2014; Kim et al., 2014 and Dosio et al., 2015) and at the regional level (e.g. Klutse et al., 2014; Abiodun et al., 2015 and Endris et al., 2015) have shown that CORDEX RCMs simulate well the spatial and temporal distributions of the West African precipitation with some seasonal and sub-regional biases.

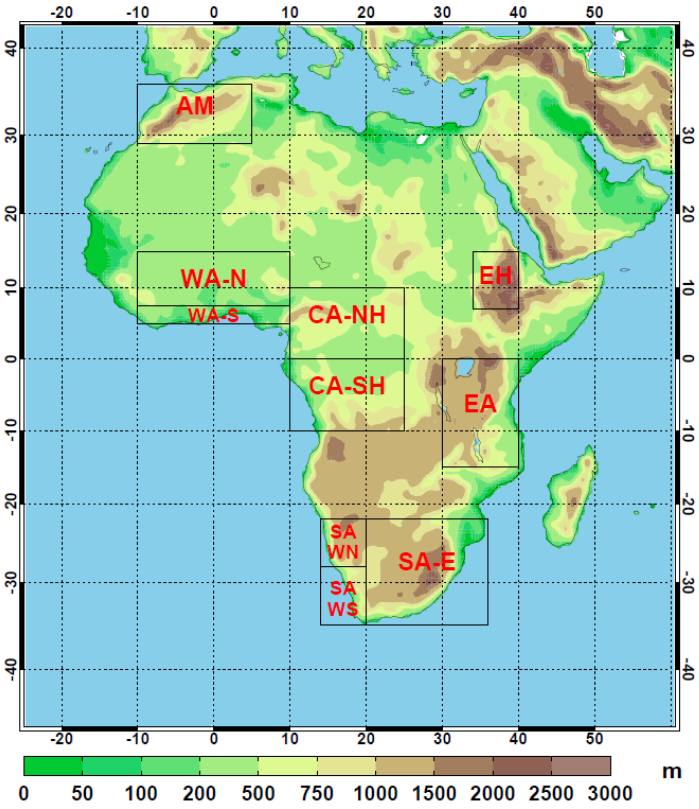

Figure 1.1: CORDEX Africa domain 0.44deg, 50-km (Swedish Meteorological and Hydrological Institute, 2016)

The Rossby Centre (SMHI) regional climate model, RCA4 and the Regional Atmospheric Climate Model (RACMO) are examples of RCMs used in generating data for the West Africa Region through the CORDEX experiment.

1.2.13. The Rossby Centre (SMHI) regional climate model, RCA4

RCA fourth generation is based on the HIRLAM, a numerical weather prediction model (Undén et al., 2002). Earlier versions of the model include RCAO, RCA1, RCA2 and RCA3. Detailed descriptions of the earlier versions have been given by Rummukainen et al. (1998, 2001); Räisänen et al. (2003, 2004), Jones et al. (2004), Kjellström et al. (2005) and Samuelsson et al. (2011). The current version, the RCA4, is an improvement of the RCA3 (Samuelsson et al. 2011) and has

undergone physical and technical changes to make it applicable for any domain worldwide. In addition, the improvement was aimed at making the model easy to use (Strandberg et al., 2014). Within the CORDEX project framework, the Swedish Meteorological and Hydrological Institute (SMHI) using RCA4 (Strandberg et al., 2014) has downscaled the ERA-Interim Reanalysis (1980-2010) and eight (8) different GCMs from the CMIP5 archives over the African domain (Jones et al., 2011, Nikulin et al., 2012). The data are available for RCP 2.6, RCP4.5 and 8.5 and cover the period 1951(1960) - 2100. The 8 GCMs employed by the SMHI for the dynamical downscaling are shown in Table 1.2.

Table 1.2: GCMs employed by the SMHI for the dynamical downscaling with RCA4

NO.	GCM NAME	INSTITUTE NAME
1	CanESM2	CCCma (Canada)
2	CNRM-CM5	CNRM-CERFACS (France)
3	HadGEM2-ES	MOHC (UK)
4	NorESM1-M	NCC (Norway)
5	EC-EARTH	ICHEC (Europian consortium)
6	MIROC5	MIROC (Japan)
7	GFDL-ESM2M	NOAA-GFDL (USA)
8	MPI-ESM-LR	MPI-M (Germany)

1.2.14. The Regional Atmospheric Climate Model (RACMO)

The Regional Atmospheric Climate Model (RACMO) is a hydrostatic limited-area model developed and maintained by the modeling group at the Royal Netherlands Meteorological Institute (KNMI) (van Meijgaard et al., 2008). The first version of the model, RACMO1 combines the HIRLAM model with the physics of ECHAM4. The second version, RACMO2, was developed based on the ECMWF-NWP release cy23r4 and the Numerical Weather Prediction (NWP) model HIRLAM version 5.0.6 (Lenderink et al., 2003). Climate change simulations of the RACMO22T

model, driven by the EC-EARTH for RCP 4.5 and 8.5 within the CORDEX project are used in this study.

1.2.15. Hydrological Models - SWAT model description

Several hydrological models have been developed and used by a wide scientific audience for studying the impacts of climate change on water resources. A hydrological model is a simplified representation of the hydrological system for studying watershed hydrology. Examples of hydrological models include the VIC model (Liang et al., 1994), HEC-HMS (Fleming and Neary, 2004), SWAT (Arnold et al., 1998) model and WaSiM-ETH (Schulla, 1997). Over the past few years, the SWAT model has gained worldwide recognition for its strengths compared to other hydrological models. It is considered a versatile model for water resource and nonpoint source pollution problems for a wide range of scales and environmental conditions (Gassman et al., 2007). Presently, more than 2,000 peer-reviewed articles on the model have been published with hundreds more published in other formats such as conference proceedings (Gassman, 2015). Globally, SWAT has been used in studying impact of climate change and/or land use change on hydrology of watersheds. Schoul and Abbaspour (2006) used SWAT to model river discharges of Niger, Volta and Senegal rivers in West Africa. Awotwi et al. (2015) used the model to assess the impact of land cover changes on water balance components of the White Volta Basin and concluded that in such "a poorly gauged rural West African catchment, the model could provide reliable results for stakeholders". In assessing the climate change impact on streamflow in selected river basins in Ghana, Kankam-Yeboah et al. (2013) successfully calibrated and validated the SWAT model for Nawuni (on the White Volta River Basin) and Twifo Praso (on the Pra River Basin). Other SWAT related studies in the Volta Basin and in Ghana include the works of Sood et al. (2013) and Obuobie et al. (2010) respectively.

The SWAT model is a physically-based medium- to large-scale watershed model developed by the United States Department of Agriculture-Agricultural Research Service (USDA-ARS) and is used for studying long-term impacts of climate, land use and agricultural management on water quality and quantity (Neitsch et al., 2005; Arnold et al., 1998). It is a very flexible and robust tool that can be used for simulating a variety of catchment problems. The model derives many of its modelling processes from some earlier models like: Chemicals, Runoff, and Erosion from Agricultural Management Systems (CREAMS) model (Knisel, 1980), the Groundwater Loading Effects on Agricultural Management Systems (GLEAMS) model (Leonard et al., 1987), and the Erosion Predictability Impact Calculator (EPIC) model (Arnold et al., 1998).

1.2.15.1. Watershed simulation in SWAT

The first and basic step in setting up a watershed simulation is the partitioning of the watershed into subunits. SWAT allows the following subunits to be defined within a watershed;

- ✓ Sub-basins
- unlimited number of Hydrologic Response Units (HRUs) [1 per sub-basin required]
- Ponds [optional]
- Wetlands [optional]
- ✓ Reach/main channel segments [1 per subbasin required]
- ✓ Impoundments on main channel network [optional]
- ✓ Point sources [optional]

Sub-basins are the first level of watershed subdivisions. They possess a geographic position in the watershed and are related to one another spatially. Sub-basin delineation may be obtained from watershed boundaries defined by surface topography. In this way the whole area within a sub-

basin flows to the sub-basin outlet. Another way to obtain sub-basin delineation is from grid cell boundaries. Generally a sub-basin contains at least one HRU, a tributary channel and a main reach. A wetland and/or pond may also be defined in a sub-basin as additional features.

Hydrologic response units (HRUs) are a further subdivision of the land area in a sub-basin and possess unique land use/management/soil attributes. Since it is often not practical to simulate individual fields with specific land use, management and soil, HRUs are used in most SWAT runs to simplify a run by lumping together all similar soil and land use areas into a single response unit. All calculations in SWAT are performed at the HRU level. The following section provides a summary of SWAT hydrology as well as the sediment component since they are important for this model application. The details of these and all the other components of the model can be found in the SWAT Input/Output Documentation (Arnold *et al*., 2012a).

1.2.15.2. Hydrology component

Simulation of watershed hydrology can be categorized into the land phase of the hydrologic cycle (Figure 1.2) and the routing phase of the hydrologic cycle. The routing phase involves movement through the channel network. The water balance equation (1.1) is the basic driver of the SWAT model hydrology. The model calculates daily water balances from meteorological, soil and land use data (Arnold et al., 1998).

$$SW_t = SW_o + \sum_{i=1}^{t} \left(R_{day} - Q_{surf} - E_a - W_{seep} - Q_{gw}\right) \quad \text{..... (1.1)}$$

where SWt is the final soil water content (mm); SW0 is the initial soil water content on day i (mm); t is the time (days), Rday is the amount of precipitation on day i (mm); Qsurf is the amount of surface runoff on day i (mm); Ea is the amount of evapotranspiration on day i (mm); Wseep is the

amount of water entering the vadose zone from the soil profile on day i (mm), and Qgw is the amount of return flow on day i (mm).

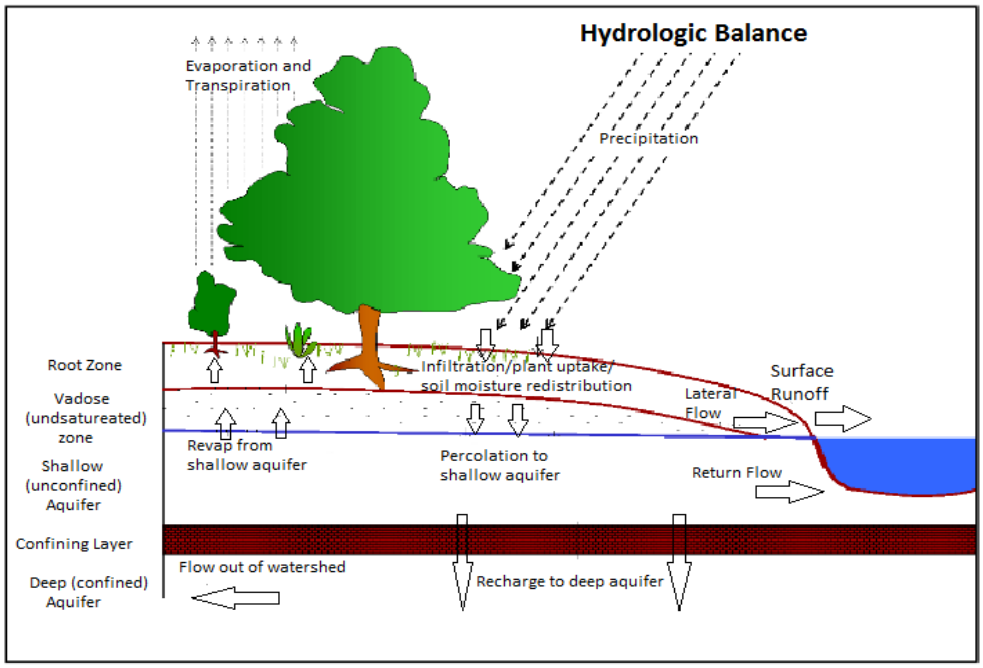

Figure 1.2: Schematic daigram of the hydrologic cycle used in the SWAT Model (Neitsch et al., 2005)

1.2.15.3. Surface runoff

Surface runoff occurs each time water application rate to the ground surface exceeds infiltration rate. The methods for surface runoff estimation in the SWAT model include the SCS curve number procedure (Soil Conservation Service 1972) and the Green & Ampt infiltration method (Green & Ampt 1911). Compared with the SCS curve number procedure, the Green & Ampt infiltration method is data intensive. For instance, whereas the former uses daily precipitation data, the latter needs hourly precipitation data. The SCS curve number method was employed in this study.

1.2.15.4. Percolation

The SWAT model categorizes soil into multiple layers. Percolation of water through these soil layers is allowed when soil moisture content in a layer exceeds its field capacity. The rate of percolation in each of the layers is highest at saturation and reduces to zero when the field capacity is reached. The flow from one layer to the underlying layer is modeled using the storage routing technique aggregated with crack flow. For dry and cracked soils, percolation of water occurs through the cracked layers without any impact on the water content of the soil. Percolated water through all the soil layers forms part of the groundwater and contributes to a stream as part of baseflow.

1.2.15.5. Lateral flow

The model uses a kinematic storage technique (Sloan et al., 1983, 1984) to compute lateral flow through each soil layer as a function of soil layer properties (saturated hydraulic conductivity, drainable porosity), soil slope and hill slope length.

1.2.15.6. Groundwater flow

The groundwater component in the SWAT model is simulated as two aquifers in each sub-basin; a shallow (unconfined aquifer which contributes to the flow in the main channel of the sub-basin) and a deep (confined) aquifer. Shallow aquifer recharge from percolation is also grouped into two; a part that percolates into deep aquifer and never gets to the stream, and a remaining part in shallow aquifer that adds to the stream as base flow and satisfies a portion of evaporative demand in the root zone (revap). Arnold et al., (1993) presume that water that enters the deep aquifer contributes to streamflow somewhere outside the watershed. Groundwater storage loses water either by seepage to the deep aquifer, upward movement from the water table into the capillary fringe or by

discharging to rivers and lakes. The model simulates the contribution of groundwater to streamflow by creating shallow aquifer storage rechargeable by percolation from the unsaturated zone. The shallow aquifer storage is reduced by withdrawal, baseflow, deep aquifer recharge and upward flows into the soil zone.

1.2.15.7. Evapotranspiration

SWAT provides three methods for computing potential evapotranspiration (PET). These are the: Penman- Monteith (Monteith, 1965), Hargreaves (Hargreaves *et al*., 1985) and Priestley-Taylor (Priestley and Taylor, 1972). The model also provides an option to use daily PET values computed with other methods. Due to the lack of long-term good quality data on relative humidity, wind speed, and solar radiation, the Hargreaves method, which requires only minimum and maximum temperature data was used for computing PET in this study.

1.2.15.8. Transmission loss

According to Lane (1982) many watersheds in the semiarid regions have ephemeral channels that abstract large quantities of streamflow. SWAT calculates all transmission losses using the method by Lane (1983).

1.2.15.9. Flow routing

Water can be routed though channel network in the SWAT model by selecting the variable storage method or Muskingum River routing method using daily time step. The model estimates the volume of water to be routed (surface runoff + lateral flow + baseflow– transmission loss) first in each HRU and then sums the values up to calculate total volume of water to be routed from a sub watershed. Apart from transmission loss, the channel can also loose water via evaporation, which

is a function of water surface area in the channel. Evaporation loss in each channel segment is subtracted from total volume before routing the flow through the next channel segment.

1.2.15.10. Erosion and sediment yield

The SWAT model estimates erosion and sediment yield for each hydrologic response unit (HRU) using the Modified Universal Soil Loss Equation (MUSLE) (Williams, 1975). The MUSLE is a revision of the Universal Soil Loss Equation (USLE) developed by Wischmeier & Smith (1965, 1978). The USLE uses the delivery ratios (the sediment yield at any point along the channel divided by the source erosion above that point) since the rainfall factor represents energy used in detachment only. In the MUSLE, the energy factor used in the USLE is replaced with a runoff factor. As a result of this improvement, sediment yield prediction using the MUSLE approach eliminates the need for delivery ratios since the runoff factor represents the energy for detaching and transporting sediment. For comparison purposes SWAT computes the USLE.

The MUSLE (Williams, 1995) is given as:

$$SY = 11.8(Q_{surf} * q_{peak} * area_{hru})^{0.56} * K_{USLE} * C_{USLE} * P_{USLE} * LS_{USLE} * CFRG \quad \text{(1.2)}$$

$$CFRG = e^{(-0.053\text{rock})} \quad \text{(1.3)}$$

where SY is the sediment yield (t/ha), 11.8 is a unit conversion constant, Q_{surf} is the surface runoff volume (mm), q_{peak} is the peak runoff rate (m^3/s), $area_{hru}$ is the area of the hydrologic unit area (HRU) (in ha), K_{USLE} is the USLE soil erodibility factor (0.013 tm^2 h/m^3t cm), C_{USLE} is the USLE cropping and management factor (dimensionless), P_{USLE} is the USLE erosion control factor (dimensionless), and LS_{USLE} is the USLE slope length (in meter) and steepness factor (no units),

and *CFRG* is the coarse fragment factor (dimensionless) and rock represents the rock fragments in the first soil layer (%).

1.3. Thesis Objectives

1.3.1. Main Objective

The overall objective of the study is to contribute to the sustainable water resources management and hydropower generation in the Black Volta River Basin by investigating the impacts of climate change and the sensitivity of land use/land cover change on streamflow and sediment yield in the basin.

1.3.2. Specific objectives

The specific objectives were to:

1. Adapt a hydrological model to simulate the streamflow and sediment yield in the BVRB;

2. Develop and analyze local climate scenarios for impact assessment in the basin mainly through statistical downscaling of projections from regional climate models;

3. Assess the impacts of climate change on the streamflow and sediment yield in the basin;

4. Analyze the sensitivity of streamflow to changes in LULC in the studied basin; and

5. Provide recommendations for effective basin management.

1.4. Research Questions

The central research question addressed in this thesis was: How will changes in climate and land use/land cover impact on streamflow and sediment yield in the Black Volta River Basin?

1.5. Research Hypothesis

This research hypothesizes that change in land use/land cover and climate in the future will impact negatively on the streamflow and sediment yield in the BVRB, the largest sub-basin of the Volta River Basin in West Africa.

1.6. Scope of Thesis/Novelty

Climate change is expected to have severe impacts on both human and natural systems worldwide and Africa in particular (Boko et al., 2007; Chinowsky et al., 2011). The Volta basin of West Africa is by no means exempted from the impacts of climate change (Kankam-Yeboah et al., 2013). Very few studies have been conducted to assess the impact of climate change on the hydrology of the Volta basin and some of its sub-basins, namely, the White Volta, Black Volta and Pru (Kankam-Yeboah et al., 2013; Sood, 2013; Obuobie et al., 2013; Obuobie et al., 2012; Obuobie, 2008; Andah et al., 2004; Opoku-Ankomah, 2000). However, nearly all the studies used climate projections from a single Regional Climate Model (RCM) driven by one Global Climate Model (GCM) and based on one IPCC Scenario experiment. Therefore, these studies were unable to adequately quantify the uncertainties associated with the climate projections used in their analysis. To overcome this drawback this study makes use of the multimodal ensemble approach. Regarding land use/land cover, its impact or sensitivity to streamflow in the studied basin has not been researched. Such information is important for sustainable water resources management including reliable hydropower generation in the Black Volta Basin as well as the entire Volta Basin.

1.7. Expected Results and Benefits

This study will generate impact specific information and data for informing water management decisions, climate change adaptation and land-use/-cover planning in the Black Volta Basin. The

results from the study can contribute to attaining the UN Sustainable Development goal 6 ("ensure availability and sustainable management on water and sanitation for all") in addition to goals 1, 2, 3 and 7 which all have linkages to water.

1.8. Outline of the Thesis

This thesis has 9 chapters, each of which contains information, data, and knowledge that contribute to addressing the overall objective of the research.

Chapter 1 provides a general introduction of the research. The chapter also contains review of literature on the subject matter. Definitions and concepts of key terminology of the research have been defined and explained in this chapter. The overview of the hydrological model used in the research, the Soil and Water Assessment Tool (SWAT), is presented. An overview of downscaling techniques, climate scenarios and the Coordinated Regional Downscaling experiment (CORDEX) are provided. The research background, problem statement, objectives, hypothesis and significance of the study are presented in this chapter.

Chapter 2 describes the study area, starting with a general description of the main Volta River Basin and narrowing it down to the Black Volta River Basin. The physical features, climatic conditions, hydrology and surface water use and development are presented.

Chapter 3 deals with the data sets, materials and methodology used in achieving the objectives of this research. The details of the modelling process with SWAT are provided. A description of the downscaling technique and the bias correction methods used are also presented, together with the procedure used in the climate change projects. The methodology used in the sensitivity analysis of land use/land cover change on the flow of the basin is also presented.

Chapter 4 presents and discusses the results of the hydrological modelling with SWAT. In particular the model sensitivity analysis, calibration and validation results are discussed. The results of the climate downscaling and bias correction aspect of this research are presented and discussed in Chapter 5. Chapter 6 discusses the results of climate change impact on precipitation and temperature while Chapter 7 discusses the impact of climate change on streamflow and sediment yield in the basin. The sensitivity of flow to changes in LULC in the Black Volta Basin is discussed in Chapter 8.

Chapter 9 presents the conclusion and perspective of the study and provides recommendations for the sustainable management of the water resources of the basin informed by the results of this study.

2. THE STUDY AREA

2.1. Introduction

This chapter first presents a general description of the Volta River Basin (VRB) and goes further to provide detailed description of the Black Volta River Basin (a major sub-basin of the Volta Basin) where the study was conducted.

2.2. General overview of the Volta River Basin

The 400,000 km² Volta River Basin is located in West Africa and stretches between latitudes 5 ^{o}N and 14 ^{o}N and longitudes 2 ^{o}E and 5 ^{o}W. The Basin is shared by six West African countries, namely, Benin, Burkina Faso, Côte d'Ivoire Ghana, Mali, and Togo (Figure 2.1). The major part of the Basin is shared by Burkina Faso and Ghana (about 82%) with the remaining 18% shared by the other four countries (Rodgers et al., 2007). The basin had an estimated population of 18.6 million in 2000, projected to reach 33.9 million by 2025 (Biney, 2010). A highly variable geographic distribution exists within the basin, with densities ranging from 8 to 104 persons/km^2 (Barry et al., 2005).

The Volta Basin has 4 main sub-basins, namely, Black Volta (147,000 km^2), White Volta (106, 000 km^2), Oti (72,000 km^2) and Lower Volta. The Lower Volta is formed through the joining of the Black and White Volta Rivers in the north of Ghana. The Volta Basin is largely flat with a mean elevation of about 257 m **(**Obuobie, 2008**).** The lowest point is found in the Lower Volta (elevations of about 1 m) and the highest point in the Oti Basin (elevations of about 920 m) (Barry et al., 2005). Agriculture is the main economic activity in the Volta baisn with about 70 to 90% of the population depending on subsistence farming (Rodgers et al., 2006, *cited in* Obuobie, 2008). The population also exploits the natural resources for survival (Barry et al., 2005).

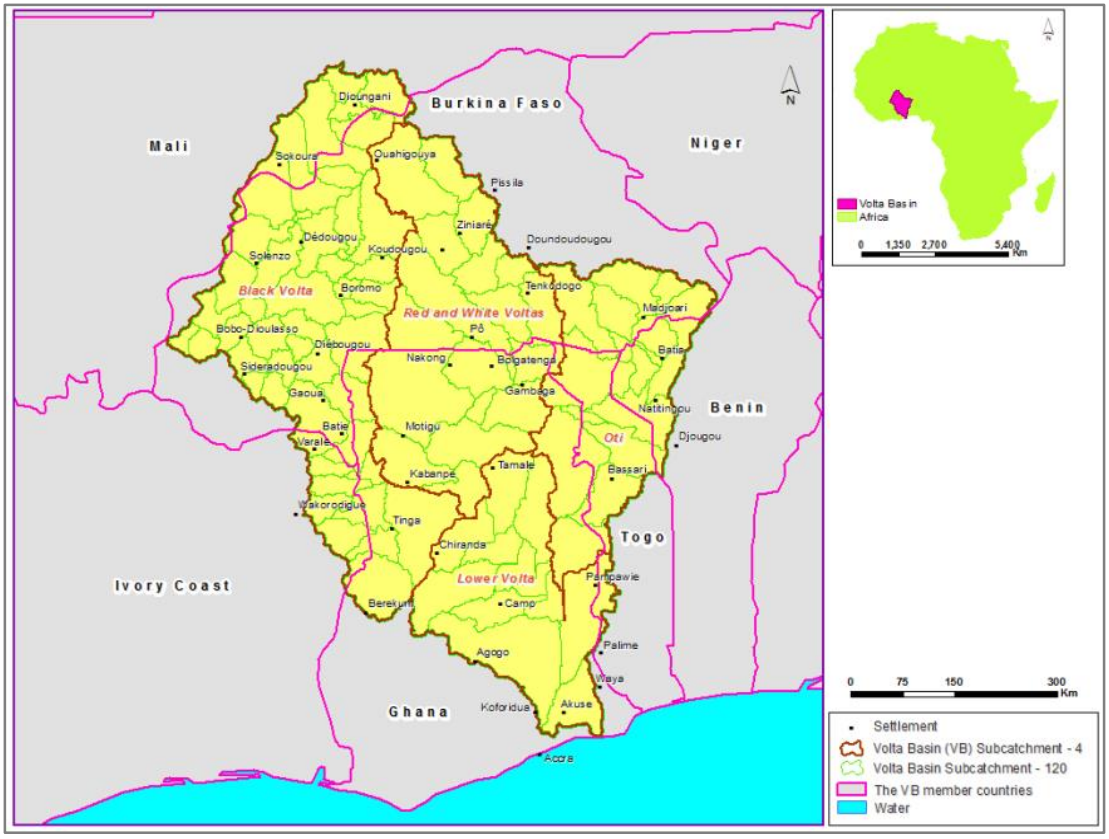

Figure 2.1: Map of Volta River Basin showing the four major sub-catchments (Geoportal of Volta Basin Authority, 2015)

2.3. Climate and hydrology

The climate of the Volta Basin is largely dependent on the movement of the dry North-East Trade winds from the interior of the African continent and the moist South-West Trade winds that blow from the seas (Amisigo, 2005 *cited in* Obuobie, 2008). The basin area has three climate zones; the humid south, the tropical transition zone and the tropical zone. The humid south and tropical transition zones each experience two rainfall seasons. While the rainfall seasons in the humid south are strongly bi-modal (peaking in June and September), those in the tropical transition zone are weakly bi-modal (Figures 2.2 and 2.3). The tropical zone on the other hand has just one rainfall season (Figure 2.4) which peaks in August/September (Barry et al., 2005). Rainfall is distributed

evenly in the humid zone throughout the year but poorly distributed in the tropic north zone. Over 70% of the total annual rainfall in the tropic north zone falls between June and September (Amisigo, 2005).

In general, higher rainfall amounts are experienced in some parts of the basin (e.g. 1600mm in the south-eastern section in Ghana) with smaller amounts in other parts (e.g. approximately 360 mm in the northern part of Burkina Faso). There have been some changes in the rainfall patterns in some of the Volta Basin's sub-catchments since the 1970's with a reduction in rainfall and runoff (Opoku-Ankomah, 2000). The beginning of the rainy season has also become difficult to predict (Obuobie, 2008).

Mean annual temperature in the Basin is higher in the northern half of the basin than in the southern half. According to Oguntunde (2004), mean daily temperature is about 36^{o}C in the north and 27^{o}C in the south. Humidity is between 6% and 83% (Barry et al., 2005). Mean annual potential evaporation is about 1,500 mm in the south and above 2,500 mm in the north of the Basin (Kasei, 2009). Annual mean potential evapotranspiration ranges from 1,800 mm in the coastal zone to 2,500 mm in the northern portions of the Basin (Green Cross International, 2001). Oguntunde (2004) estimated that about 80% of the rain which falls in the Basin during the rainy season is lost to evapotranspiration. Potential evapotranspiration exceeds rainfall for most parts of the year (Obuobie, 2008).

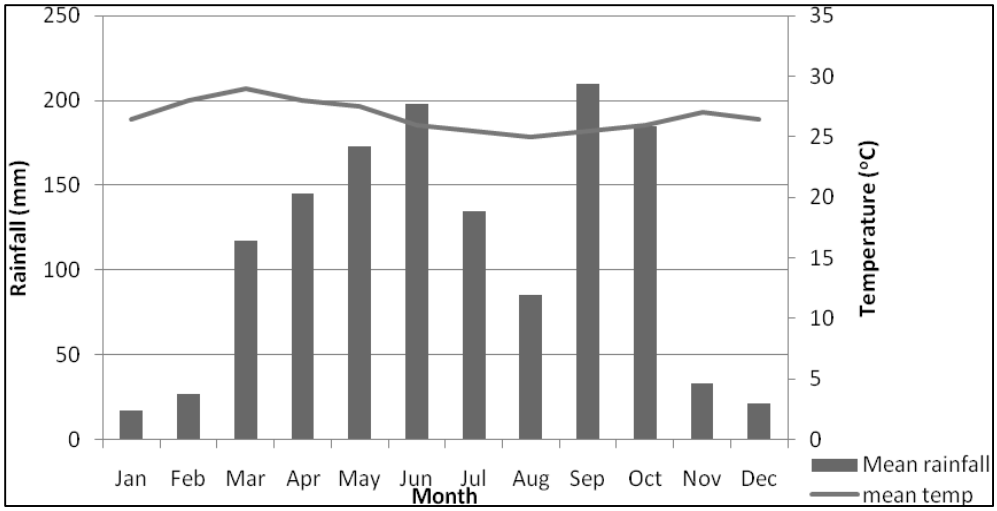

Figure 2.2: Mean monthly rainfall and temperature (1970-2000) at Ejura-Ghana, representing the humid south climate zone of the Volta Basin and showing two distinct rainfall seasons (Kasei, 2009)

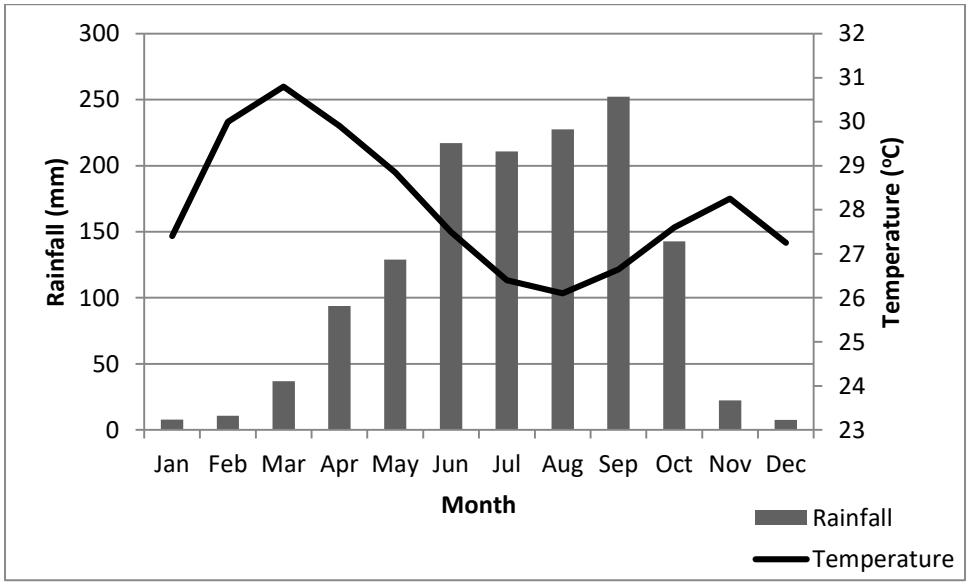

Figure 2.3: Mean monthly rainfall and temperature (1981-2010) at Kete Krachi - Ghana, representing the tropical transition climate zone and showing weakly bi-modal rainfall pattern (Data source: Ghana Meteorological Agency)

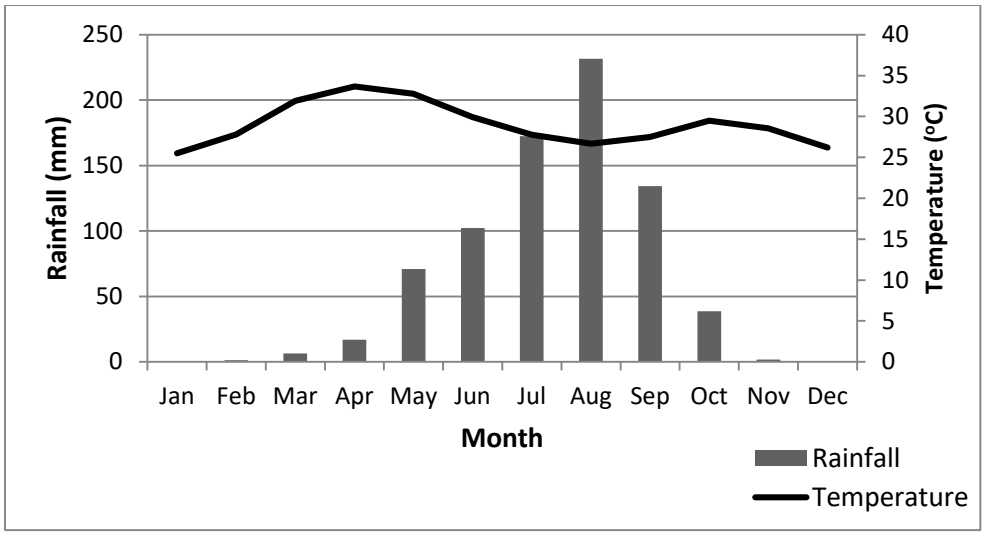

Figure 2.4: Mean monthly rainfall and temperature (1981-2010) at Dedougou in the tropical climate zone of the basin in Burkina Faso and showing a single rainfall peak (Data Source: Meteorological Agency of Burkina Faso)

2.4. Geology and soils

The geology of the Volta Basin (Figure 2.5) is largely (over 90%) comprised of the Precambrian basement crystalline formation that are related to the West African Craton and the Proterozoic to Paleozoic consolidated sedimentary formation (Obuobie et al., 2016; Mul et al., 2015). According to Key (1992) and MWH (1998), both *cited in* Mul et al. (2016), the basement crystalline formation consists of igneous rocks, metamorphic rocks, granite-gneiss-greenstone rocks, and anorogenic intrusions while the consolidated sedimentary formation consists of shales, mudstones, arkose, limestones, sandstones and sandy and pebbly beds. Other geological formation of importance in the basin is the unconsolidated sedimentary formation that consists of the recent tertiary sandstones and thick layers of sandstones together with schists, conglomerate and dolomite (Martin 2006; Obuobie and Barry 2012). Detailed information on the geology of the Volta Basin can be obtained from Obuobie et al., (2016), Mul et al. (2015), Obuobie and Barry (2012) and Martin (2006). The soils of the Basin (Figure 2.6) are derived from weathered parent material of the mid Palaezoic age

(Andah et al., 2005 *cited in* Obuobie, 2008) with the topsoil characterized by the buildup of organic matter (Kasei, 2009). The soils in the north of the basin (Burkina Faso) are mostly of lateritic type while that in the south (Ghana) is mainly lixosols. These weathered soils are mostly kaolinite clays high in iron, aluminium and titanium oxide. The soils in the northern savannah part of the Basin have less organic matter and lower nutrient content than the forest soils in the south (Kasei, 2009). The arenosols, mostly found in the arid northern portion of the basin, constitute the other main group of soils in the basin (Jung, 2006). These soils have high infiltration rates and are red in colour due to the sand being coated with iron oxides (Jung, 2006).

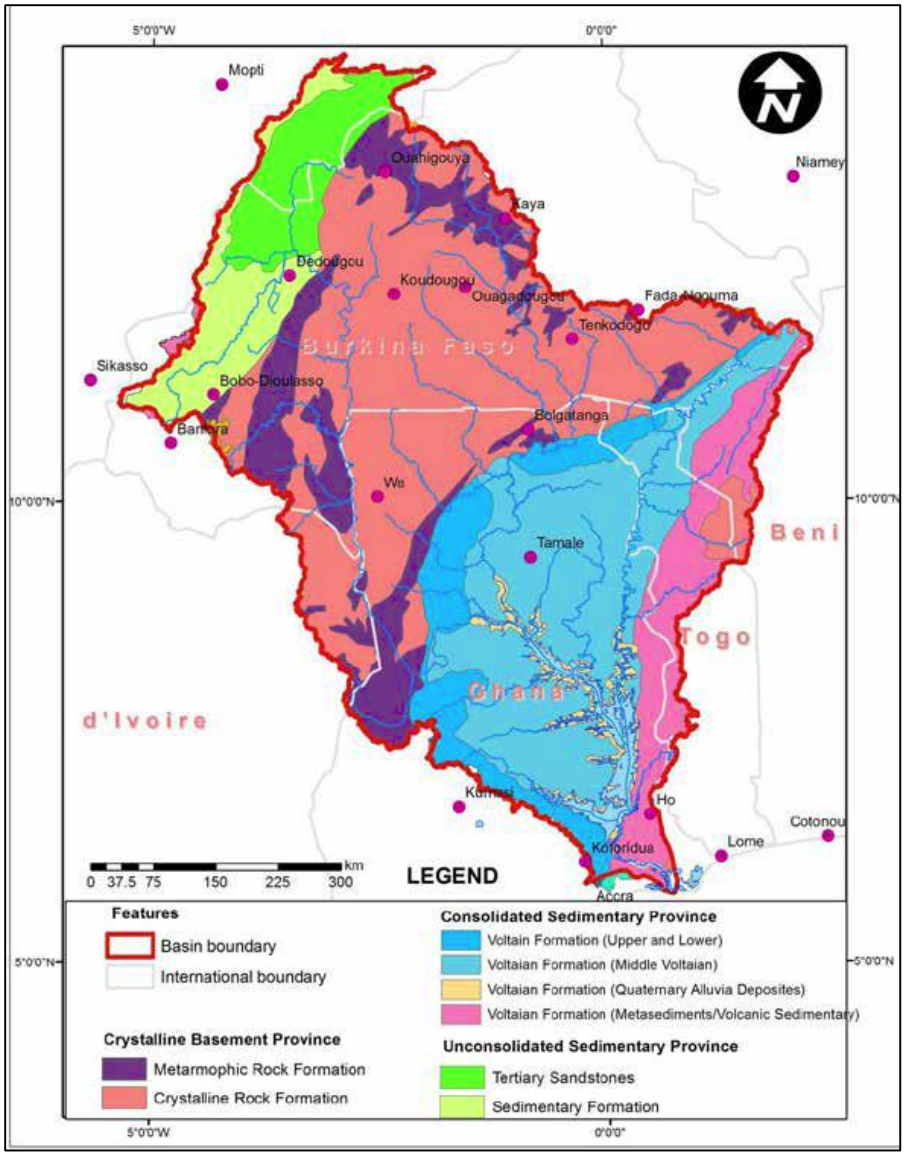

Figure 2.5: Volta Basin Geology (Glowa Volta Project)

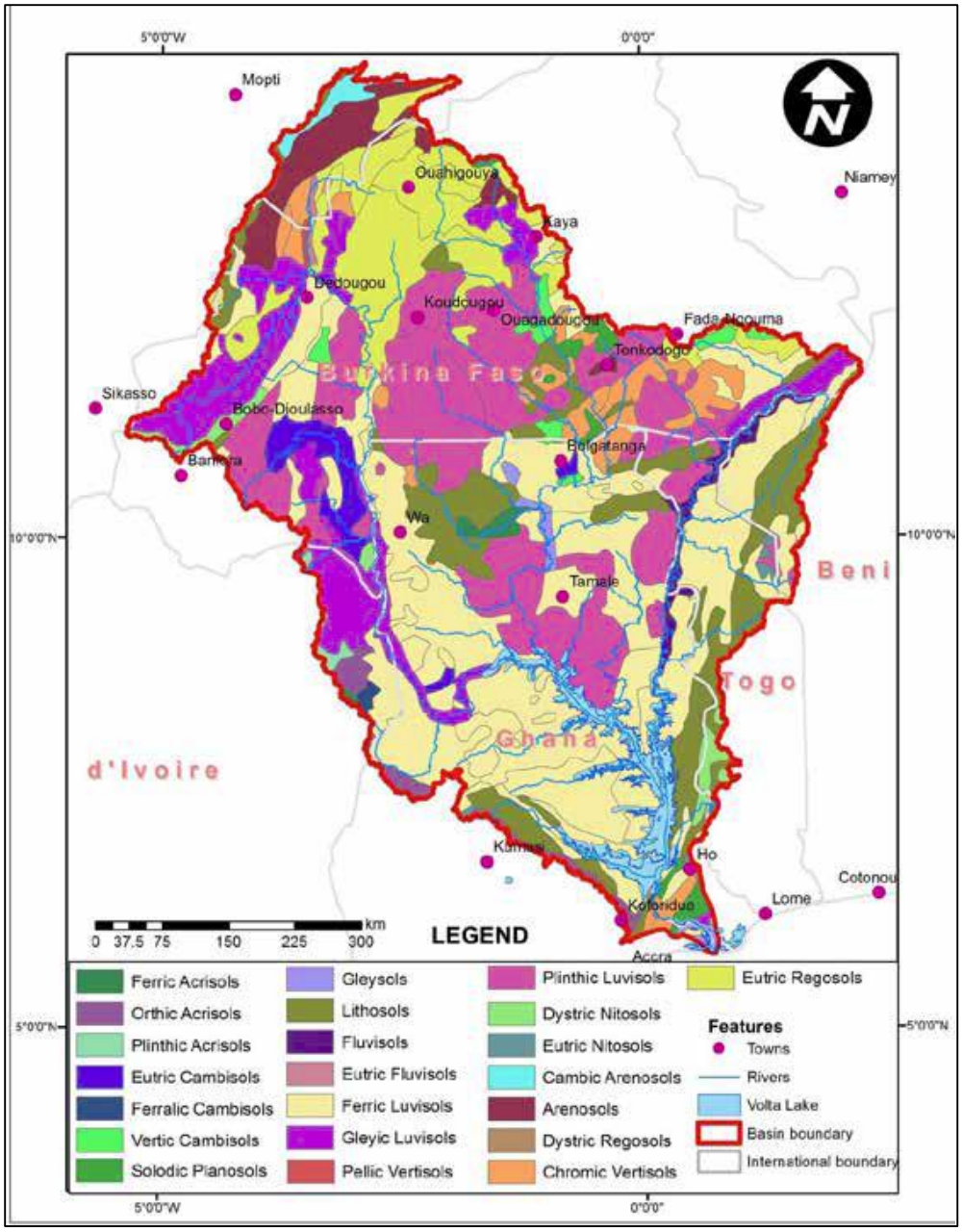

Figure 2.6: Volta River Basin soil map (Mul et al., 2015)

2.5. Land cover and land use

Land cover in the Volta Basin is dominated by the savannah land cover (Figure 2.7), which is made up of grassland interspersed with trees and shrubs and covers about 86% of the basin (Obuobie 2008). The rest of the land cover is made up of croplands and natural vegetation wetland,

forest cover and urban/industrial, with area coverage of 10.4%, 4.6%, 0.7% and 0.5%, respectively (WRI, 2003 *cited in* Obuobie 2008). Land cover type has a major influence on runoff processes including infiltration (Chevallier and Planchon, 1993; Giertz, 2004). Agriculture is the predominant land use type in the Basin. Cultivated crops include cereals such as maize and millet, root crops and vegetables (Obuobie, 2008).

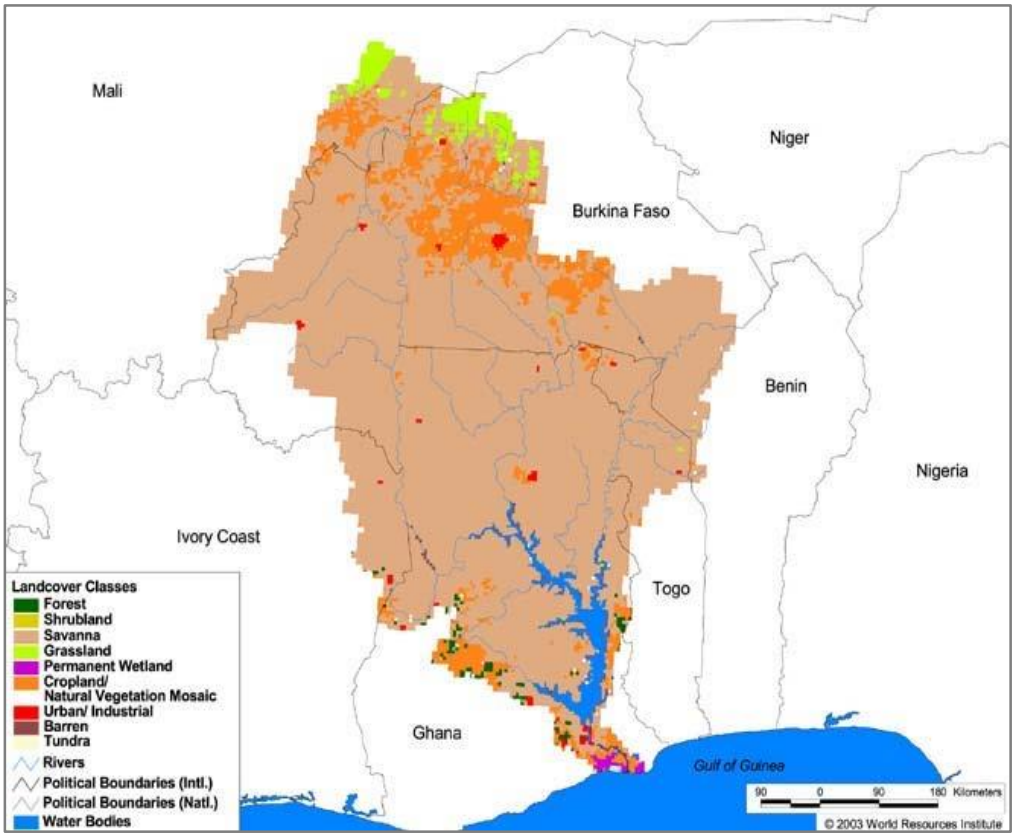

Figure 2.7: Land cover map of the Volta River Basin (Barry et al., 2005)

2.6. Surface water development and use

The Volta River Basin has a number of reservoirs constructed to mobilize water for agriculture, energy generation and water supply. The basin houses one of the world's largest man-made lakes, the Volta Lake, which resulted from the construction of the Akosombo Dam in Ghana in 1964 for

hydropower generation. The lake has a surface area of 8,500 km^2 and a storage capacity of 148 km^3 (FAO, 1997b). The Kpong Headpond is a relatively smaller hydroelectric dam constructed in 1981 at Kpong, 20 km downstream of Akosombo with an area of about 40 km^2 (WRC, 2016). Together the Akosombo dam and Kpong headpond generate about 1,180 MW of hydropower (Ghana Energy Commission, 2015). The ever increasing energy demands and high energy costs in the country has, however, led to the establishment of a third dam, the Bui, located in the Bui Gorge of the Black Volta Basin, approximately 150 km upstream of Lake Volta (Environmental Resources Management, 2007). The construction of the main dam began in 2009 and started operation in May 2013 with a hydropower generation of about 400 MW.

A number of other small and large dams have also been constructed by governments, local populace and Non-governmental Organizations (NGOs) in the other 5 riparian countries of the basin. These constructions occurred after the severe droughts of 1970s and 1980s and are mainly for irrigation and watering of livestock for food security. A typical example is the case of the Nakambe (White Volta) sub-basin in Burkina Faso where more than 600 small dams have been built (Barry et al., 2005). Power generating dams have also been constructed on the Oti River at the border between Togo and Benin and in some of the Volta main tributaries (e.g., Bagre on White Volta and Kompienga on Oti in Burkina Faso). The power generating capacities of the Bagre and Kompienga dams are 16MW and 14MW, respectively (Mul et al., 2015).

The mean annual groundwater recharge of the Volta River system is approximately 5-13% of annual precipitation (Martin, 2006). Since surface water is becoming increasingly insufficient for many communities in the basin, most of the people have resorted to the use of groundwater for everyday domestic purposes and for irrigation.

2.7. The Black Volta River Basin

2.7.1. Location and administrative boundaries

The Black Volta River Basin (Figure 2.8) is located between Latitude 7º00'00"N and 14º30'00"N and Longitude 5º30'00"W and 1º30'00"W (Annor, 2012). With a total area of about 142,056 km ^{2} (Kasei, 2009), it is the largest sub-catchment of the Volta River Basin. It is shared by Ghana, Burkina Faso and Cote D'Ivoire.

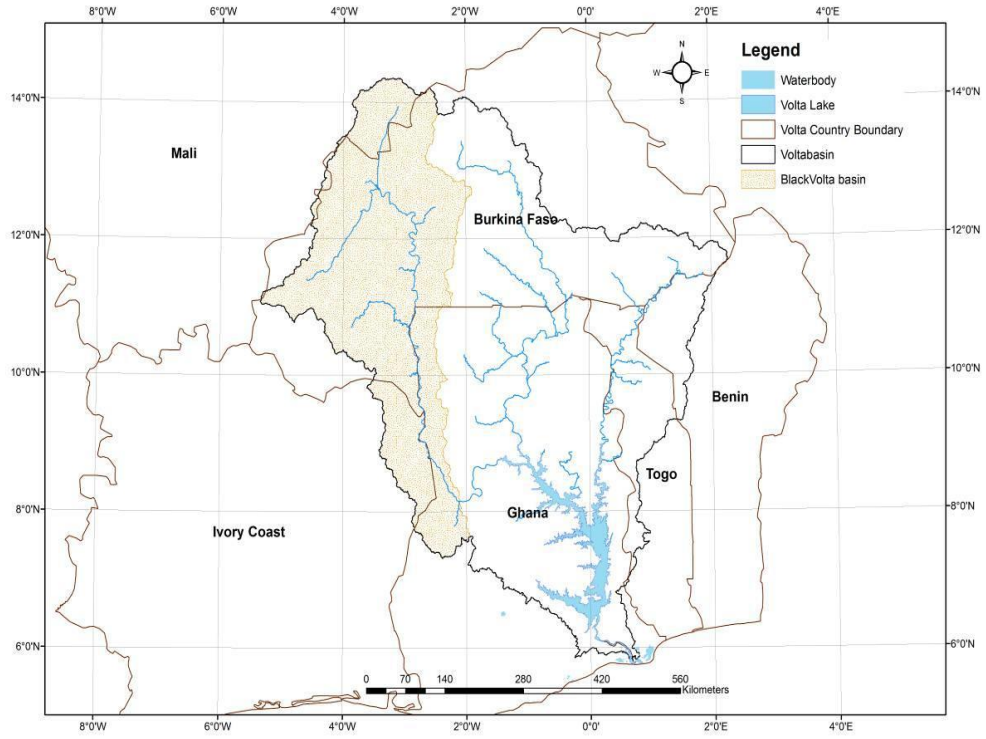

Figure 2.8: The Black Volta sub-catchment within the Volta Basin (Annor, 2012)

2.7.2. Rainfall, temperature and evaporation

The BVRB experiences two contrasting rainfall seasons: the rainy season and the dry season. Rainy season spans from May to September during which over 76% of the total annual rainfall occurs (Amisigo, 2005 *cited in* Obuobie, 2008) with the remaining months being dry and hot. Mean annual rainfall ranges between 1,043 mm-1,270 mm, with annual evapotranspiration of

about 1,450 mm/year to 1,800 mm/year. Mean monthly minimum temperature for the basin ranges between 18°C in December to 25°C in April while mean maximum temperatures vary from 30°C in August to 37°C in April (Figure 2.9). The spatial distribution of rainfall in the BVRB is presented in Figures 2.10 and 2.11.

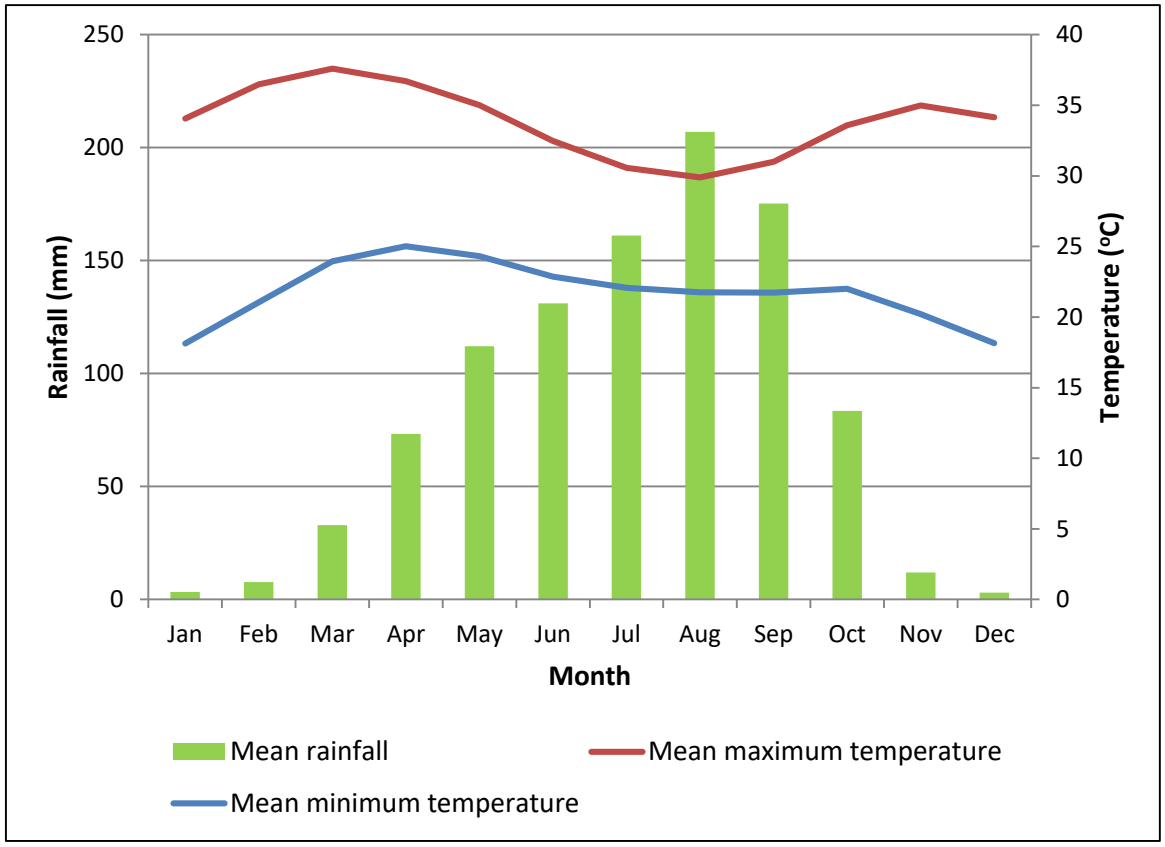

Figure 2.9: Mean monthly rainfall and temperature in the Black Volta Basin (1981-2010) (Data source; Ghana and Burkina Faso Meteorological Agencies)

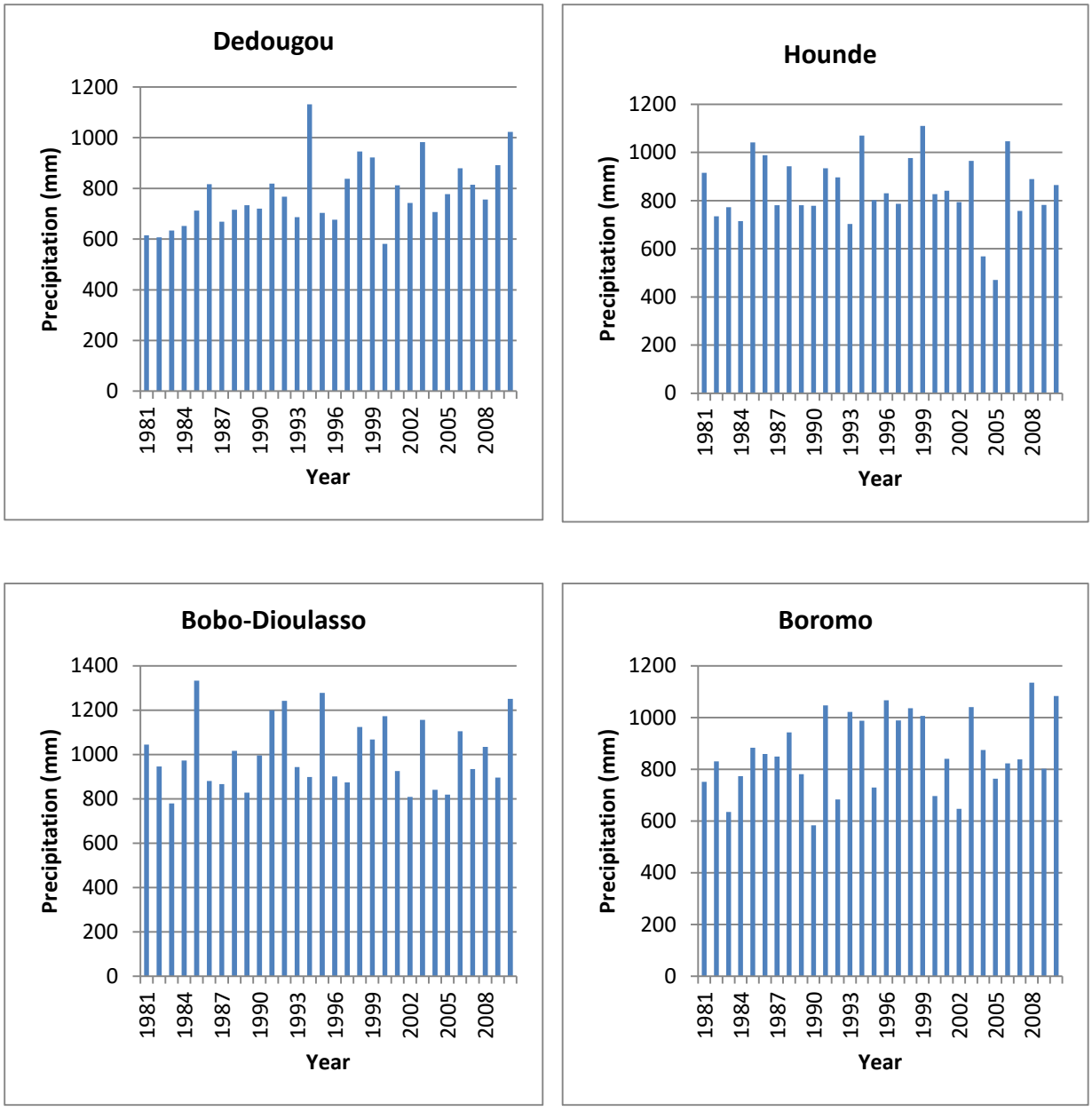

Figure 2.10: Inter-annual rainfall (1981-2010) at 4 gauge stations in the north of the basin in Burkina Faso: (Data source; Burkina Faso Meteorological Agency; Volta Basin Authority Geoportal)

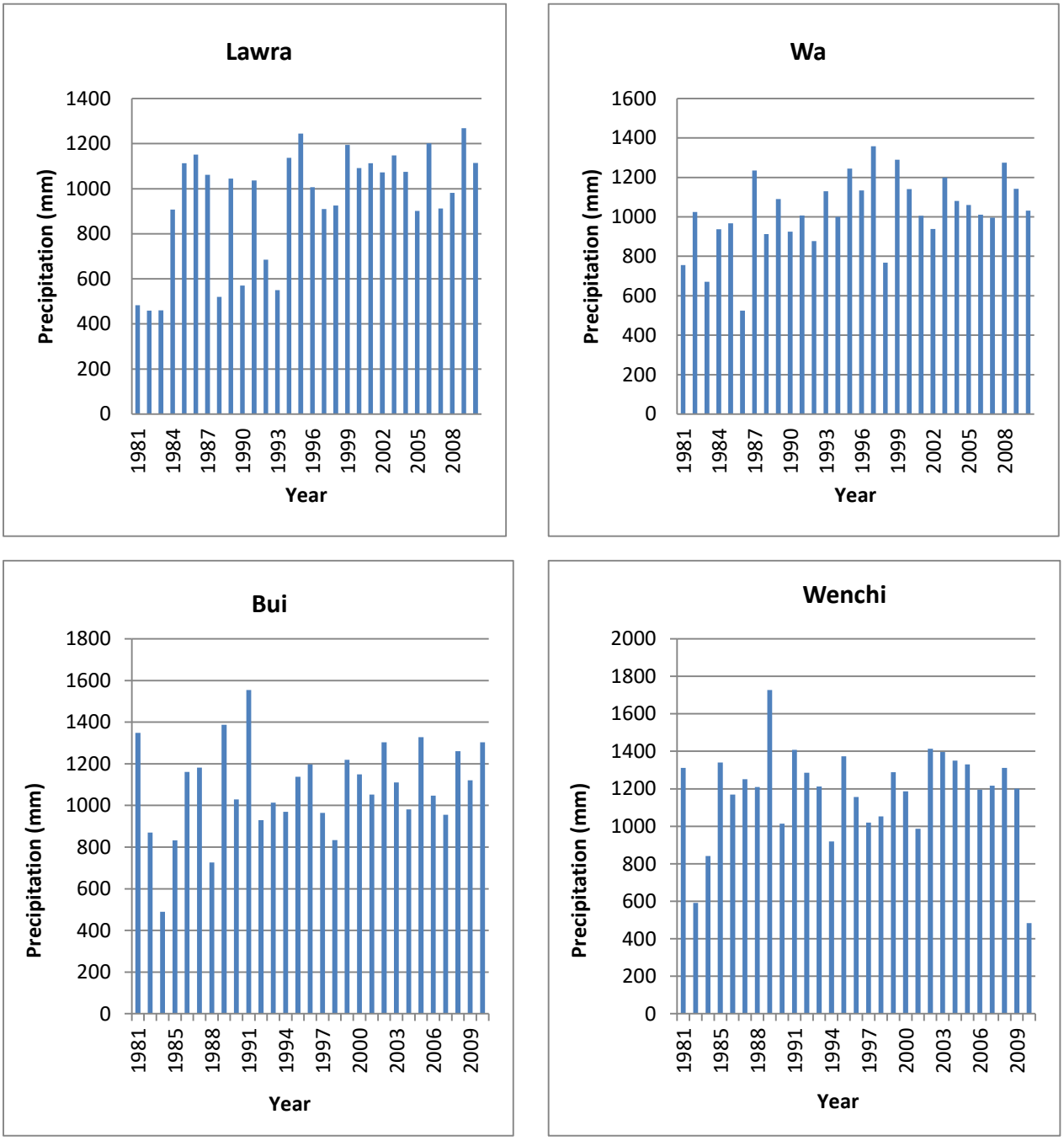

Figure 2.11: Inter-annual rainfall (1981-2010) at 4 gauge stations in the south of the basin in Ghana: (Data source; Ghana Meteorological Services; Volta Basin Authority Geoportal)

2.7.3. Vegetation and land use /land cover

2.7.4. Geology and soil

The Black Volta Basin geology consists mainly of granite, Birimian, Voltaian and Tarkwaian systems (Gordon and Amatkpor, 1999; Barry et al., 2005). The Birimian system is made of gneiss, granite-gneiss, phyllite, migmatite, schist and quartzite (Gyau-Boakye and Tumbulto, 2006). The Voltaian system is made of Precambrian to Paleozoic sandstones, shale and conglomerates. The Tarkwaian system consists of quartzites, phyllites, grits, conglomerates, and schists. The underlying rocks of the basin are without inherent porosity and so groundwater is stored only in fractures in the rocks (Barry et al., 2005). Based on the FAO claissification, the soils of the BVRB are dominantly Luvisols and Gleysols (Figure 2.12).

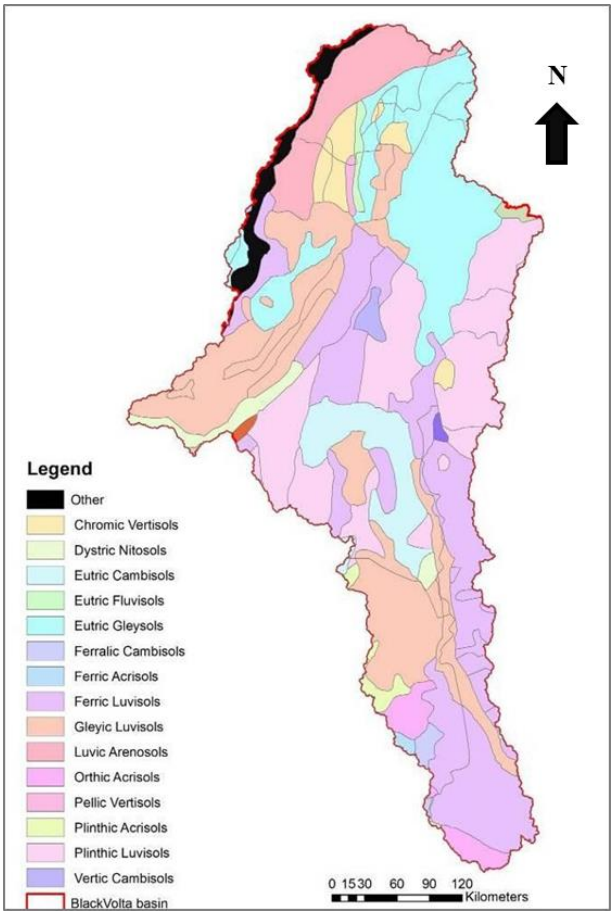

Figure 2.12: Dominant Soil types in the Black Volta River Basin (Annor, 2012)

2.7.5. Population

The population of the BVRB was around 4.5 million as of year 2000 and projected to reach 8 million by 2025 (Annor, 2012). The basin's population density ranges between 8 and 123 people/km^2 (Allwaters Consult, 2012), with a population growth rate of around 3% per annum (Green Cross International, 2001).

3. DATA, MATERIALS AND METHODS

This chapter describes in detail the data, materials and procedure followed in achieving the objectives of the study.

3.1. Data

3.1.1. SWAT input data

The input data used for setting up the SWAT model for the Black Volta basin included a digital elevation model (DEM), the year 2000 land-use/land cover (LULC) map, soil map and data, data on climate, plant growth, management and the Bui reservoir. Streamflow and sediment yield data covering a period of eleven years (2000-2010) and eight years (2000-2007) respectively, were used for calibrating and validating the model.

3.1.1.1. Digital elevation model (DEM)

The Shuttle Radar Topographic Mission (SRTM) Digital Elevation Model (DEM) provides reliable global coverage of topography and stream network and was used in this study for watershed delineation. The DEM (Figure 3.1) was obtained from the CGIAR-CSI Consortium for Spatial Information server (http://srtm.csi.cgiar.org/index.asp) and had a resolution of 90m. All data voids had been filled when the DEM was obtained.

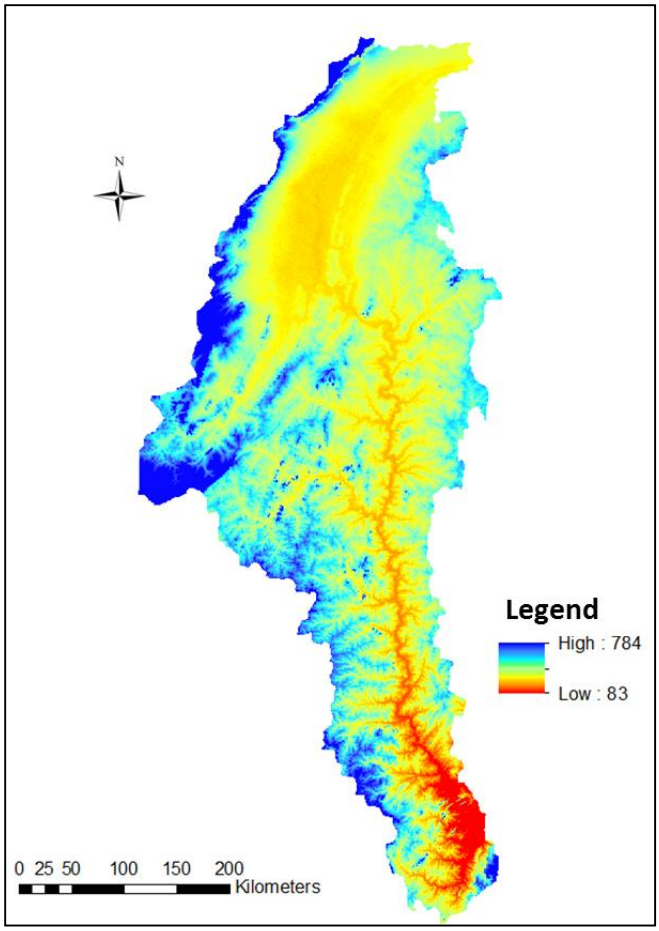

Figure 3.1: SRTM DEM of the Black Volta Basin (Source: The CGIAR-CSI Consortium for Spatial Information server - http://srtm.csi.cgiar.org/index.asp)

3.1.1.2. Land use/land cover map and data

The year 2000 land-use/-cover map (Figure 3.2) with a resolution of 250m obtained from the GLOWA Volta project of the Center for Development Research (ZEF), Germany, was used in setting up the SWAT model. The original legend of the map was modified to allow for modelling in SWAT as shown in Table 3.1. The existing SWAT look up table was also modified to include land use/land cover types that were not already present (e.g. savanna) in SWAT 2012.

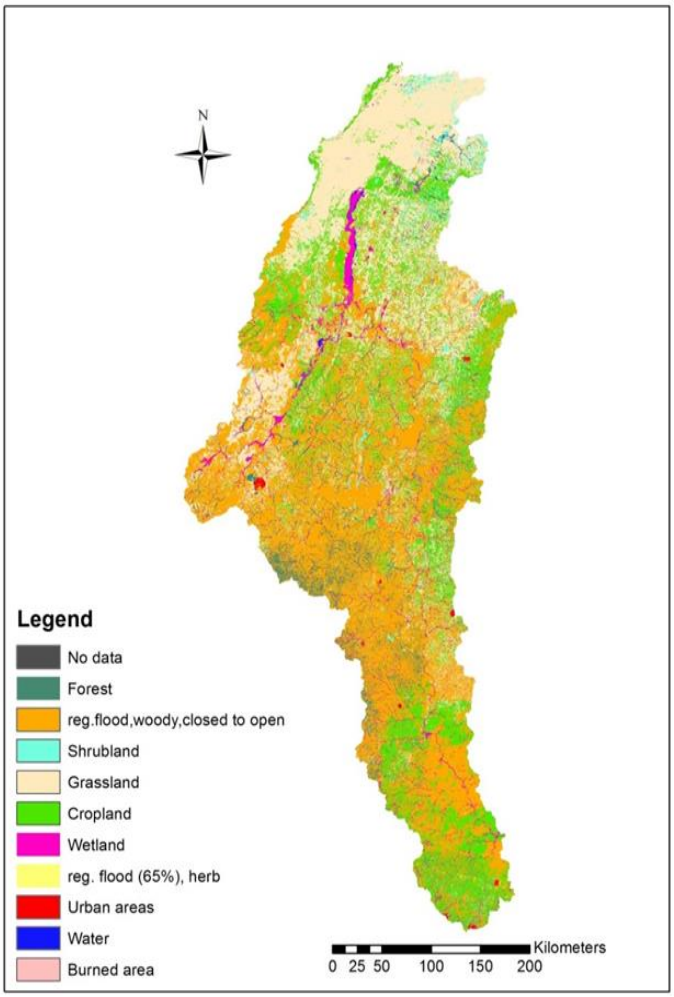

Figure 3.2: Land use/land cover map used as input in SWAT (Data source: Glowa Volta project)

Table 3.1: User-defined SWAT LULC classes for the Black Volta Basin

No.	Land use class	Description
1	SAVA	Savanna
2	FRSE	Forest-Evergreen
3	SHRB	Shrubland
4	GRAS	Grassland
5	AGRL	Agricultural Land-Generic
6	WETN	Wetlands-Non-Forested
7	WEHB	Herbaceous wetland
8	URMD	Urban Medium Density
9	WATR	Water Body
10	BARR	Barren

3.1.1.3. Soil map and data

The BVRB soil map (Figure 3.3) used in this study was obtained from the FAO digital soil map of the world and derived soil properties (FAO, 1995). Soil properties play an important role in the hydrological process of watersheds. Soil physical characteristics determine the movement of water and air within the HRU and are required for modelling in SWAT. In addition to the digital soil map, the SWAT model requires information on the physical and chemical properties (e.g. soil depth, soil texture, hydraulic conductivity and bulk density, and organic carbon) of each soil layer modeled. These data were obtained from the FAO digital soil map of the world and derived soil properties (FAO, 1995) and the Soil Research Institute (SRI) in Ghana. A user table specific for the Black Volta River basin soil layers was appended to the existing soil table in the SWAT database using Arc toolbox in ArcGIS since the soil types found in the study area are not included

in the US soils database. A list of soil properties required for modelling in SWAT is listed in Table 3.2.

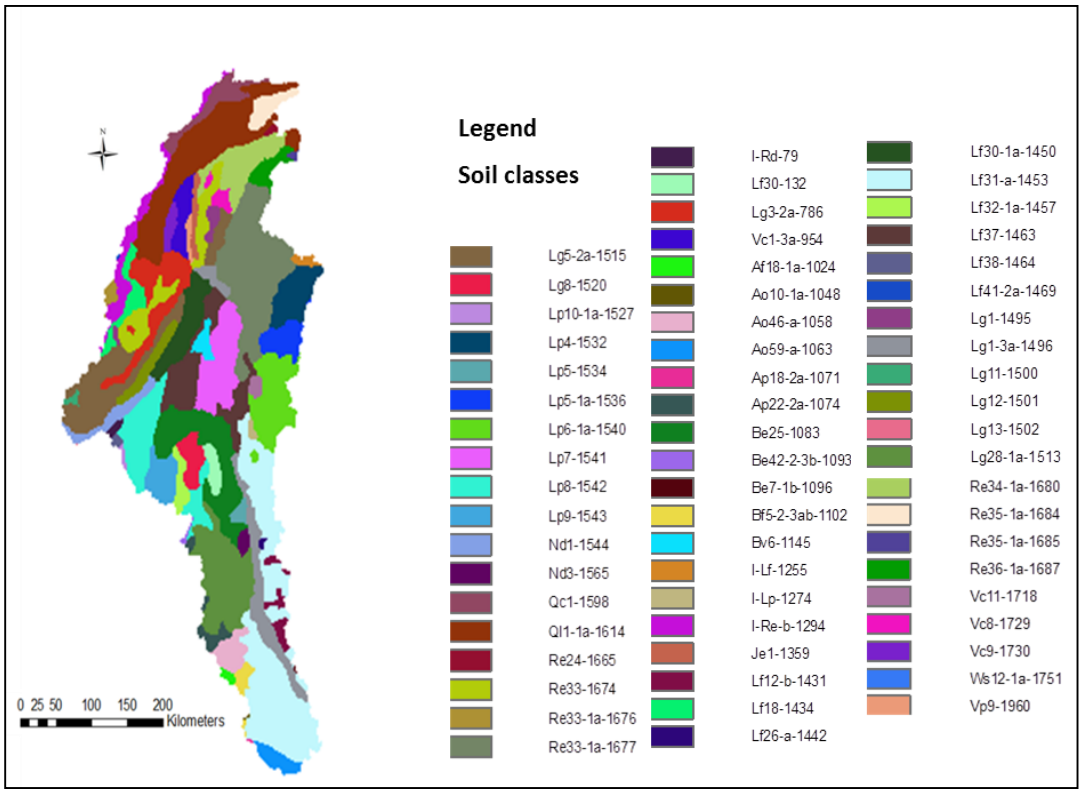

Figure 3.3: Soil map of the Black Volta Basin used as input in SWAT

Table 3.2: Soil physical properties required for modelling in SWAT (Arnold et al., 2012a)

Soil parameter	Description	Unit
NLAYERS	Number of layers in the soil (min 1, max 10)	-
HYDGRP	Soil hydrologic group (A, B, C, D)	-
SOL_ZMX	Maximum rooting depth of soil profile	mm
ANION_EXCL	Fraction of porosity from which anions are excluded	-
SOL_CRK	Potential or maximum crack volume of the soil profile expressed as a fraction of the total soil volume [optional]	-
TEXTURE	Texture of soil layer [optional]	-
SOL_Z	Depth from soil surface to bottom of layer	mm
SOL_BD	Moist bulk density	Mg/m^3 or g/cm^3
SOL_AWC	Available water capacity of the soil layer	mm H_2O/mm soil
SOL_K	Saturated hydraulic conductivity	mm/hr
SOL_CBN	Organic carbon content	% soil weight
CLAY	Clay content	% soil weight
SILT	Silt content	% soil weight
SAND	Sand content	% soil weight
ROCK	Rock fragment content	% total weight
SOL_ALB	Moist soil albedo	-
USLE_K	Soil erodibility factor	0.013 (metric ton m^2 hr)/(m^3-metric ton cm)

3.1.1.4. Climate data

SWAT requires climate data such as precipitation, maximum and minimum air temperature, solar radiation, wind speed and relative humidity to calculate the water balance of a river basin. The observed daily climate data used in this study were obtained from the Ghana Meteorological Agency and the Direction Generale de la Météorologie, Burkina Faso, and included daily precipitation and minimum/maximum air temperature. The data were from 11 synoptic climate stations (Figure 3.4 and Table 3.3) in the BVRB and covered the period 1981-2010. The SWAT model reads the values for weather parameters directly from records but in cases where there is missing data in any of the weather data, a weather generator incorporated in SWAT can be used to fill in gaps in data and/or simulate data. Three climate stations (Bobo-Dioulasso, Bole and Dedougou) in the BVRB, with almost complete (> 98%) climate data were used for generating missing records in the data of the other stations (Annex 2).

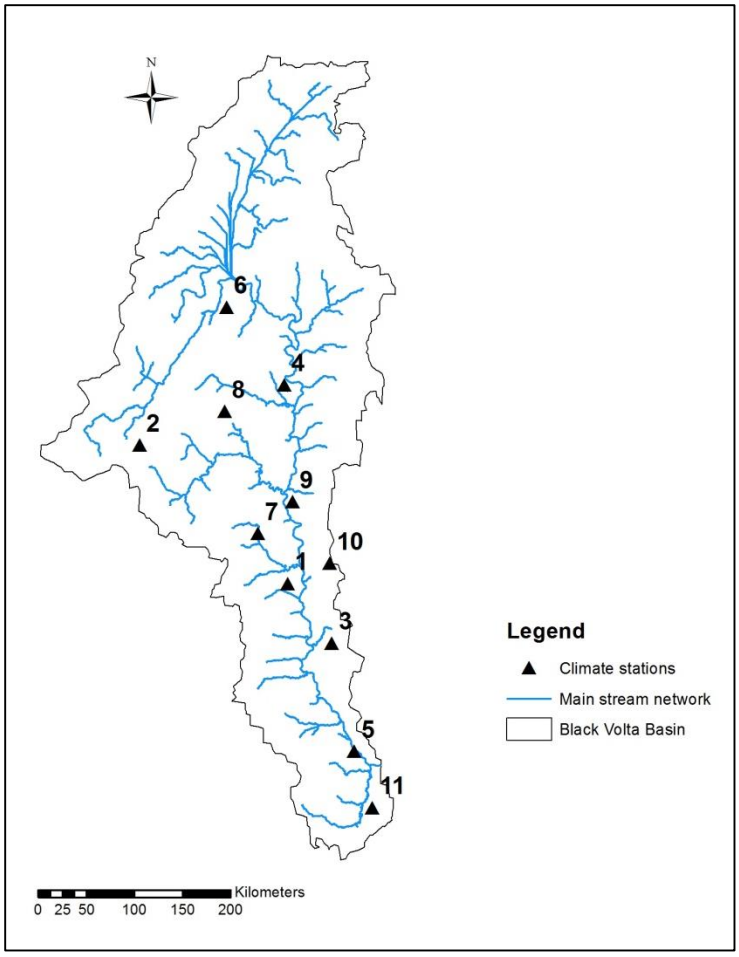

Figure 3.4: Location of synoptic climate stations in the Black Volta River Basin

Table 3.3: Details of weather stations used for SWAT modelling in the Black Volta Basin

No.	Station Name	Latitude (^{o})	Longitude (^{o})
1	Batie (BF)	9.86	-2.9
2	Bobo-Dioulasso (BF)	11.17	-4.3
3	Bole (GH)	9.03	-2.48
4	Boromo (BF)	11.73	-2.92
5	Bui (GH)	8.28	-2.27
6	Dedougou (BF)	12.46	-3.48
7	Gaoua (BF)	10.33	-3.18
8	Hounde (BF)	11.48	-3.5
9	Lawra (GH)	10.63	-2.85
10	Wa (GH)	10.05	-2.5
11	Wenchi (GH)	7.75	-2.1

3.1.1.5. Discharge data

Monthly discharge data from the streamflow gauge at Bui on the main course of the BVRB (Figure 3.5) was used for calibrating and validating the SWAT model. The discharge data, covering a period of eleven years from 2000 to 2010 was obtained from the Ghana Hydrological Services Department and the Water Research Institute (WRI) of Ghana. Bui has a drainage area of about 127,926 km^2.

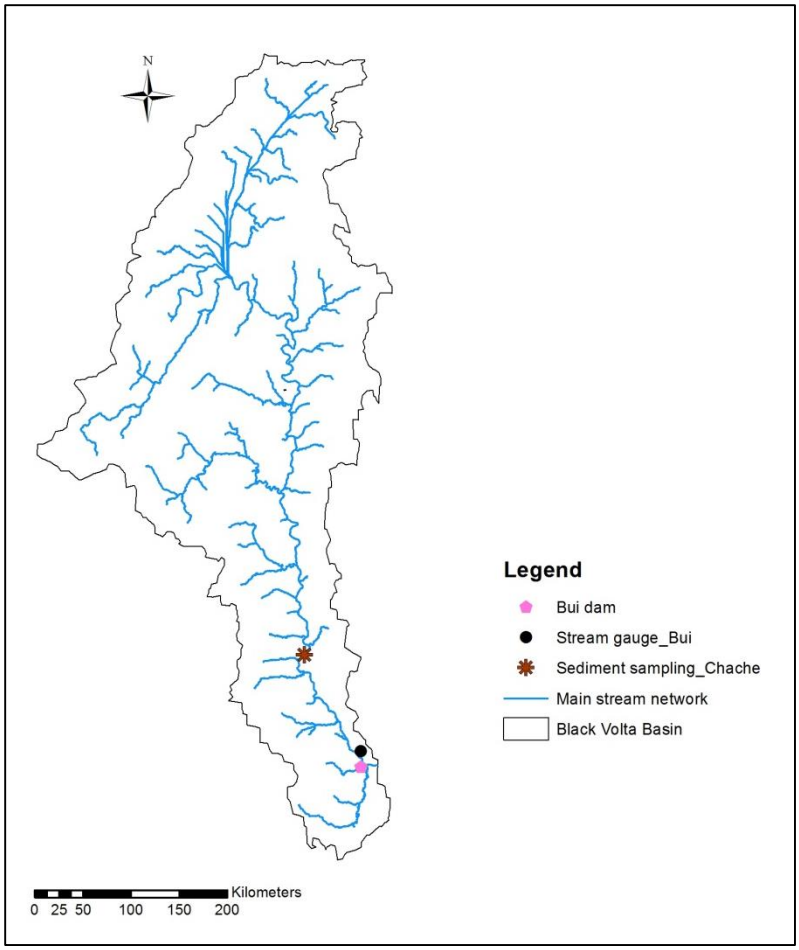

Figure 3.5: Location of sediment sampling site, Bui dam and Bui discharge station in the Black Volta Basin.

3.1.1.6. Reservoir data

The 400-megawatt Bui dam (Figure 3.5) is the main reservoir located on the main course of the Black Volta River. The data required for reservoir water balance modelling in SWAT (shown in Table 3.4) were obtained from literature, Water Research Institute in Ghana and the Bui Dam Authority in Ghana.

Table 3.4: Characteristics of the Bui dam

Parameter	Description	Value	Unit
MORES	Month the reservoir became operational	May	_
IYRES	Year of the simulation the reservoir became operational	2013	_
RES_ESA	Reservoir surface area when the reservoir is filled to the emergency spillway	44000	ha
RES_EVOL	Volume of water needed to fill the reservoir to the emergency spillway	1257000*10E4	m^3
RES_PSA	Reservoir surface area when the reservoir is filled to the principal spillway	35000	ha
RES_PVOL	Volume of water needed to fill the reservoir to the principal spillway	772000*10E4	m^3
RES_VOL	Initial reservoir volume	694800*10E4	m^3

3.1.1.7. Sediment data

Measured data on sediment yield are very limited in developing countries including the riparian countries of the Black Volta River Basin. In Ghana, for example, sediment yield data is limited due to the high cost associated with sampling and lack of logistics (Akrasi, 2011). The problems of lack of continuous suspended sediment concentration records and hence sediment load data can be overcome through development of sediment rating curves (e.g.,Walling 1977). In a number of studies (e.g., Walling, 1977 and Zhang et al., 2012) suspended sediment load have been estimated using sediment rating equations. For this research, sediment yield data for calibrating the SWAT model were generated from sediment rating curve established for the Black Volta Basin at Chache. Chache is located on the lower course of the main BVRB (Figure 3.5) and was chosen for sediment sampling because of the availability of historic flow discharge data for the development of sediment rating curve for the Basin. Sediment sampling for laboratory analysis of sediment

concentration was done once every month from May 2014 to June 2015 using the depth integration procedure (Guy and Norman, 1970). Flow measurements were also taken with the mobile OTT Qliner 2 each time sampling was done. When maintained in a stationary location in a river, the Qliner measures the water depth and velocities of water passing through the vertical axis of the instrument and calculates the average flow velocity of each vertical as well as the partial discharge of a discharge segment in accordance with the mid-section method (Rantz *et al.*, 1982). The final stream discharge is calculated as the total of all sub discharges when the measurement is completed. Details of the operating principles and instructions of the OTT Qliner 2 can be found in the OTT Hydromet 2011 user manual. Following the evaporation method (Tilrem, 1979) suspended sediment concentration was calculated using equation 3.1 below.

$$\mathrm{Cs} = \frac{\text{sediment weight (total weight of sand+clay+silt)}}{\text{smple weight (weight of water+sediment)}} * 10^{6} \quad \text{..... (3.1)}$$

Cs = sediment concentration (ppm, same as mg/l for sediment concentration between 0 - 15,900 parts per million)

The suspended sediment concentration was converted to values of tons/day using equation 3.2 below:

$$Q_s = k * Q_w * C_S \quad \text{..... (3.2)}$$

where *Qs* is sediment discharge (tons/day), Q_w is water discharge (m^3/s), C_S is sediment concentration (mg/l), and *k* is 0.0864

Suspended sediments move at a close velocity with flow velocity (McMahon et al., 2004) making sediment load a function of water discharge. After obtaining the sediment discharge (tons/day),

the sediment rating curve was developed for suspended sediment load (*Load*) and water discharge (*Q*) for Chache (see Annex 3) using equation 3.3.

$$Load = aQ^b \quad \text{(3.3)}$$

where *a* and *b* are empirical parameters.

The resulting sediment rating equation $\boldsymbol{S = 1.1168Q^{1.342}}$ developed for Chache was used together with historic streamflow data to generate historical suspended sediment yield data for the BVRB.

Bedload was estimated as 25% of suspended load using Maddock's (1975) ratios for estimation of bedload (Annex 4). The total sediment yield for Chache was obtained by taking the sum of suspended sediment yield and bedload (Annex 5).

3.1.1.8. Other data

Other data e.g., plant-cover and land use factor, and potential heat unit that were used in setting up the SWAT model for the Black Volta Basin were obtained from literature.

3.1.2. Scenarios data

The scenarios data used for climate change impact assessment in this study were obtained from the CORDEX archives for the West African region. The data included daily precipitation and maximum and minimum temperature series for the 11 climate stations used in this study for the period 1981-2005 (control run) and 2051-2100 (future horizon). The data consisted of projection from 2 RCMs driven by 3 GCMs for two of the IPCC Scenarios, RCP 4.5 and RCP 8.5 (Table 3.5). The choice of RCMs was based on data availability at the beginning of this study. The RCP

4.5 and RCP 8.5 were chosen because they represent the low-end and high-end emission scenarios, respectively.

Table 3.5: Regional Climate models (RCMs) with driving Global Climate Models (GCMs) used in this study (modified from Nikulin et al., 2012)

RCMs	RCA4 (SMHI)	KNMI Regional ClimateModel, (RACMO22T)	RCA4 (SMHI)
Institute	Swedish Meteorological and Hydrological Institute	Koninklijk Netherlands Meteorologisch Instituut (KNMI) Netherlands	Swedish Meteorological and Hydrological Institute
Short name	RCA4	RACMO	RCA4
Resolution	0.44º	0.44 º	0.44 º
Reference	Samuelsson et al. 2011; Kupiainen et al. 2011; Strandberg et al., 2014	van Meijgaard et al. 2008	Samuelsson et al. 2011; Kupiainen et al. 2011; Strandberg et al., 2014
Boundary forcing (GCMs)	MPI-ESM-LR (MPI-M) Stevens et al. 2013	ICHEC-EC-EARTH Hazeleger et al. 2010	CCCma-CanESM2 Chylek et al., 2011

3.2. Materials

As mentioned in section 3.1.2, the data used for the climate change impact assessment were obtained from the CORDEX archives for the West African region and consisted of projection from the RCMs the Rossby Centre (SMHI) regional climate model, RCA4 and the Regional Atmospheric Climate Model (RACMO). The Soil and Water Assessment Tool (SWAT) model was employed in this study for analyzing the impact of climate change and assessing the sensitivity

of land use/land cover change on streamflow and sediment yield of the Black Volta River Basin. The two RCMs and the SWAT model are described in detail in the literature review.

3.3. Methods

3.3.1. Hydrological modelling with SWAT

The processes followed to setup the SWAT model for the Black Volta included watershed delineation, determination of hydrological response units, weather data definition and finally the writing of input tables. The detail of each of the processes is described below.

3.3.1.1. Watershed delineation

The SRTM DEM was used to delineate the BVRB watershed and to analyze the drainage pattern of the land surface in ArcGIS with ArcSWAT extension. The BVRB watershed was divided into 167 sub-basins (Figure 3.6) to allow for capturing of the heterogeneity in the catchment's physical properties.

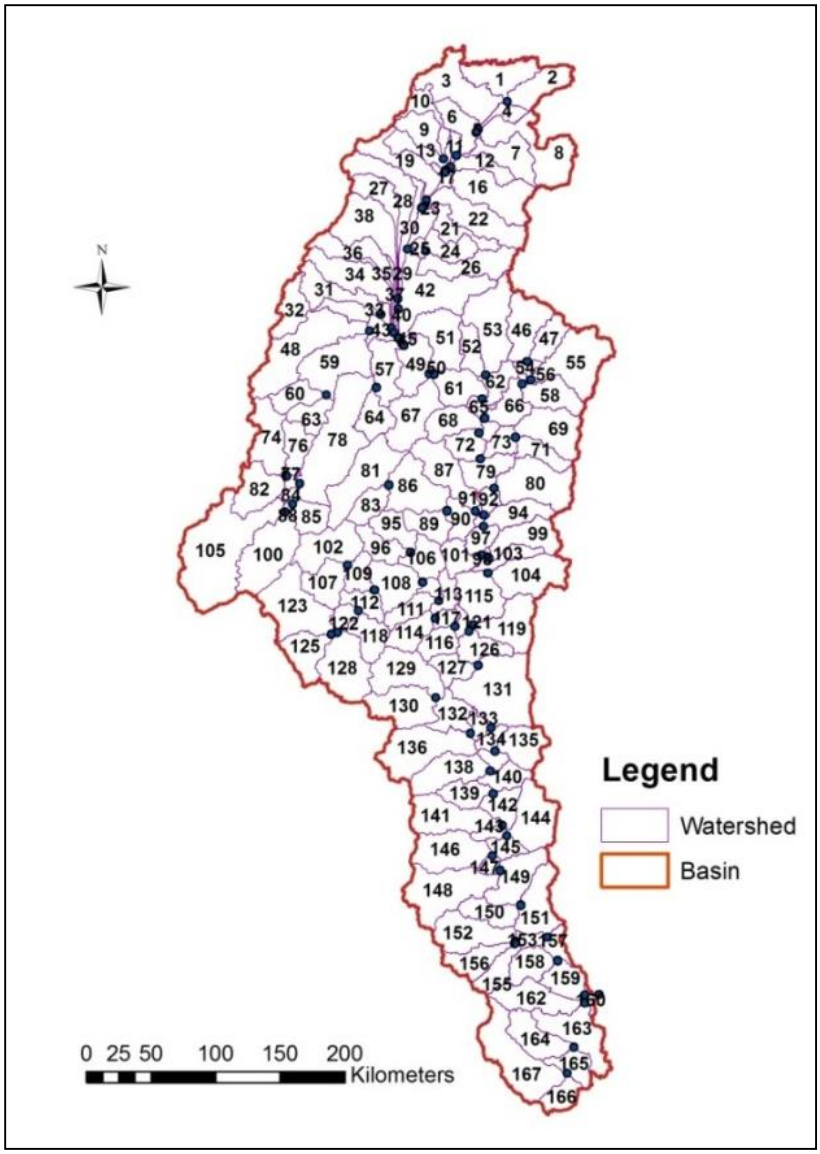

Figure 3.6: SWAT-delineated sub-basins in the Black Volta Basin

3.3.1.2. HRU definition

To account for differences in hydrologic conditions and evapotranspiration, the delineated sub-basins were further divided into 2,539 hydrologic response units (HRUs) based on differences in land use, soil and slope. To achieve this, the modified land use dataset was loaded and reclassified

based on the land use SWAT code assigned to the map. In a similar manner, the soil map was also loaded and reclassified by linking it to the SWAT soil database information. Finally the the slope characteristics were identified based on the DEM. The reclassification processes yielded 7 LULC classes (Table 3.6), 56 soil classes (Annex 6) and 3 slope classes (Figures 3.7 and 3.8). The BVRB is largely flat resulting in over 50% of the watershed falling within the slope class 0-2%. The overlay operation was carried out after the reclassification process.

The final step in the HRU analysis was the definition of the HRU. In defining HRUs, the SWAT model gives the option to have one or multiple HRUs per each sub-basin. For single HRUs per sub-basin, the model uses the dominant land category, soil type and slope class within each watershed for the designation process. For multiple HRUs in a sub-basin the user needs to select a threshold percentage value of land use, soil and slope data that will be used to determine the number and kind of HRUs in each watershed. In this simulation the multiple HRUs per sub-basin was selected. Subsequently, unique HRUs with the following parameter values were created;

- land use percentage (%) over sub-basin area = 5%
- soil class percentage (%) over land use area = 5%
- slope class percentage (%) over soil area = 5%

Table 3.6: Final land use classification of the Black Volta Basin used in the SWAT modelling

Watershed				Area [km^2]	
				135,003.18	
				Area [ha]	%Wat.Area
LANDUSE:	Shrubland	-->	SHRB	1585.91	1.17
	Grassland	-->	GRAS	36542.37	27.07
	Agricultural Land-Generic	-->	AGRL	27273.91	20.2
	Wetlands-Non-Forested	-->	WETN	2396.40	1.78
	Savanna	-->	SAVA	60874.79	45.09
	Water	-->	WATR	2.89	0
	Forest-Evergreen	-->	FRSE	6326.91	4.69

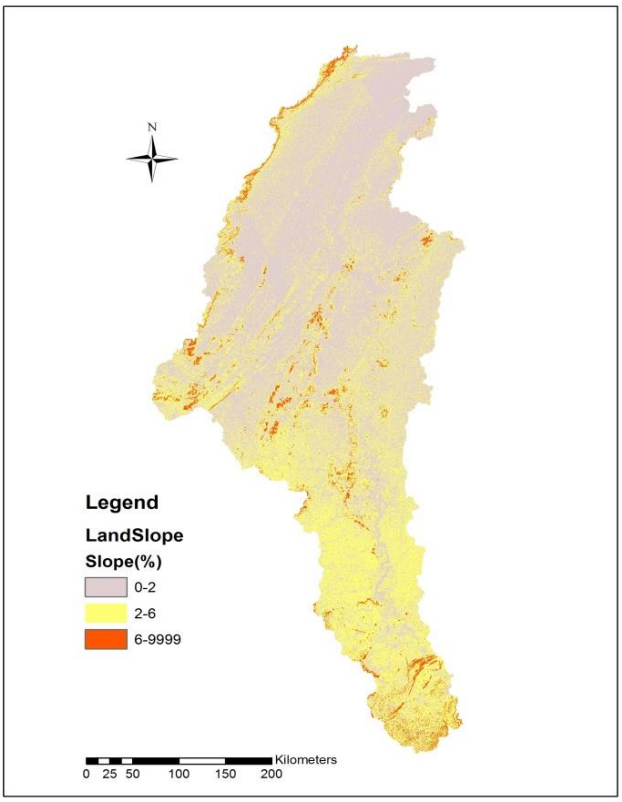

Figure 3.7: SWAT slope classes in the Black Volta River Basin

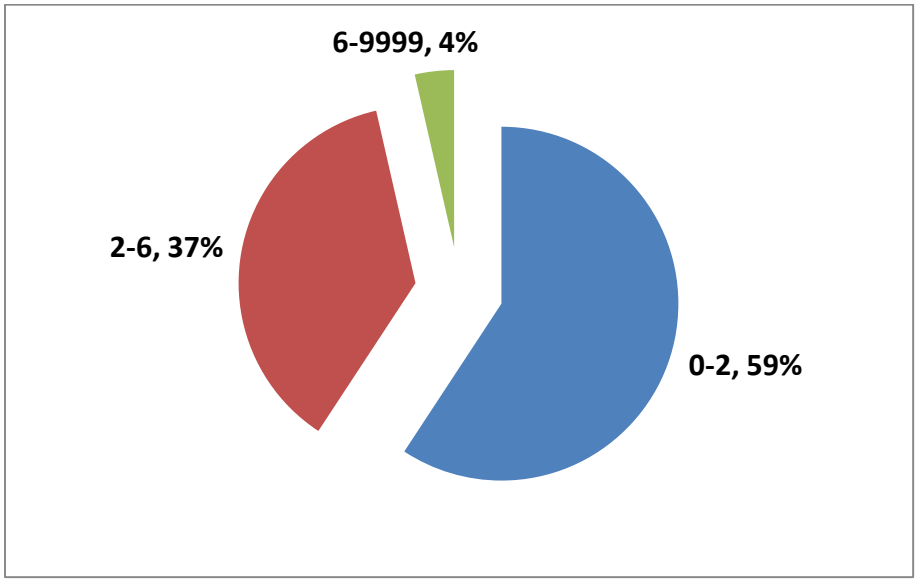

Figure 3.8: Land slope categories in the Black Volta River Basin, in percentage watershed area

3.3.1.3. Model calibration and validation using SUFI-2 in SWAT-CUP

Model calibration involves the adjustment of sensitive parameters of the model so as to mimic the hydrologic and other processes in a basin. The SWAT model has lots of parameters (physical and process) that needed to be adjusted through calibration. During the calibration process, model parameter values are selected and adjusted within recommended ranges and output variables compared with observed data (Arnold et al., 2012b). After model calibration it is important to verify that the model can make accurate simulations in different time period from the period of calibration without further adjustment in the values of the model parameters (Refsgaard, 1997). This verification process is termed validation. Prior to calibration and validation, sensitivity analysis was done to identify the most sensitive model parameters. Model uncertainty analysis was also undertaken to quantify the uncertainties in the modelling process. The aforementioned processes were achieved using SWAT-CUP (SWAT Calibration Uncertainty Programs: Abbaspour, 2007), which is a program developed at the Swiss Federal Institute of Aquatic Science and Technology (EAWAG) for the calibration of SWAT. Sensitivity analysis, calibration, validation, and uncertainty analysis can be achieved using any of the five algorithms present in the SWAT-CUP program (Abbaspour, 2015). The procedures are the Particle Swarm Optimization-PSO (Eberhart and Kennedy 1995); the Sequential Uncertainty Fitting-SUFI-2 (Abbaspour et al., 2007); the Generalized Likelihood Uncertainty Estimation-GLUE (Beven and Binley, 1992); the Markov Chain Monte Carlo-MCMC (Vrugt et al., 2003) and the Parameter Solution-ParaSol (van Griensven and Meixner, 2006) to SWAT. In this study the SUFI-2 optimization algorithm for model calibration and validation was used since it represents all the sources of uncertainties (Yang et al., 2008). The details of each of the processes are described below. Further details of SWAT model calibration using the SWAT-CUP program can be found in Abbaspour (2015).

3.3.1.4. Model parameter sensitivity analysis

Before model calibration, sensitivity analysis needs to be carried out to determine how model outputs change when model input parameters are changed (Arnold et al., 2012b). Since the SWAT model has a lot of parameters, it is necessary to carry out sensitivity analysis to identify and select the most sensitive parameters for the calibration process. In addition to reducing computation time, sensitivity analysis makes calibration much easier since one is left to deal with a relatively small number of parameters. After pre-selection of parameters sensitive to flow based on literature search and expert knowledge, the "global sensitivity analysis" of the SUFI-2 program was used in identifying the most sensitive parameters and the relative significance of each of the parameters to flow output. A t-test which provides a t-stat summary and p-value helped in ranking the model parameters after the sensitivity analysis. Larger t-stats indicate more sensitivity while smaller P-values indicate higher significance of the parameter to the system and vice-versa. For this study eighteen parameters (shown in Table 3.7) were taken through sensitivity analysis and the 13 most sensitive parameters to flow output used in model calibration.

Table 3.7: Parameters selected for sensitivity analysis with respect to streamflow

No.	Parameter Name	Description
1	R__CH_S2.rte	Average slope of main channel along the channel length (m/m)
2	R__CN2.mgt	SCS runoff curve number
3	R__SHALLST.gw	Initial depth of water in the shallow aquifer (mm)
4	R__SLSUBBSN.hru	Average slope length (m)
5	R__SOL_AWC(..).sol	Available water content of soil layer (mmH_20/mm soil)
6	R__SOL_K(..).sol	Saturated hydraulic conductivity (mm/hr)
7	V__ALPHA_BF.gw	Baseflow alpha factor (days)
8	V__ALPHA_BNK.rte	Baseflow alpha factor for bank storage (days)
9	V__CANMX.hru	Canopy storage (mm)
10	V__CH_K2.rte	Effective hydraulic conductivity in the main channel (mm/hr)
11	V__CH_N2.rte	Manning's "n" value for the main channel
12	V__ESCO.hru	Soil evaporation compensation factor
13	V__GW_DELAY.gw	Groundwater delay (days)
14	V__GW_REVAP.gw	Groundwater revaporation coefficient
15	V__GWQMN.gw	Threshold depth of water in the shallow aquifer required for return flow to occur (mm)
16	V__RCHRG_DP.gw	Deep aquifer percolation fraction
17	V__REVAPMN.gw	Threshold depth of water in the shallow aquifer for "revap" to occur (mm)
18	V_SURLAG.bsn	Surface runoff lag time

Note: 'r__' – indicates relative change in the parameter value which implies multiplying the existing parameter value by 1 plus a given value; 'v__' – indicates replacement by a new value which implies substitution of a parameter by a value from the given range.

3.3.1.5. Calibration and validation of flow and sediment

The model was calibrated on a monthly basis first for discharge and thereafter for sediment (also on a monthly time step) as recommended by Abbaspour (2015). The model calibration for flow was carried out using six years (1995-2000) observed monthly discharge data at Bui, close to the outlet of the modeled basin. A warm-up period of three years (1992-1994) prior to the calibration period was allowed to stabilize the initial soil moisture content. The SUFI-2 program is iterative, with around 200 to 500 simulations recommended per iteration. Parameter ranges were used in

achieving the calibration instead of single parameters. These parameter ranges were implemented in two different ways: (i) multiplying the existing parameter value by 1 plus a given value (represented by r_) and (ii) replacing the existing parameter value by the given value (represented by v_). The calibration process was ended when satisfactory values of the objective function (Nash-Sutcliffe efficiency-NSE), other goodness-of-fit parameters (coefficient of determination – R^2, percent bias – PBIAS, and RMSR observations standard deviation ratio - RSR) and uncertainty parameters (P-factor and R-factor) used in this study were achieved.

After calibrating for streamflow, the model was calibrated for sediment by selecting (based on literature and expert knowledge) and adding 2 parameters that affect only sediment: SPEXP (Channel re-entrained exponent parameter) and SPCON (channel re-entrained linear parameter) to the 13 calibrated runoff parameters. The sediment data also spanned a period of five years (2000 to 2004). A total of 350 simulations resulted in a successful calibration of flow and total sediment yield.

Thereafter the model was validated for flow and sediment yield by using the calibrated model to simulate streamflow and sediment for periods other than those used for the calibration and without any further changes to the model streamflow and sediment parameters. The streamflow was validated with five years (2002-2006) monthly observed discharge data and the sediment yield, three years (2005 to 2007) monthly sediment yield data.

3.3.1.6. Model performance evaluation

As mentioned under section 3.3.1.5, four quantitative statistics were used in evaluating the performance of the SWAT model with respect to streamflow and sediment yields in the calibration and validation periods. These were the NSE (eqn. 3.4), R^2 (eqn. 3.5), PBIAS (eqn. 3.6), and RSR (eqn. 3.7). The four statistics are widely used for the assessment of the performance of the SWAT

model and have been recommended by Singh et al. (2004), Moriasi et al. (2007) and Duan et al. (2009), among others. The NSE is said to be one of the best fit estimators and evaluation methods for monthly comparison in SWAT hydrological studies (Coffey et al., 2004). Moriasi et al. (2007) describes it as a statistic which "indicates how well the plot of observed versus simulated values fits the 1:1 line". It ranges between -∞ and 1.0 with 1 being the optimal NSE value. The R^2 describes the strength between observed and simulated values and range from 0 to 1, with 1 being the optimal value. PBIAS measures the average tendency of simulated data to be either on the higher or lower side of the corresponding observed data (Gupta et al., 1999). Positive PBIAS values represent model underestimation while negative values show overestimation. As such PBIAS values of 0.0 are desired (Gupta et al., 1999). The RSR is computed as the ratio of RMSE and the standard deviation of the observation data (STDEV), with values ranging from zero (zero RMSE means perfect model) to large values (large RMSE means unsatisfactory model).

A summary of the general performance ratings of the quantitative statistics for flow and sediment load on a monthly time step are shown in Table 3.8.

$$\mathrm{NSE} = 1 - \frac{\sum_{i=1}^{N}(O_i - P_i)^2}{\sum_{i=1}^{N}(O_i - \overline{O})^2} \qquad (3.4)$$

$$R^2 = \frac{\sum_{i=1}^{N}\left[(O_i - \overline{O})\,(O_i - \overline{O})\right]^2}{\sum_{i=1}^{N}(O_i - \overline{O})^2 \sum_{i=1}^{N}(O_i - \overline{O})^2} \qquad (3.5)$$

$$PBIAS = \frac{\sum_{i=1}^{N}(O_i - P_i)*(100)}{\sum_{i=1}^{N}(O_i)} \quad (3.6)$$

$$RSR = \frac{RMSE}{STDEV} = \frac{\sqrt{\sum_{i=1}^{N}(O_i - P_i)^2}}{\sqrt{\sum_{i=1}^{N}(O_i - \overline{O})^2}} \quad (3.7)$$

where O_i is the measured data; P_i is the simulated data; $\overline{O}$ is the mean of the measured data; $\overline{P}$ is the mean of the simulated data; and N is the number of compared values.

Table 3.8: General Performance ratings for recommended statistics for flow and sediment load on a monthly time step (Moriasi et al., 2007; Santhi et al., 2001).

Performance rating	RSR	NSE	R^2	PBIAS (%)	
				Streamflow	Sediment
Very good	0.00 ≤ RSR ≤ 0.50	0.75 < NSE ≤ 1.00		PBIAS < ±10	PBIAS < ±15
Good	0.50 < RSR ≤ 0.60	0.65 < NSE ≤ 0.75		±10 ≤ PBIAS < ±15	±15 ≤ PBIAS < ±30
Satisfactory	0.60 < RSR ≤ 0.70	0.50 < NSE ≤ 0.65	>0.6	±15 ≤ PBIAS < ±25	±30 ≤ PBIAS < ±55
Unsatisfactory	RSR > 0.70	NSE ≤ 0.50	<0.6	PBIAS ≥ ±25	PBIAS ≥ ±55

3.3.1.7. Uncertainty analysis

Quantification of model uncertainty is highly necessary in hydrological modelling studies. Experience from modelling studies has shown that proper model calibration and validation reduce errors in model simulations, but does not necessarily guarantee error-free simulations (Moriasi et al., 2007). For this reason, it was necessary to include uncertainty analysis in the model evaluation

of this study. The parameter uncertainty in the SUFI-2 program accounts for all sources of uncertainties including that in the conceptual model, measured data, parameters and in the driving variables. Two important factors, the P- and R-factors (Abbaspour et al., 2004, 2007) were used in measuring uncertainties in the Black Volta SWAT model. The P-factor denotes the percentage of measured data enveloped by a 95% prediction uncertainty (or 95PPU) and measures the ability of a model to capture uncertainties. A P-factor of 1, means 100% bracketing of measured data by the 95PPU which means that all the correct processes have been accounted for. The R-factor gives the thickness of the 95PPU and is a measure of the quality of calibration. It is the average width of the 95PPU divided by the standard deviation of the observed data (Abbaspour, 2015). Ideally, R-factor value should be close to zero (matching with measured data). A simulation which corresponds exactly to measured data will therefore have a P-factor of 1 and an R-factor of 0. Based on how close or far away the P- and R-factors are to the ideal corresponding values, one can judge the goodness of prediction uncertainty and calibration. During calibration attention was paid to the P- and R- factors to ensure a good balance between the two.

3.3.2. Climate downscaling and bias correction

To improve projections of future precipitation and temperature (maximum and minimum) data, each of the RCM data was corrected using the Quantile-Quantile downscaling technique and Quantile-Quantile transformation (Q-Q) (Maraun et al., 2010; Themeßl et al., 2011) to obtain station-specific future climate scenario data with reduced RCM biases for the hydrological impact study. This empirical statistical technique was applied to adjust the statistical distribution of the RCM data to match the statistical distribution of the observed data. The Q-Q transformation procedure was applied on a monthly basis on each of the data set as described by Amadou et al., (2015) and Sarr et al., (2015), as follows;

The historical data set was split into two, one half for calibration and the other half for validation. In order to avoid issues due to non-stationarity in hydrologic time series, the calibration period consisted of every odd year starting from the beginning of the historical period (i.e. years 1, 3, 5, etc.). The performance of the downscaling was tested on even years (years 2, 4, etc.). The daily time series of the month were extracted for both calibration and validation periods from both observation and RCM simulation data.

Two empirical cumulative distribution functions, F_{obs} and F_{RCM} , were then developed. F_{obs} was generated using observations on the calibration period and F_{RCM}, using RCM outputs on the calibration period.Corrected RCM simulations, X_{CORR}, were generated on the validation period and future periods using the transformation: $X_{CORR} = F_{obs}^{-1}\left(F_{RCM}(X_{RCM})\right)$, where X_{RCM} refers to the variable extracted from raw simulated RCM data.

The probability mass function (PMF) of precipitation occurrence (i.e intensity greater than 1mm/day) and probability density function (PDF) of precipitation intensity on wet/rainy days, maximum and minimum temperatures were built. The quantile-quantile transformation was applied to produce improved (corrected) future RCM simulations of a variable if it was noticed that the PDF (or (PMF) of a corrected variable was closer to the PDF of the observations than the PDF (or PMF) of the raw non-corrected variable.

3.3.2.1. Evaluation of model-simulated historical climate of the BVRB

Assessment of the performance of models in simulating historical climate is the first and necessary step for model projections. This is to help establish whether a model is credible enough to be used for climate projections. In this regard, the performance of the individual RCMs in simulating the historical (1981-2005) precipitation and temperature of the BVRB was evaluated. The

performance of the mean of the RCMs was also assessed. The historical period was set from 1981 to 2005 to allow for comparison among the RCMs since some of the RCA4 generated historical data sets (e.g. precipitation) were only until the end of 2005.

3.3.2.2. Multi-model ensemble scenarios

In view of the disagreement in models regarding the trend of change and variability in precipitation over West Africa and indeed the entire continent of Africa (Hewitson and Crane 2006; IPCC-AR4, 2005), several studies (e.g. Owusu and Klutse 2013: Klutse et al., 2014; Panitz et al., 2014; Abiodun et al. 2015 and Endris et al. 2015; Dosio et al., 2015) have recommended the use of multi-model RCM ensemble means for more robust results. Therefore, to account for uncertainties in the projections (especially precipitation), the model scenarios developed included the individual RCM outputs as well as the ensemble mean of the RCMs. Two future time horizons, 2051-2075 representing the late 21st century (also the 2060s) and 2076-2100 representing the end of the 21st century (also the 2080s) were considered. Altogether, sixteen model scenarios for climate change impact assessment were formed (Table 3.9).

Table 3.9: Model scenarios for climate change impact assessment in the Black Volta Basin

Scenario Number	Model Scenarios
1	RACMO22T/ ICHEC-EC-EARTH (RCP4.5/Late 21st century)
2	RACMO22T/ ICHEC-EC-EARTH (RCP4.5/End of 21st century)
3	RACMO22T/ ICHEC-EC-EARTH (RCP8.5/Late 21st century)
4	RACMO22T/ ICHEC-EC-EARTH (RCP8.5/End of 21st century)
5	RCA4/CanESM2 (RCP4.5/Late 21st century)
6	RCA4/CanESM2 (RCP4.5/End of 21st century)
7	RCA4/CanESM2 (RCP8.5/Late 21st century)
8	RCA4/CanESM2 (RCP8.5/End of 21st century)
9	RCA4/MPI-ESM-LR (RCP4.5/Late 21st century)
10	RCA4/MPI-ESM-LR (RCP4.5/End of 21st century)
11	RCA4/MPI-ESM-LR (RCP8.5/Late 21st century)
12	RCA4/MPI-ESM-LR (RCP8.5/End of 21st century)
13	ENSEMBLE (RCP4.5/Late 21st century)
14	ENSEMBLE (RCP4.5/End of 21st century)
15	ENSEMBLE (RCP8.5/Late 21st century)
16	ENSEMBLE (RCP8.5/End of 21st century)

3.3.3. Impact of climate change on temperature and precipitation of the BVRB

The corrected future precipitation and temperature (maximum and minimum) data were used in projecting the future change in precipitation and temperature data using Microsoft Excel software. The Mann-Kendall test (Mann, 1945; Kendall 1975; Gilbert 1987) was used in analyzing the trends of the projected changes while the magnitude (slope) of the trends were estimated using the Sen's slope estimator (Sen, 1968). The details of the Mann-Kendall test and the Sen's slope estimator are presented in Appendix 1A and 1B respectively.

3.3.4. Impact of climate change on flow and sediment yield of the BVRB

The impacts of climate change on the flow and sediment yield of the BVRB was assessed by driving the calibrated and validated SWAT model with the 16 sets of future climate scenarios developed under section 3.3.2.2 and comparing the seasonal trend and annual magnitude of the resulting stream flow and sediment yield with those of the baseline (1984-2010) period. Three years of warm up (1981-1983) was allowed during the model runs.

3.3.5. Sensitivity of streamflow to land use/land cover changes in the Black Volta Basin

3.3.5.1. Land use/land cover change detection analysis

Change detection of LULC of the BVRB was carried out based on the 1990 and 2000 LULC change maps developed for the basin. Using the overlay function in ArcGIS 10.2.2 and Microsoft Excel 2010, the percentage changes in land use/ land cover was calculated for the ten (10) year period.

3.3.5.2. Sensitivity of streamflow to land use/land cover change

Land use/land cover changes play important roles in rainfall-runoff processes (Elfert and Bormann, 2010; Ghaffari et al., 2010). A recent study by Akpoti et al. (2016) showed that increasing urbanization and bare land in the Black Volta River Basin (BVRB) caused an increase in surface runoff and a reduction in groundwater. In order to test the sensitivity of changes in LULC on streamflow of the BVRB, further simulations using the 1990 LULC map were carried out with the calibrated Soil and Water Assessment Tool (SWAT) model after running the model with the 2000 LULC map. For this sensitivity analysis, all the input variables (e.g. rainfall, temperature, soil data) with the exception of the LULC data set remained unchanged. The 1990 LULC dataset was used instead of the 2000 dataset. All the processes, from model set up until model run (section 3.3.1),

also remained as in the case of the 2000 LULC map. After calibrating the SWAT model for the 1990 LULC data, the flow output at Bamboi was compared with that from the 2000 LULC data. The period of analysis was from 1984 to 2010.

4. HYDROLOGICAL MODELLING WITH SWAT

4.1. Introduction

This section presents the results of the hydrological modelling with SWAT. The results of the model sensitivity analysis, calibration and validation are presented discussed.

4.1.1. Model sensitivity analysis

Results of the model sensitivity analysis show that the most sensitive parameter to streamflow in BVRB is the curve number (CN2), followed by threshold depth of water in the shallow aquifer required for return flow to occur (GWQMN), and baseflow alpha factor for bank storage (ALPHA_BNK) (Table 4.1). Canopy storage (CANMX) was the least sensitive of the eighteen (18) model parameters analyzed.

Table 4.1: Global sensitivity analysis of flow parameters of SWAT for the Black Volta Basin

Rank	Parameter Name	t-Stat[1]	P-Value[2]
1	r_CN2.mgt	-13.57	0.05
2	v_GWQMN.gw	13.01	0.05
3	v_ALPHA_BNK.rte	-11.44	0.06
4	v_ REVAPMN.gw	10.68	0.06
5	v_GW_DELAY.gw	8.89	0.07
6	v _RCHRG_DP.gw	-7.22	0.09
7	v_CH_N2.rte	-6.85	0.09
8	v_ESCO.hru	-6.33	0.10
9	r __SHALLST.gw	-5.77	0.11
10	r__SLSUBBSN.hru	5.71	0.11
11	r __SOL_AWC.sol	5.00	0.13
12	r_SOL_K.sol	-4.58	0.14
13	v_ALPHA_BF.gw	3.98	0.16
14	r__CH_S2.rte	3.80	0.16
15	v__ CH_K2.rte	3.11	0.20
16	v__GW_REVAP.gw	1.87	0.31
17	v__SURLAG.hru	-1.60	0.35
18	v__CANMX.hru	-0.29	0.82

[1] t-stat provides the sensitivity measure. The larger the absolute value the more sensitive the parameter.
[2] p-value determines a sensitivity's significance. A value closer to zero indicates more significance.

4.1.2. Calibration and validation results for streamflow and sediment yield

The final parameter value ranges used in SUFI-2 for the calibration and subsequently for validation are presented in Table 4.2. Figure 4.1 presents results of the simulated monthly streamflow with observed data for the calibration and validation periods. Performance assessment via quantitative statistics during the calibration period resulted in R^2 of 0.86, RSR of 0.38 and NSE of 0.85 (Table 4.3), indicating that the model simulated the streamflow with reasonable accuracy. The model was able to replicate the low flow fairly well and captured most of the peak flows. In comparison with the general statistical performance ratings given by Moriasi et al. (2007) and Santhi et al. (2001)

and provided in Table 3.5, the overall discharge calibration results indicates “very good” model performance. The PBIAS value of 8.1% indicates that the model has the tendency to under-predict flows. The flow validation results were generally “satisfactory” (NSE; 0.60, R^2; 0.62, RSR; 0.64, PBIAS; 20.1%). The calibration and validation plots of total sediment yield are presented in Figure 4.2. The PBIAS value of 27.5% obtained during the calibration period shows under-prediction of sediment yield by the model. Overall, the evaluation results (NSE; 0.68, R^2; 0.77 and RSR; 0.57) indicates “good” model performance. The sediment yield validation results (NSE; 0.65, R^2; 0.74, RSR; 0.59 and PBIAS; 39.1) were satisfactory.

Table 4.2. Final parameter value ranges at calibration of discharge and total sediment in the Black Volta River Basin via SUFI-2 of SWAT-CUP

Variable	Parameter name	Parameter value		
		Fitted	Min	Max
FLOW	r_CN2.mgt	-0.120	-0.168	-0.107
	v_GWQMN.gw	1344.085	1261.467	1393.655
	v_ALPHA_BNK.rte	0.6705	0.649	0.683
	v_ REVAPMN.gw	459.941	455.758	462.451
	v_GW_DELAY.gw	483.756	482.813	484.798
	v _RCHRG_DP.gw	0.041	0.040	0.100
	v_CH_N2.rte	0.238	0.202	0.243
	v_ESCO.hru	0.643	0.642	0.653
	r __SHALLST.gw	0.265	0.261	0.267
	r__SLSUBBSN.hru	-0.506	-0.543	-0.506
	r __SOL_AWC.sol	0.542	0.534	0.556
	r_SOL_K.sol	-0.660	-0.685	-0.650
	v_ALPHA_BF.gw	0.373	0.366	0.385
SEDIMENT	v __SPEXP.bsn	1.194	1.192	1.199
	v __SPCON.bsn	0.007	0.007	0.007

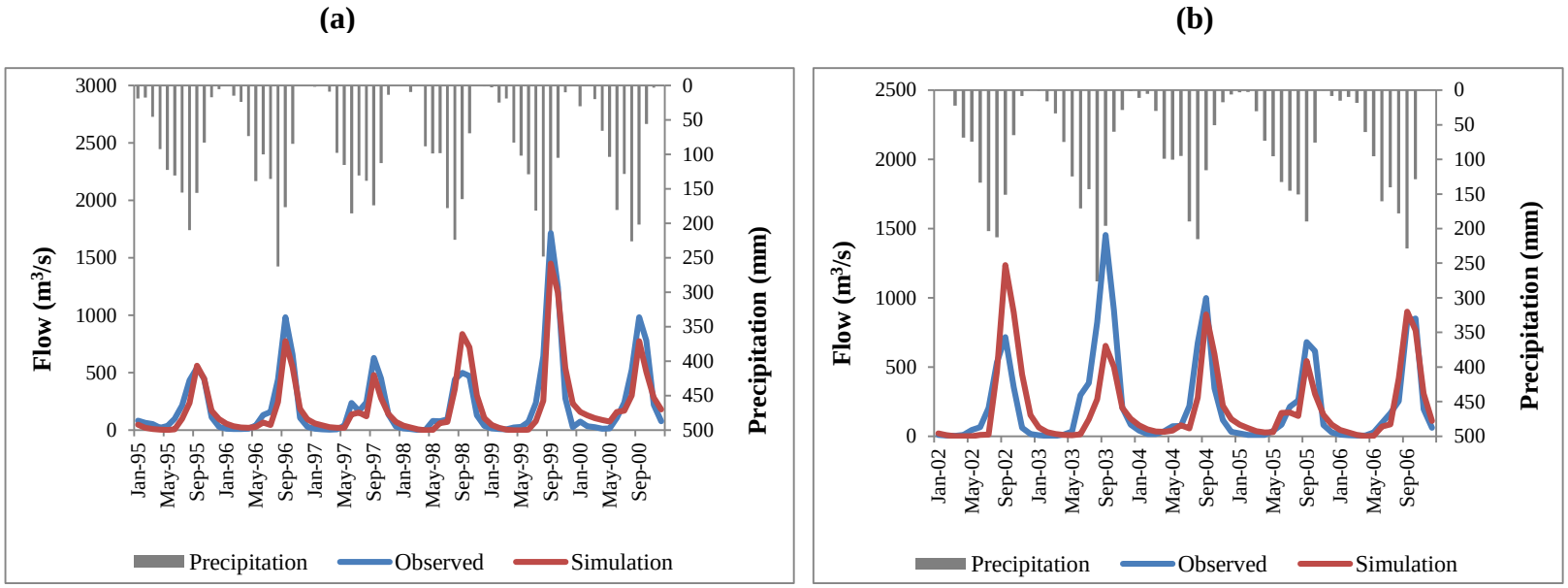

Figure 4.1: Plots of precipitation and comparison of observed and simulated discharges during (a) calibration and (b) validation of SWAT for the Black Volta River Basin

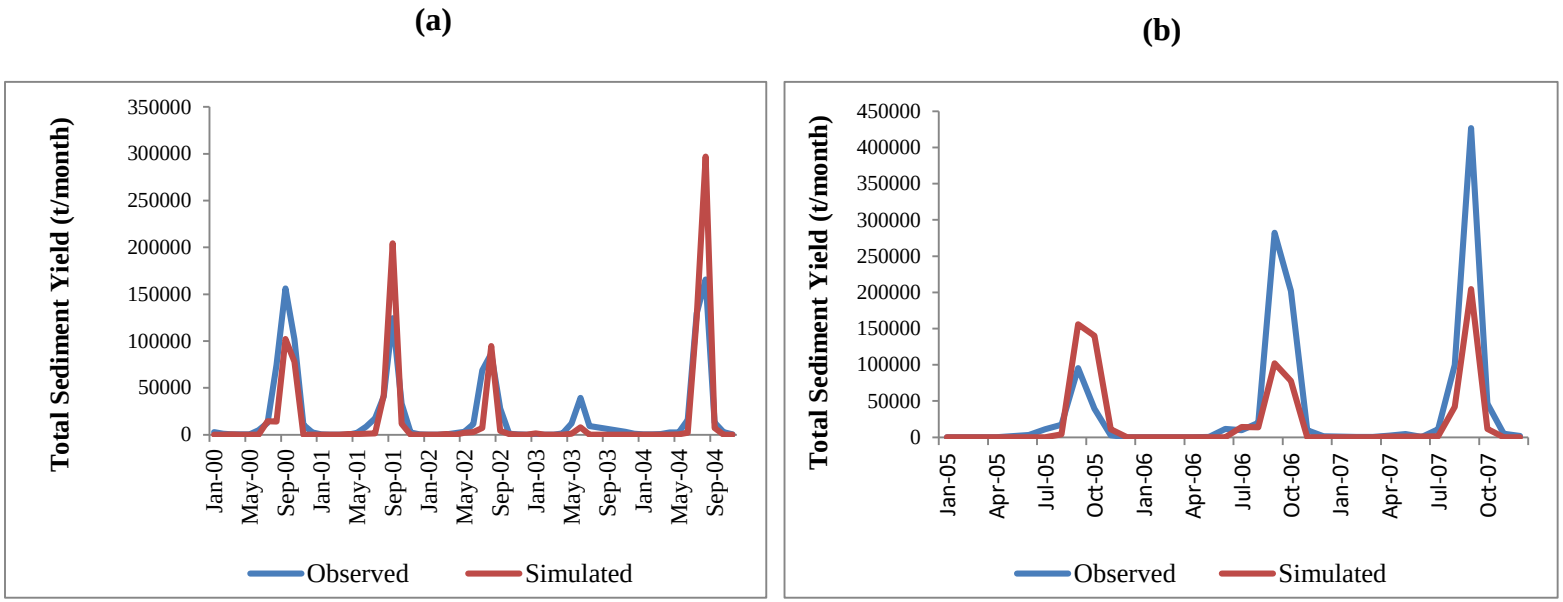

Figure 4.2: Plots of observed and simulated total sediment yield during (a) calibration and (b) validation of SWAT for the Black Volta River Basin

Table 4.3: Results of SWAT calibration and validation for streamflow and sediment yield for the Black Volta River Basin

Component	Simulated period	R^2	RSR	NSE	PBIAS
Runoff	Calibration	0.86	0.38	0.85	8.1
	Validation	0.62	0.64	0.60	20.1
Total Sediment yield	Calibration	0.76	0.57	0.68	27.5
	Validation	0.74	0.59	0.65	39.1

4.1.3. Uncertainty analysis

The uncertainty analysis results for monthly discharge and sediment yield of the study basin during the calibration period are shown in Figure 4.3. Low levels of uncertainty exist in the simulation results as seen from the graphs. For discharge simulations, P-factor values of 0.21 and 0.25 were obtained during the calibration and validation periods respectively. The R-factor values were 0.21 during calibration and 0.19 during validation. This result indicates that the uncertainty measures were better in the discharge validation period than in the calibration period.

For total sediment yield, a low proportion of the observed yields were enveloped within the simulated yields for calibration (11%) and validation (14%) periods. The R-factor value was better (0.10) in the validation period than in the calibration period (0.22). Similar to the discharge results, the sediment yield validation period had better uncertainty measures than the calibration period. In general the uncertainty level in the streamflow calibration was better in comparison with sediment yield calibration.

(a) (b)

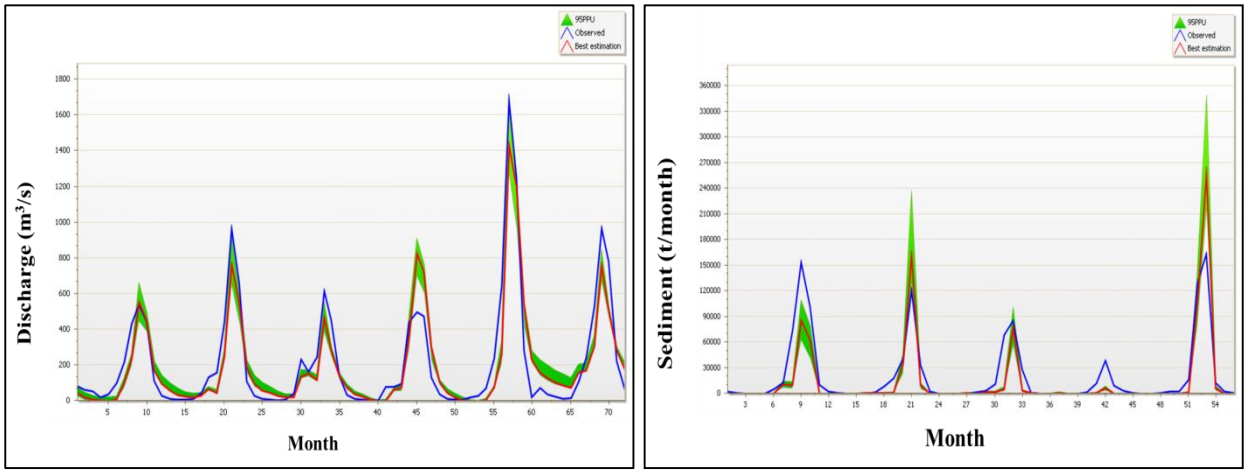

Figure 4.3: Plot of 95PPU for (a) discharge and (b) total sediment yield at calibration in SWAT-CUP

5. CLIMATE DOWNSCALING AND BIAS CORRECTION

5.1. Introduction

This section presents and discusses the results of the downscaling and bias correction of future datasets used in modelling streamflow and sediment yield of the BVRB.

5.1.1. Assessment of model-simulated uncorrected and bias-corrected historical climate of the BVRB

To establish the importance of bias-correction of RCM data for use in impact studies, plots of mean monthly precipitation and temperature of the model-simulated uncorrected, model-simulated bias-corrected and observed data were made for four of the 11 climate stations used in this study (depicted in Figures 5.1 and 5.2) and analyzed to determine which of the two model simulated dataset fits more closely to the observed. The analysis included the computation of annual mean and standard deviation (Table 5.1) as well as probability of exceedence of precipitation thresholds (Figure 5.3). It can be observed that the trend and monthly values of precipitation and temperature computed with the bias-corrected projections fit much better to the observed data than those computed with the uncorrected model output. The use of the uncorrected RCM projection data resulted in an overall overestimation of peak rainfall at Bole. For BoBo-Dioulasso the uncorrected model data underestimated precipitation. The uncorrected output from RACMO22T/ EC-EARTH resulted in an underestimation of maximum temperature at Bui (Figure 5.2). The results of the computed mean, standard deviation and probability of exceedence of precipitation thresholds for the selected stations proved further that the corrected data was much closer to the observed data than the uncorrected data was. The use of uncorrected modeled data for impact assessment may lead to wrong climate change projections. As shown in Figure 5.3b for example, the probability of exceedence of precipitation events between 11mm and 50mm was underestimated by the

uncorrected modeled data for station Bole. The use of such data my lead to the missing of flash floods.

(a) (b)

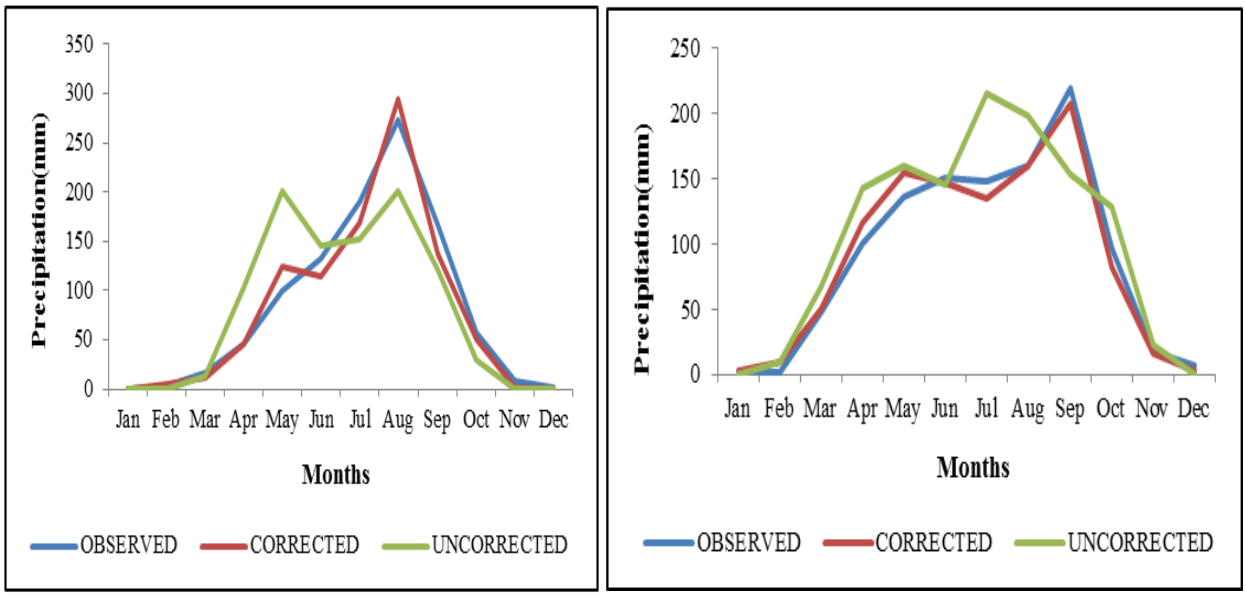

Figure 5.1: Uncorrected and bias-corrected RCM model simulations of historical (1981-2005) precipitation of (a) BoBo-Dioulasso, RCA4/ CanESM2 (b) Bole, RACMO22T/ EC-EARTH

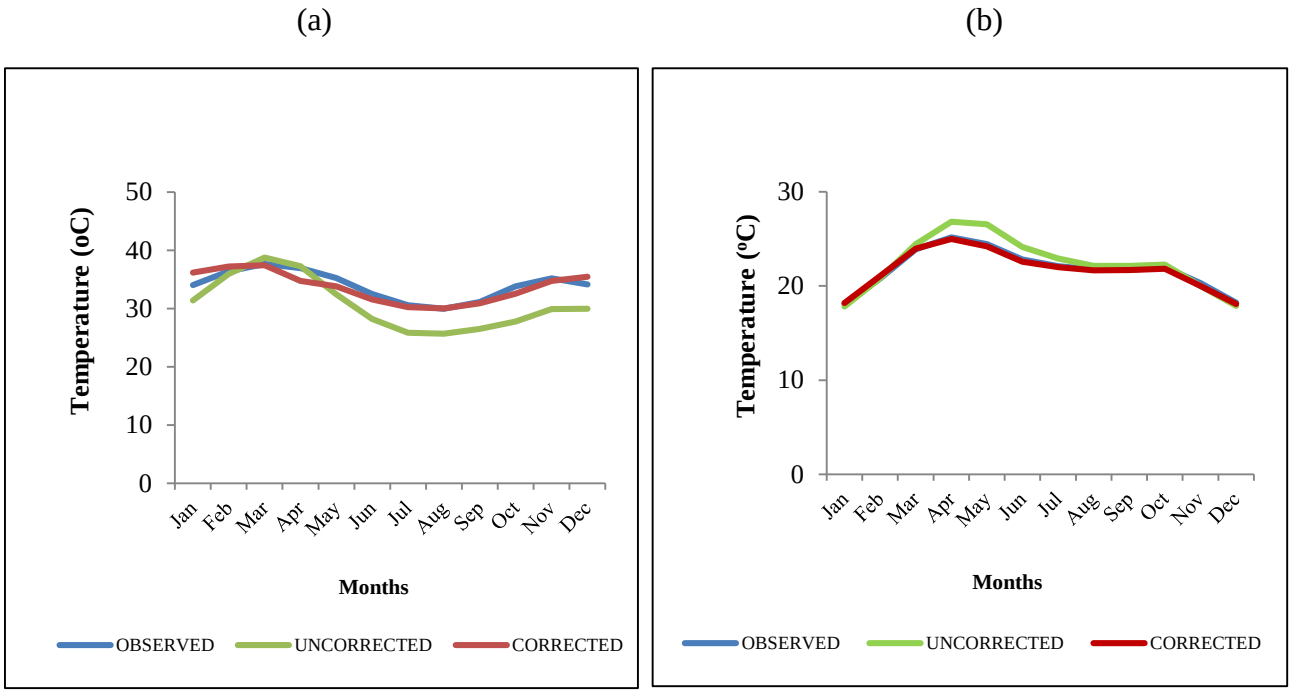

Figure 5.2: Uncorrected and bias-corrected RCM model simulations of historical (1981-2005) maximum and minimum temperature of (a) Bui, RACMO22T/ EC-EARTH (b) Dedougou, RCA4/ CanESM2

Table 5.1: Analysis of uncorrected and bias-corrected RCM model simulations of historical (1981-2005) temperature and precipitation of the Black Volta Basin

Variables	**Climate stations**	**Mean**			**Standard Deviation**		
		Observed	Corrected	Uncorrected	Observed	Corrected	Uncorrected
Temperature	Bui	33.97	33.75	30.81	2.51	2.64	4.49
	Dedougou	21.76	21.68	22.32	2.20	2.17	2.92
Precipitation	Bobo-Dioulasso	2075.73	1985.02	2009.56	2256.24	2278.57	2039.16
	Bole	2267.48	2252.74	2593.02	1853.43	1811.85	1988.75

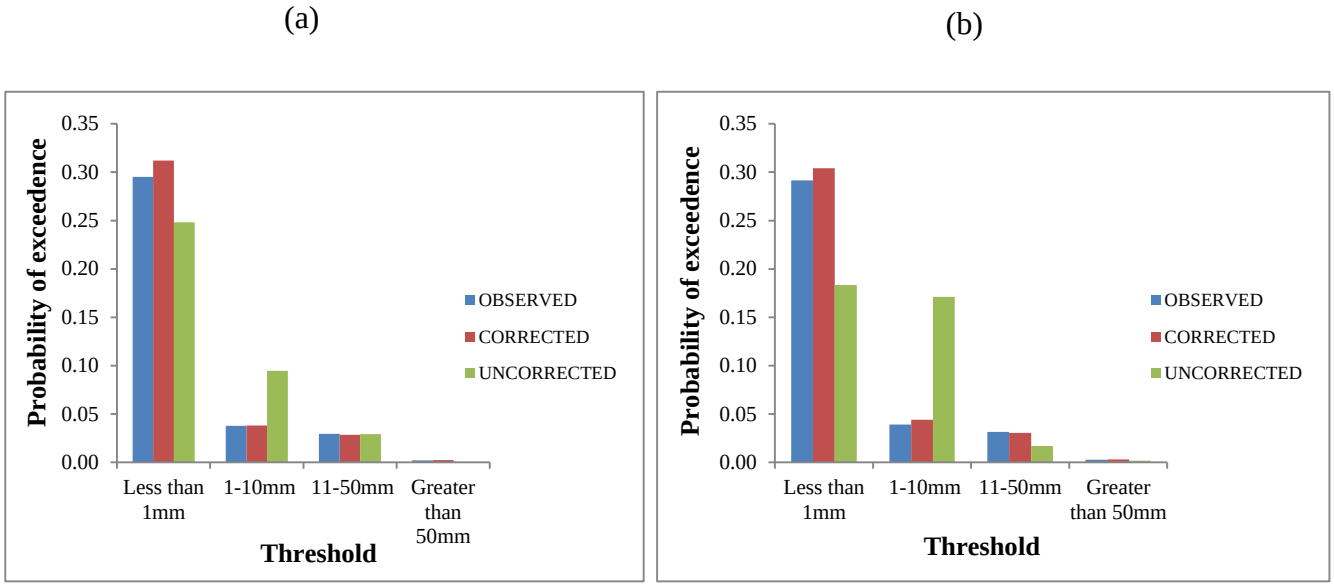

Figure 5.3: Probability of exceedence of precipitation thresholds for the bias-corrected and uncorrected RCM model simulations of historical (1981-2005) precipitation of (a) BoBo-Dioulasso, RCA4/ CanESM2 (b) Bole, RACMO22T/ EC-EARTH

5.2. Evaluation of RCM performance in simulating of historical climate of the BVRB

Results of the historical simulation of precipitation over the BVRB by the 3RCM/GCM pairs and their ensemble mean are presented in Figure 5.4. The intra-annual precipitation plots show that the RCMs RCA4/MPI-ESM-LR and RACMO22T/ ICHEC-EC-EARTH replicated quite well the precipitation pattern of the basin, capturing the beginning of the rainfall months (April-June; AMJ) as well as the wet season (July-September; JAS). Unlike the other 2 models, RCA4/CanESM2 did not capture the period May-July very well, and overestimated the rainfall amount for most parts of the wet period (May-September; MJJAS). In mid-September and during the wet-dry transition (October-December; OND) the model underestimated rainfall amounts. Since simulations by the RCA4/MPI-ESM-LR performed quite well, the biases shown by RCA4/CanESM2 can be linked to biases inherited through the lateral boundary conditions of the driving GCM (Hong and Kanamitsu 2014) CanESM2.The simulated precipitation by the mean of the RCMs fitted much better to the observed than that by the individual models. This good performance may be attributed

to the counterbalancing of opposite-signed biases in the individual models (Nikulin et. al., 2012). Several studies (e.g. Diallo et. al., 2012; Nikulin et. al., 2012; Paeth et. al., 2011) have reported similar results of best performance by multi-model ensemble means. Historical temperature simulations by the RCMs are displayed in Figure 5.5. Unlike the biases exhibited during rainfall simulation, the RCMs simulated the historical tmax and tmin of the basin very well, capturing the trends and peaks. The RCM RACMO22T/ICHEC-EC-EARTH slightly overestimated the average maximum temperature for the months of February and August-September (Figure 5.5).

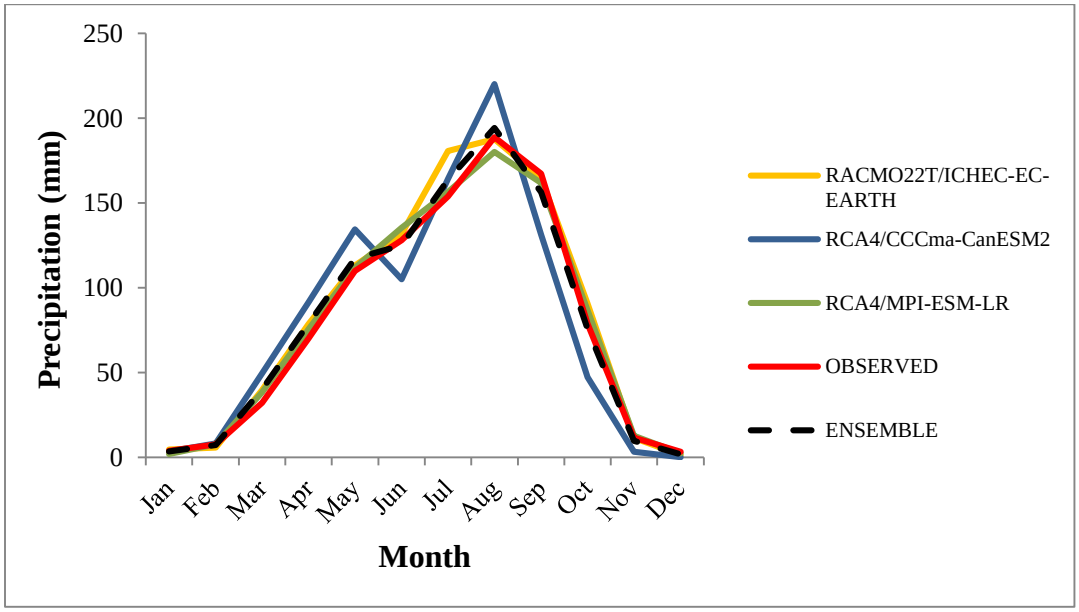

Figure 5.4: Observed and simulated intra-annual precipitation over the Black Volta River Basin from 1981 to 2005

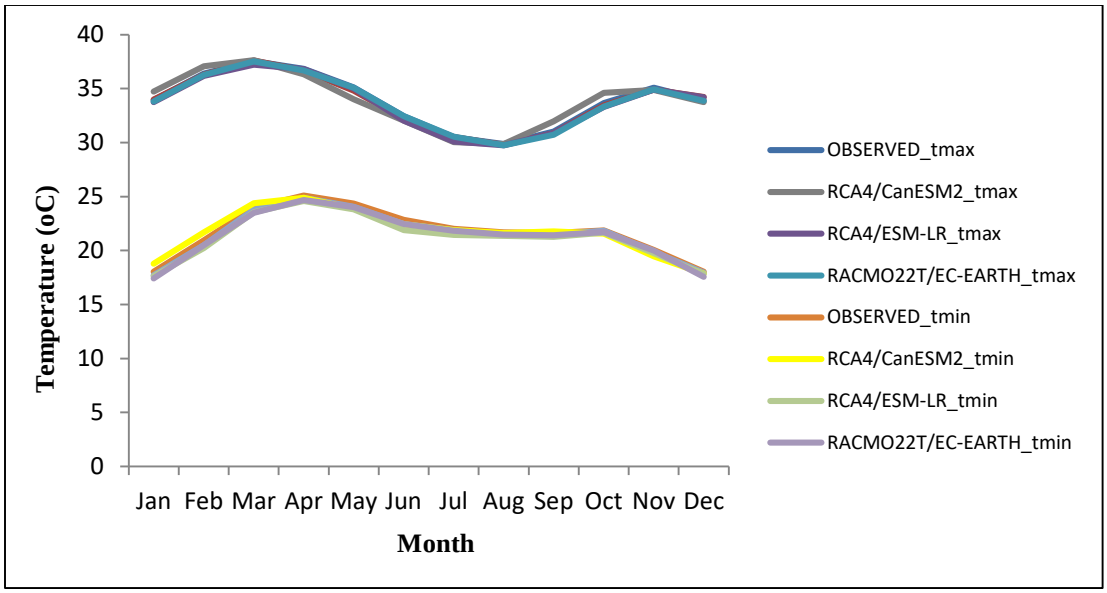

Figure 5.5: Observed and simulated intra-annual maximum and minimum temperature (tmax and tmin respectively) over the Black Volta River Basin from 1981–2005

6. IMPACT OF CLIMATE CHANGE ON PRECIPITATION AND TEMPERATURE OVER THE BVRB

6.1. Introduction

The results of the impact of climate change on precipitation and temperature over the basin are presented and discussed in this chapter. The time periods considered are the late (2051-2075) and end (2076-2100) of the 21st century.

6.1.1. Projected changes in precipitation over the BVRB

The analysis of average annual precipitation over the basin for the late- and end of the 21st century showed high level of uncertainties, with mixed signals of increases and decreases in precipitation amounts across the models (Table 6.1). Relative to the baseline, mean annual precipitation for the late 21st century ranged between -16% and +6%, with a mean of -2% under the RCP4.5 scenario and between -27% and +14%, with a mean of -1% under the RCP8.5 scenario. The end of the 21st century projection showed precipitation changes of between -23% and +2%, with a mean of -7% under the RCP4.5 scenario. The high emission RCP8.5 scenario projects changes ranging between -33% and +13%, with a mean of -4%. From the results, it is established that the uncertainty in the projections increases with increasing RCP forcing and increasing time frames. Similar observations were made by Sylla *et al*. (2016).

Figure 6.1 and 6.2 show the projected changes in intra-annual precipitation over the BVRB for the late and end of 21st century, respectively. As shown in both graphs (6.1a and 6.1b), future rainfall projections by the models show high variability consistent with findings for the West African region reported in the IPCC 5th Assessment report (IPCC, 2013). The variability is mostly pronounced during the wet season. Precipitation amount for the month of July for example is projected to range between +51mm and -16mm under the RCP 4.5 scenario and between +81mm and -30mm under the RCP8.5 scenario in the 2060s. From the months of October through

December however, the variability is highly reduced, especially under the RCP4.5 scenario. The end of the 21st century rainfall projections also shows substantial variability, in this case especially in the months of February through September, which reduces from October through December. Changes in precipitation for the dry (January-March) and wet (August-October) seasons are presented in Figures 6.3 and 6.4. In the late 21st century, the ensemble runs project a change in the range of +6% to -35% in the dry season precipitation, with a mean change of 11% for the RCP4.5 scenario. The change in wet season precipitation is projected to range from +4% to -10%, with a mean of -3%. Under the RCP8.5 scenario, the change in dry and wet season precipitations are projected to range from +22% to -67%, with a mean of -26%, and +9% to -16%, with a mean of -1%. Similarly, the dry and wet season precipitations over the basin for the end of the 21st century are projected to range between +20% and -48%, with a mean of -11% and from -2% to -16%, with a mean of -8% for the RCP4.5 scenario. The high emission RCP8.5 scenario projections show a rate of change in dry season precipitation ranging from +48% and -68%, with a mean of -18% while for the wet season the projected changes are between +16% and -23%. The high variability in the projections across the models and the opposing change in signals are indications of uncertainty surrounding precipitation projections in the basin. Whereas a decrease in precipitation over the region may cause droughts, affect agriculture development and cause a decline in hydropower generation, increases in precipitation may cause floods in the basin.

Table 6.1: Projected changes in precipitation for the late and end of 21st century in the Black Volta River Basin under RCPs 4.5 and 8.5

RCMs	Baseline (1981-2010) observed mean value (mm)	Late-Century (2051-2075)				End-of-Century (2076-2100)			
		RCP4.5		RCP8.5		RCP4.5		RCP8.5	
		Ave (mm)	% change	Ave (mm)	% change	Ave (mm)	% change	Ave (mm)	% change
RACMO22T/ ICHEC-EC-EARTH	999.48	1064.12	6.47	1091.52	9.21	999.37	-0.01	1126.88	12.75
RCA4/MPI-ESM-LR		1050.77	5. 13	1136.19	13.68	1021.95	2.25	1094.23	9.48
RCA4/ CCCma-CanESM2		836.55	-16.30	728.64	-27. 10	767.69	-23.19	665.25	-33.44
ENSEMBLE		983.81	-1.57	985.45	-1.40	929.67	-6.98	926.12	-3.74

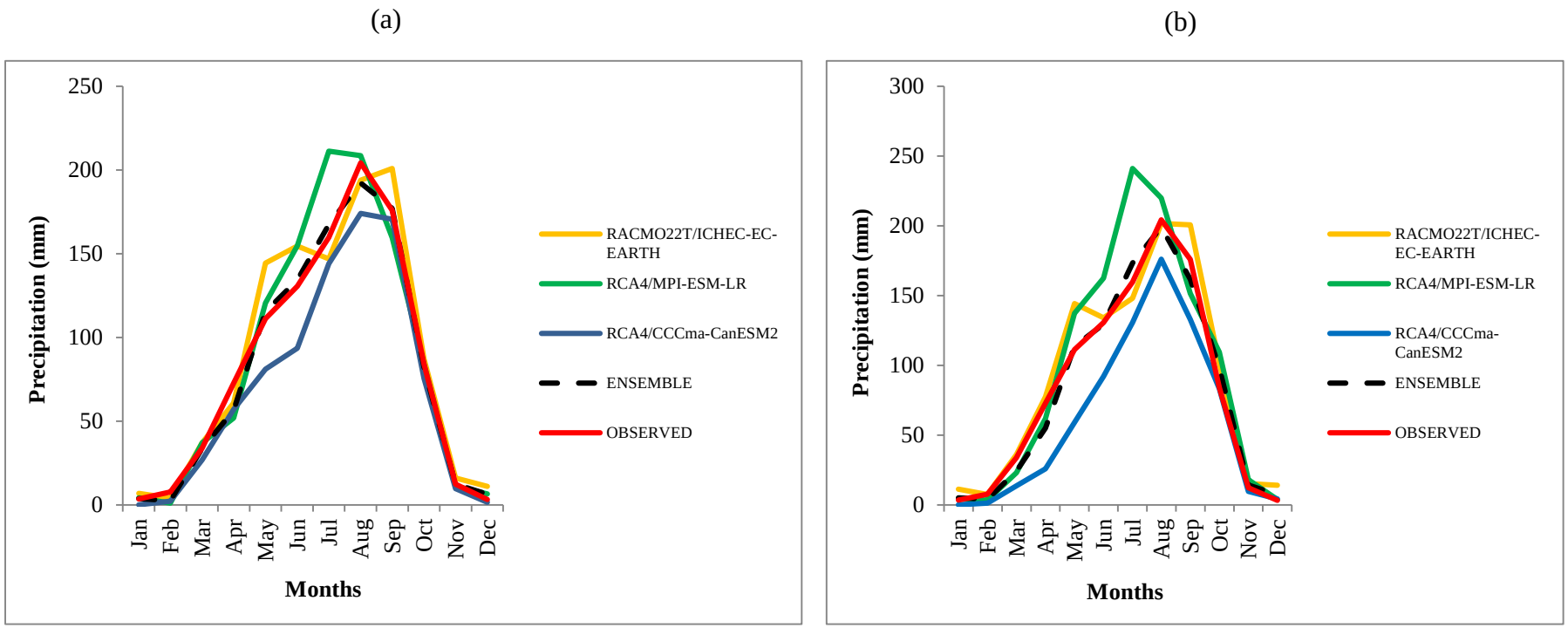

Figure 6.1: Observed and projected intra-annual precipitation under (a) RCP4.5 and (b) RCP8.5 for the 2060s (2051-2075)

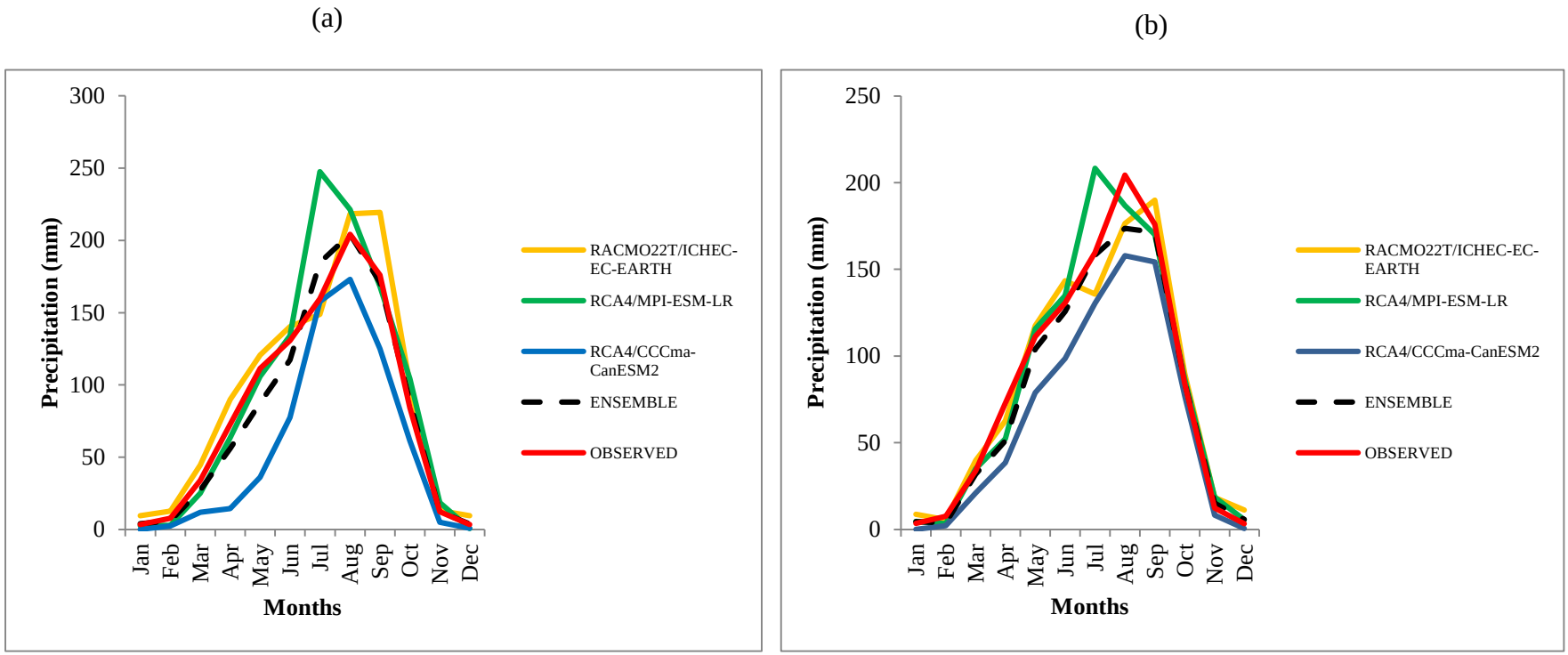

Figure 6.2: Observed and projected intra-annual precipitation under (a) RCP4.5 and (b) RCP8.5 for the 2080s (2076-2100)

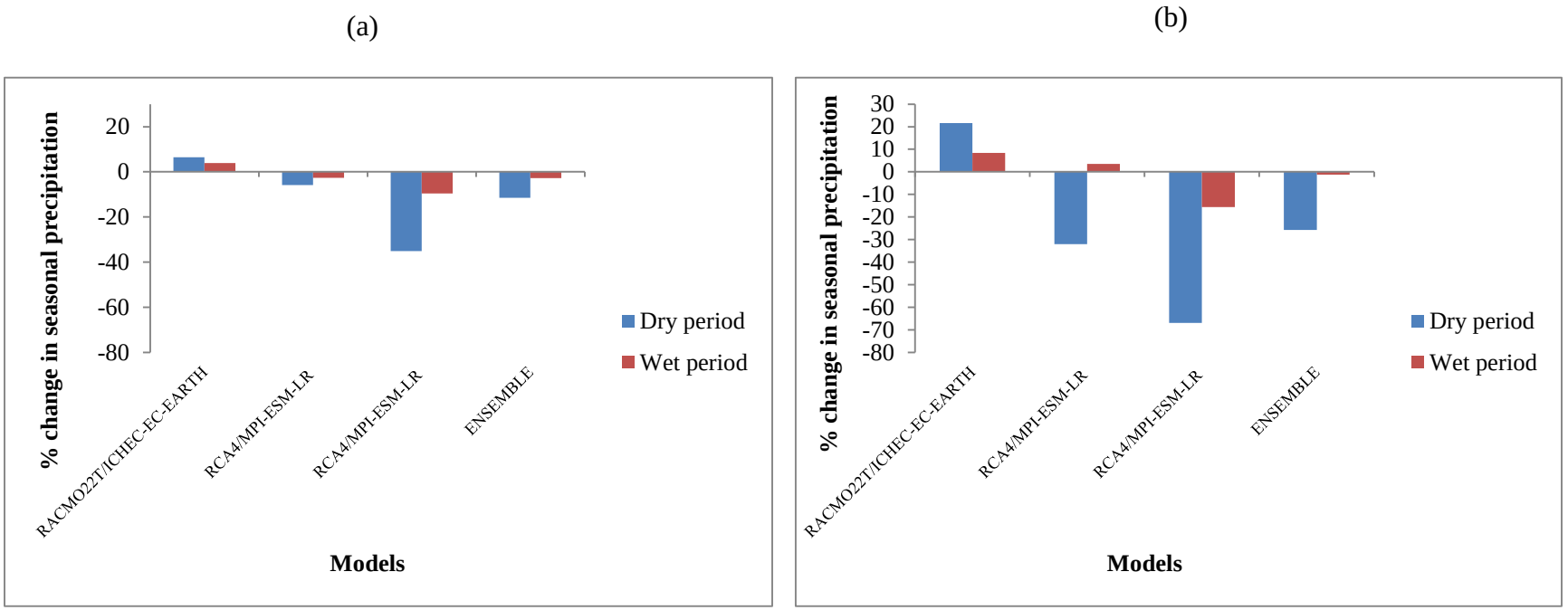

Figure 6.3: Changes in mean seasonal precipitation for the 2060s (2051-2071) under (a) RCP4.5 and (b) RCP8.5 scenarios, relative to the baseline (1981-2010).

(a)

(b)

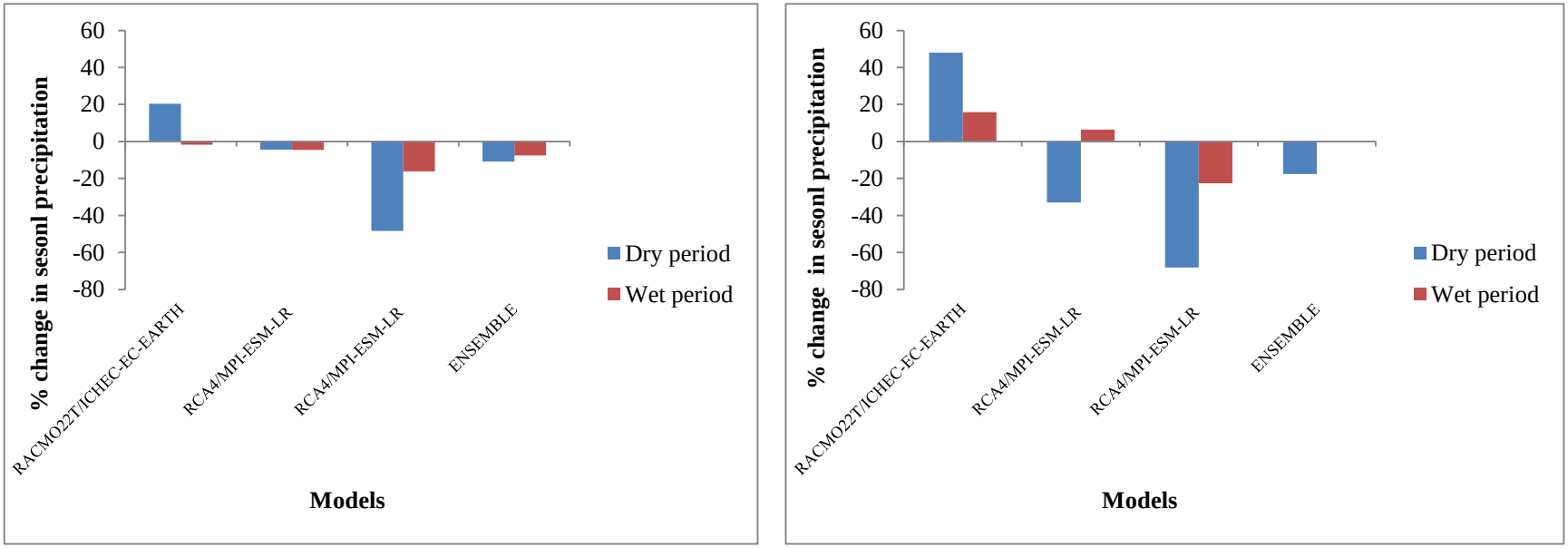

Figure 6.4: Changes in mean seasonal precipitation for the 2080s under (a) RCP4.5 and (b) RCP8.5 scenarios, relative to the baseline (1981-2010).

6.2. Projected changes in temperature over the BVRB

Consistent with the latest IPCC (2013) report, results of the temperature projections for the BVRB (Table 6.2) indicate a warmer climate in the late- and end of the 21st century under both RCP scenarios, relative to the baseline. The projected increase in temperature by all the ensemble models as well as from the mean of the ensemble is statistically significant at the 5% confidence level. As Table 6.2 shows, the magnitude of projected increase in mean temperature over the basin is greater in the 2080s compared to the 2060s. As expected, the increase in temperature is higher in the RCP8.5 scenario than in the RCP4.5 scenario. Possible rise in mean temperature for the late and end of the 21st century under the two RCP scenarios ranges between 2.0^{o}C (RCP4.5) and 3.7^{o}C (RCP8.5), in line with the projected range for West Africa (Sylla et al., 2016).

6.3. Trends in projected annual precipitation and mean temperature

The Man-Kendall trend test showed increases and decreases in future precipitation over the basin (Table 6.3) with majority of the trends (about 67%) being in the positive direction. The projected trend ranges from a decrease of 5.5mm/year to an increase of 3.6mm/year for the RCP4.5 scenario in the late century period. For the RCP8.5 scenario, the trend ranges from a decrease of 2.7mm/year to an increase of 8.6mm/year. The end of the century projected trend ranges from a decline of 3mm/year to an increase of 4.9mm/year under the RCP4.5 and from a decline of 2.7mm/year to an increase of 8.6mm/year under the RCP8.5 scenario. All the trends were however statistically insignificant at the 5% level of significance. Unlike temperature, precipitation projection in the West African Region is in general associated with higher uncertainties (Rowell 2012; Orlowsky and Seneviratne 2012). Trend analysis of temperature, revealed statistically significant (5% level of significance) increases in agreement with the IPCC (2013) report. For the late century increase in trends up to 0.03^{o}C/year is projected by both RCP4.5 and RCP8.5 scenarios. The projected trend

for the end of the century ranges from a decrease 0f 0.01^{o}C/year to an increase of 0.02^{o}C/year for the RCP4.5 scenario and from 0.02^{o}C/year to 0.06 ^{o}C/year for the RCP8.5 scenario. The decreasing trends are however not significant at the 5% level as shown in Table 6.4.

Table 6.2: Projected changes in temperature (°C) for the late and end of 21st century in the Black Volta River Basin under RCPs 4.5 and 8.5

RCMs	Baseline (1981-2010) Observed mean values	2051-2075				2076-2100			
		RCP4.5		RCP8.5		RCP4.5		RCP8.5	
	Tmean (°C)	Tmean (°C)		Tmean (°C)		Tmean (°C)		Tmean (°C)	
		Ave	Change	Ave	Change	Ave	Change	Ave	Change
RACMO22T/ICHEC-EC-EARTH	27.9	30.0	2.1	30.7	2.8	30.2	2.3	31.4	3.5
RCA4/MPI-ESM-LR		29.9	2.0	30.6	2.7	30.1	2.2	31.4	3.5
RCA4/CCCma-CanESM2		30.2	2.3	30.9	3.0	30.5	2.6	31.6	3.7
ENSEMBLE		30.0	2.1	30.7	2.8	30.2	2.3	31.4	3.5

Table6.3 Results of the Mann-Kendall test for annual precipitation (mm) for the late and end of 21st century in the Black Volta River Basin under RCPs 4.5 and 8.5

Model runs	Mann-Kendall Statistic (S)	Sen's slope	p-value	Trend
RACMO22T/ICHEC-EC-EARTH (RCP4.5/2060s)	-50.00	-5.53	0.26	Not significant
RACMO22T/ICHEC-EC-EARTH (RCP4.5/2080s)	-46.00	-2.96	0.30	Not significant
RACMO22T/ICHEC-EC-EARTH (RCP8.5/2060s)	18.00	2.53	0.70	Not significant
RACMO22T/ICHEC-EC-EARTH (RCP8.5/2080s)	18.00	2.54	0.70	Not significant
RCA4/CanESM2 (RCP4.5/2060s)	18.00	1.54	0.70	Not significant
RCA4/CanESM2 (RCP4.5/2080s)	42.00	4.90	0.34	Not significant
RCA4/CanESM2 (RCP8.5/2060s)	74.00	8.56	0.09	Not significant
RCA4/CanESM2 (RCP8.5/2080s)	74.00	8.56	0.09	Not significant
RCA4/MPI-ESM-LR (RCP4.5/2060s)	28.00	3.55	0.53	Not significant
RCA4/MPI-ESM-LR (RCP4.5/2080s)	12.00	1.86	0.80	Not significant
RCA4/MPI-ESM-LR (RCP8.5/2060s)	-28.00	-2.67	0.53	Not significant
RCA4/MPI-ESM-LR (RCP8.5/2080s)	-26.00	-2.67	0.56	Not significant

Table 6.4 Results of the Mann-Kendall test for mean annual temperature (°C) for the late and end of 21st century in the Black Volta River Basin under RCPs 4.5 and 8.5

Model runs	Mann-Kendall Statistic (S)	Sen's slope	P-value	Trend
RACMO22T/ICHEC-EC-EARTH (RCP4.5/2060s)	104.00	0.03	0.02	Significant increase
RACMO22T/ICHEC-EC-EARTH (RCP4.5/2080s)	108.00	0.02	0.01	Significant increase
RACMO22T/ICHEC-EC-EARTH (RCP8.5/2060s)	152.00	0.03	0.00	Significant increase
RACMO22T/ICHEC-EC-EARTH (RCP8.5/2080s)	190.00	0.06	< 0.00	Significant increase
RCA4/CanESM2 (RCP4.5/2060s)	-4.00	-0.00	0.94	Not significant
RCA4/CanESM2 (RCP4.5/2080s)	-44.00	-0.01	0.32	Not significant
RCA4/CanESM2 (RCP8.5/2060s)	130.00	0.02	0.00	Significant increase
RCA4/CanESM2 (RCP8.5/2080s)	132.00	0.02	0.00	Significant increase
RCA4/MPI-ESM-LR (RCP4.5/2060s)	26.00	0.00	0.56	Not significant
RCA4/MPI-ESM-LR (RCP4.5/2080s)	-28.00	-0.01	0.53	Not significant
RCA4/MPI-ESM-LR (RCP8.5/2060s)	164.00	0.02	0.00	Significant increase
RCA4/MPI-ESM-LR (RCP8.5/2080s)	148.00	0.03	0.00	Significant increase

7. PROJECTED IMPACT OF CLIMATE CHANGE ON STREAMFLOW AND SEDIMENT YIELD IN THE BVRB

7.1. Introduction

This chapter discusses the projected changes in flow and sediment yield in the basin due to the impact of climate change.

7.1.1. Impact of climate change on flow and sediment yield

The results of the seasonal change in streamflow and total sediment yield in the Black Volta Basin during the late- and end of the 21st century are presented in Figures 7.1 - 7.4. Relative to the baseline, the model scenarios projected an increase in flow and sediment yield during the dry period for the 2060s under RCP45 scenario as shown in Figure 7. 1a. The increase in flow ranged between +35% and +45% with a mean of +39% while that of sediment ranged between +51% and +120% with a mean of +85%. For the wet period, the same pattern of general increase in flow and sediment yield was recorded (Figure 7.1b). The range of change in flow was between +28% and +37% with a mean of +35% while that for sediment yield ranged between +113% and +195% with a mean of 143%. Under the high emission RCP8.5 scenario, all the models again projected increases in flow (up to +163%) and sediment yield (+704%) for both dry and wet period. The increase dry period flow ranged between +64% and +163% with a mean of +113% and that of sediment between +169% and +704% with a mean of +473%. For the wet period, the flow increase ranged between +35% and +146% with a mean of +80% while the sediment increase ranged between +179% and +365% with a mean of 279%. The end of the 21st century projection of streamflow and sediment yield for the RCP 4.5 and RCP 8.5 scenarios also showed increases (Figure 7.3a and b). The only exception to this pattern was a projected decrease in wet period flow with increasing sediment yield by the RACMO22T/ICHEC-EC-EARTH. This results of decrease

in flow with increase in sediment yields is similar to the findings of Phan et al. (2011) and Shrestha et al. (2013). Decrease in flows with corresponding increase in sediment yield in river basins can sometimes occur with precipitation decrease and temperature increase (Shrestha et al. 2013). According to Zhu et al. (2008) and Li et al. (2011), increase in temperature with decreasing precipitation reduces plant growth, exposes the soil surface and results in increasing erosion rates and sediment yields. Under RCP8.5 scenario, all the models projected increases in both flow and sediment during the dry and wet periods. The increase in flow across the models was projected to reach +309% (RCA4/CCCma/CanESM2) and 229% (RCA4/CCCma/CanESM2) compared to the historical value, for the dry and wet periods respectively. The projected increase in sediment was between approximately 112% and 750% (Figure 7.4 a and b). High sediment yields following increases in streamflow in river basins can occur from intense precipitation events, erosion and scouring at river banks. The banks of the BVB are mostly sandy and might have contributed to the high sediment yields values obtained. In general, the seasonal cycle of the sediment yield followed that of flow, with increasing flows resulting in increasing sediment yield.

The results of the impact of climate change on the mean annual flow and sediment yield are shown in Table 7.1. Relative to the baseline period, the change is projected to range between +40% and +42% with a mean +41% of for flow and between +100% and +143% with a mean of +139% for sediment yield during the late 21st century under the RCP4.5 scenario. By the end of the 21st century, the change in flow is projected to range between -6% and +78% with a mean of +22% while sediment yield will range from approximately 100% up to about 216% with a mean of +182%. Under the high emission RCP8.5 scenario, the projections showed that the change in flow during the late century period will range between +48% and up to +148% with a mean of +95% across the models. For sediment yield the projected change was from +249% to +335% with a

mean of +285. The end of century projections of flow ranged between +69% and up to +243% with a mean of +130% while that of total sediment ranged between +358% and 412% with a mean of +368% across models under this high scenario. In general, the trend analysis results of streamflow and sediment yield (Table 7.2) indicated statistically significant increase ($p<0.05$) in both streamflow and sediment yield under both emission scenarios during the late - and end of the - 21st century. Increase in streamflow my results in floods in the basin region and thereby affect livelihoods and food security. Sediment load increase in the basin may increase the turbidity of the river and cause loss of reservoir storage (Walling, 2008).

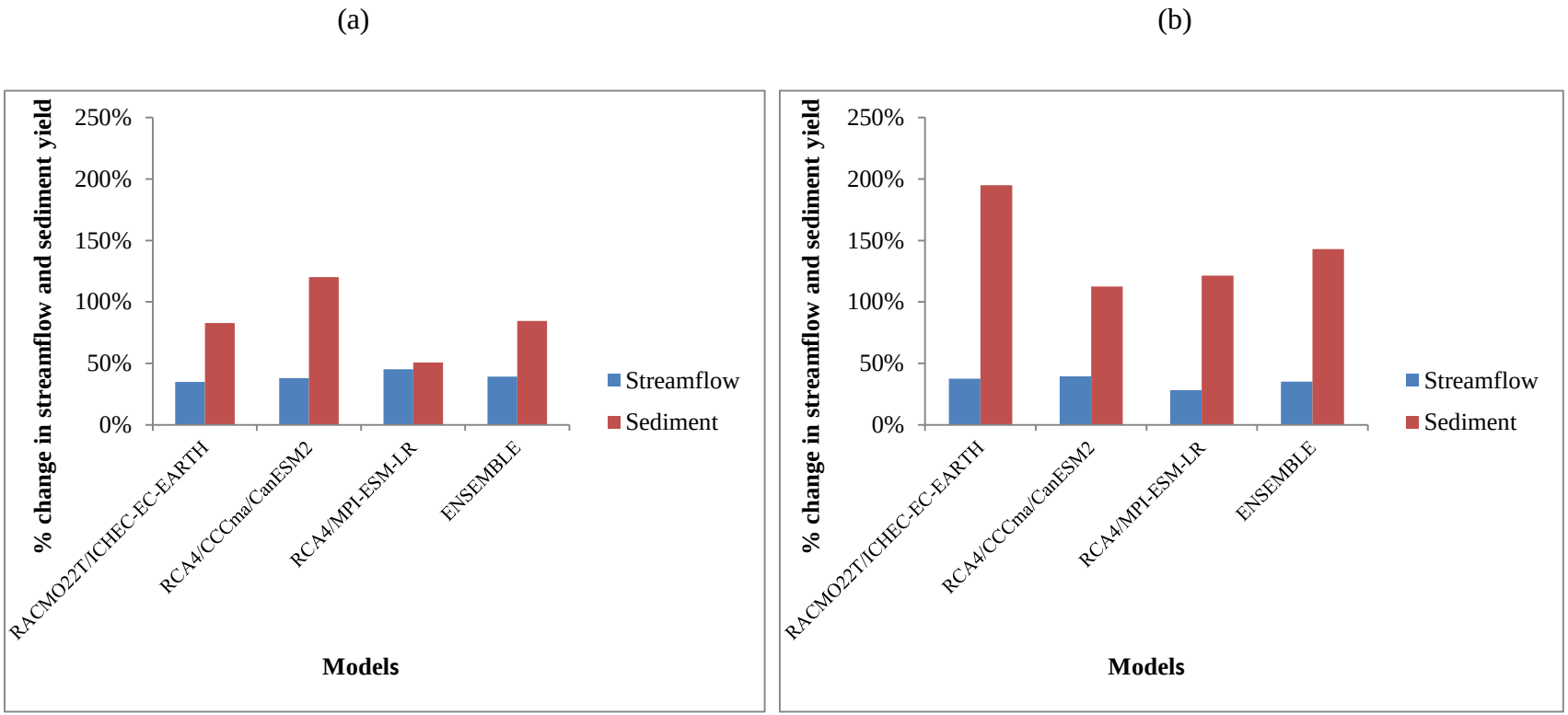

Figure 7.1: Changes in mean seasonal streamflow and sediment yield for the late 21st century (2060s) under RCP4.5 scenario compared to the baseline period. (a) Dry period (January-March) and (b) Wet period (August-October).

(a) (b)

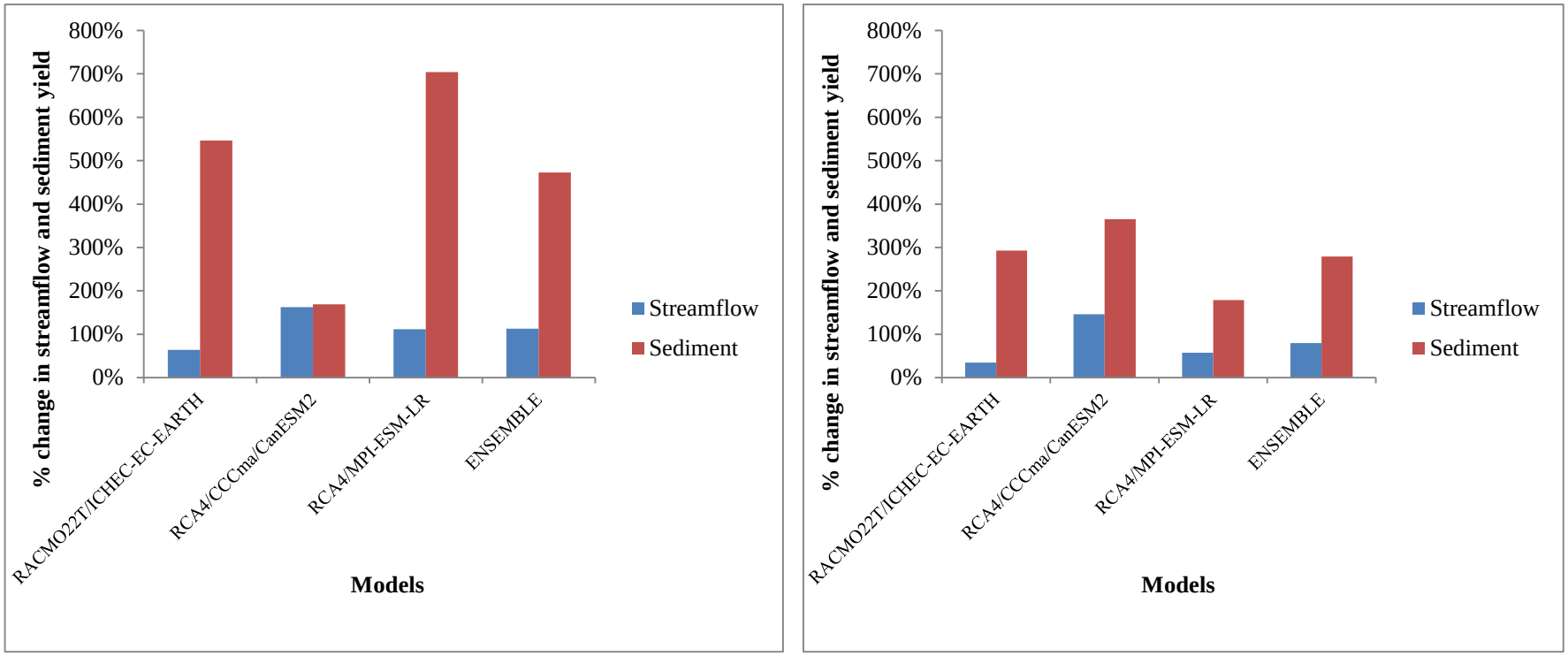

Figure 7.2: Changes in mean seasonal streamflow and sediment yield for the late 21st century (2060s) under RCP8.5 scenario compared to the baseline period. (a) Dry period (January-March) and (b) Wet period (August-October).

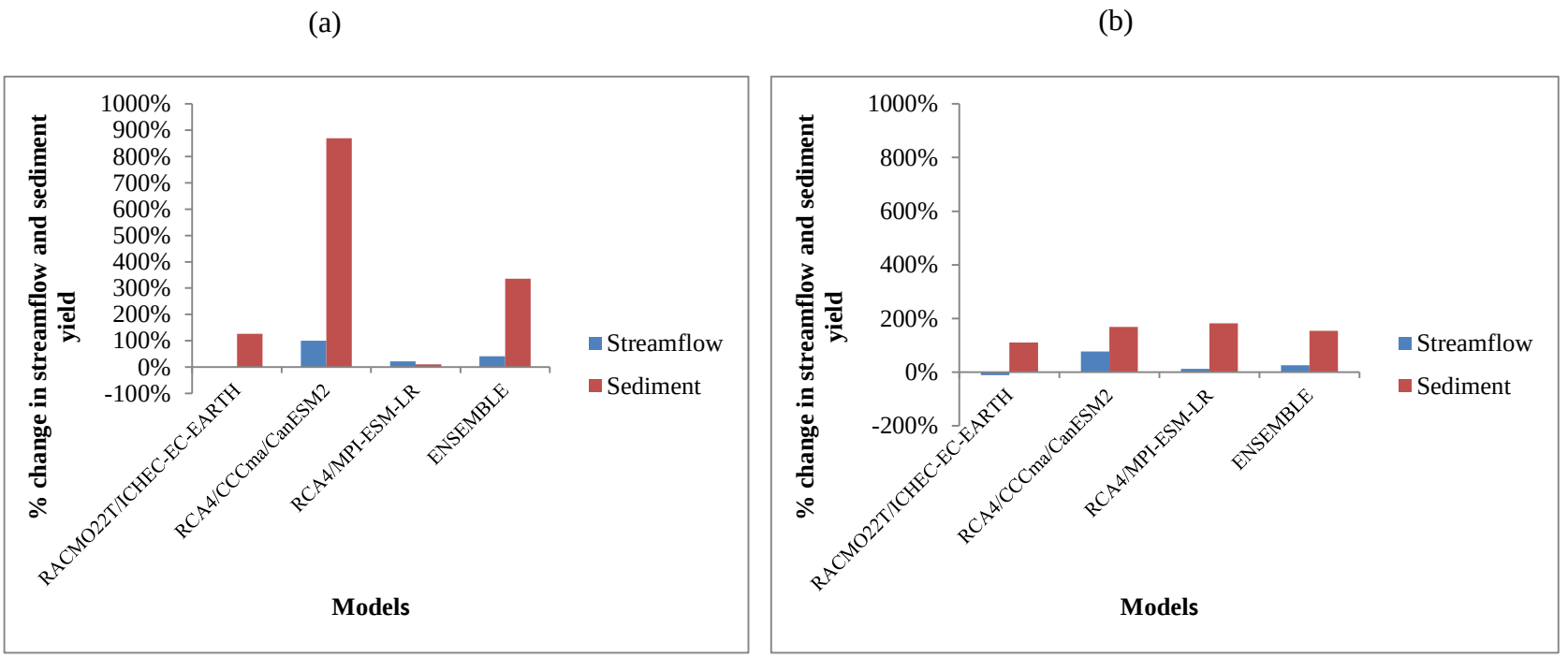

Figure 7.3: Changes in mean seasonal streamflow and sediment yield for the end of the 21st century (2080s) under RCP4.5 scenario compared to the baseline period. (a) Dry period (January-March) and (b) Wet period (August-October).

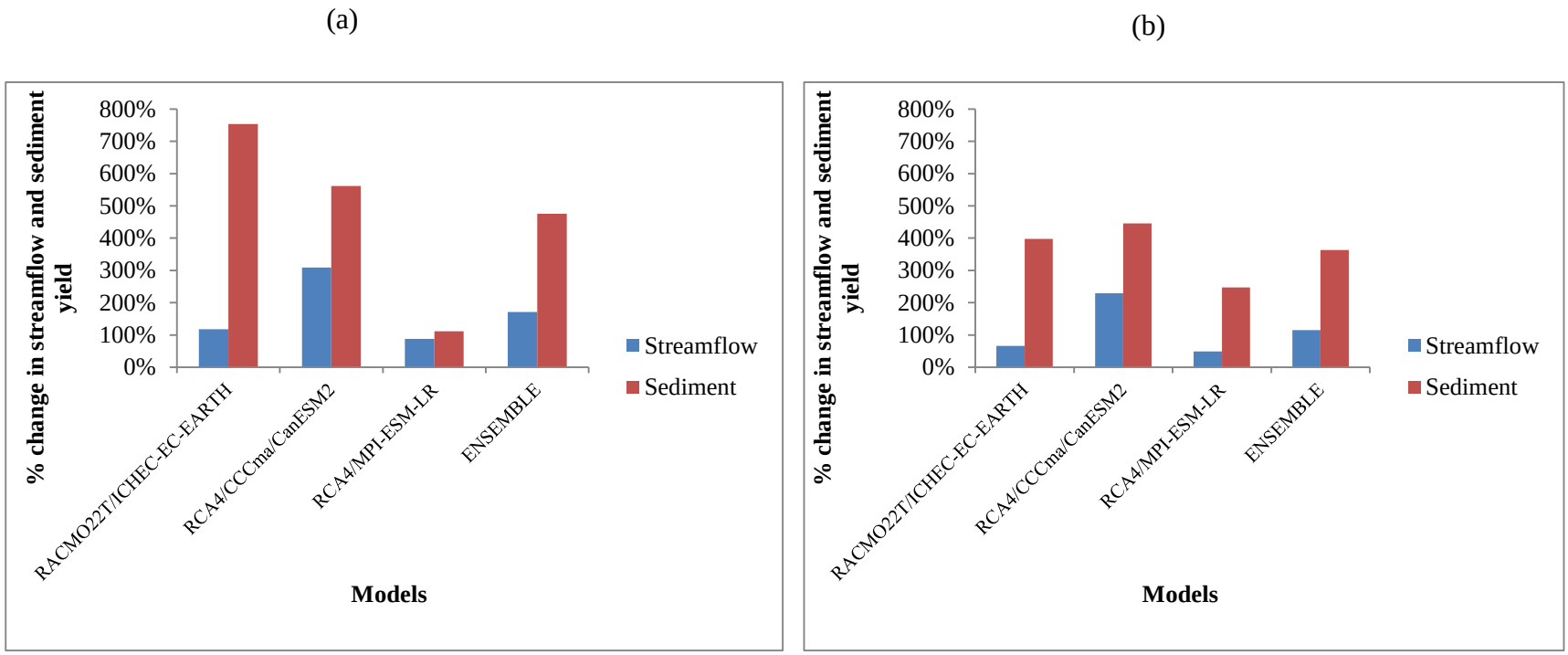

Figure 7.4: Changes in mean seasonal streamflow and sediment yield for the end of the 21st century (2080s) under RCP8.5 scenario compared to the baseline period. (a) Dry period (January-March) and (b) Wet period (August-October).

Table 7.1: Projected changes in mean annual stream flow and total sediment yield, relative to the 1984-2010 period

RCMs	Scenarios	Streamflow (m^3/s)	% Change in streamflow	Total Sediment yield (t/month)	% Change in Total Sediment yield
	Historical	309.53	0.00	155542.97	0.00
RCA4/CCCma-CanESM2	Late-Century RCP4.5	432.28	39.66	311288.78	100. 13
	Late-Century RCP8.5	769.41	148.57	676733.31	335.08
	End-of-Century RCP4.5	551.0	78.02	424965.27	173.21
	End-of-Century RCP8.5	1062.14	243.15	797398.78	412.65
RACMO22T/ICHEC-EC-EARTH	Late-Century RCP4.5	434.14	40.26	311288.78	100.13
	Late-Century RCP8.5	460.75	48.85	578270.76	271.78
	End-of-Century RCP4.5	289.65	-6.42	310308.74	99.50
	End-of-Century RCP8.5	549.27	77.45	705923.30	353.84
RCA4/MPI-ESM-LR	Late-Century RCP4.5	440.94	42.45	379010.45	143.67
	Late-Century RCP8.5	578.67	86.95	542214.66	248.59
	End-of-Century RCP4.5	382.67	23.63	492050.56	216.34
	End-of-Century RCP8.5	523.22	69.04	682351.52	338.69
MULTIMODEL ENSEMBLE MEAN	Late-Century RCP4.5	435.79	40.80	371349.60	138.74
	Late-Century RCP8.5	602.94	94.80	599072.91	285.15
	End-of-Century RCP4.5	377.86	22.08	437976.24	181.58
	End-of-Century RCP8.5	711.54	129.87	728557.87	368.39

Table 7.2: Results of Mann-Kendall trend test for average annual streamflow and total sediment yield in the BVB for the 2060s and 2080s under RCP 4.5 and RCP 8.5 emission scenarios.

Model Scenarios		Mann-Kendall's test			
		Kendall's Tau	p-value (two tiled test)	alpha	Trend
FLOW	RACMO22T/ ICHEC-EC-EARTH (RCP4.5/2060s)	0.276	0.004	0.05	Significant increase
	RACMO22T/ ICHEC-EC-EARTH (RCP4.5/2080s)	-0.051	0.597	0.05	Not significant
	RACMO22T/ ICHEC-EC-EARTH (RCP8.5/2060s)	0.389	< 0.0001	0.05	Significant increase
	RACMO22T/ ICHEC-EC-EARTH (RCP8.5/2080s)	0.474	< 0.0001	0.05	Significant increase
	RCA4/CanESM2 (RCP4.5/2060s)	-0.176	0.066	0.05	Not significant
	RCA4/CanESM2 (RCP4.5/2080s)	-0.336	0.000	0.05	Significant decrease
	RCA4/CanESM2 (RCP8.5/2060s)	0.683	< 0.0001	0.05	Significant increase
	RCA4/CanESM2 (RCP8.5/2080s)	0.624	< 0.0001	0.05	Significant increase
	RCA4/MPI-ESM-LR (RCP4.5/2060s)	0.385	< 0.0001	0.05	Significant increase
	RCA4/MPI-ESM-LR (RCP4.5/2080s)	0.210	0.029	0.05	Significant increase
	RCA4/MPI-ESM-LR (RCP8.5/2060s)	0.440	< 0.0001	0.05	Significant increase
	RCA4/MPI-ESM-LR (RCP8.5/2080s)	0.394	< 0.0001	0.05	Significant increase
SEDIMENT	RACMO22T/ ICHEC-EC-EARTH (RCP4.5/2060s)	0.275	0.004	0.05	Significant increase

	RACMO22T/ ICHEC-EC-EARTH (RCP4.5/2080s)	0.273	0.004	0.05	Significant increase
	RACMO22T/ ICHEC-EC-EARTH (RCP8.5/2060s)	0.425	< 0.0001	0.05	Significant increase
	RACMO22T/ ICHEC-EC-EARTH (RCP8.5/2080s)	0.608	< 0.0001	0.05	Significant increase
	RCA4/CanESM2 (RCP4.5/2060s)	0.290	0.003	0.05	Significant increase
	RCA4/CanESM2 (RCP4.5/2080s)	0.121	0.210	0.05	Not significant
	RCA4/CanESM2 (RCP8.5/2060s)	0.552	< 0.0001	0.05	Significant increase
	RCA4/CanESM2 (RCP8.5/2080s)	0.531	< 0.0001	0.05	Significant increase
	RCA4/MPI-ESM-LR (RCP4.5/2060s)	0.356	0.000	0.05	Significant increase
	RCA4/MPI-ESM-LR (RCP4.5/2080s)	0.410	< 0.0001	0.05	Significant increase
	RCA4/MPI-ESM-LR (RCP8.5/2060s)	0.495	< 0.0001	0.05	Significant increase
	RCA4/MPI-ESM-LR (RCP8.5/2080s)	0.475	< 0.0001	0.05	Significant increase

8. SENSITIVITY OF STEAMFLOW TO LAND USE/LAND COVER CHANGES IN THE BLACK VOLTA BASIN

8.1. Introduction

As mentioned earlier, land use/land cover changes play important roles in rainfall-runoff processes (Elfert and Bormann, 2010; Ghaffari et al., 2010). The results of the LULC change analysis of the BVB as well as the sensitivity of the basin's flow to changes in LULC are presented and discussed in this chapter.

8.1.1. Land use land cover change analysis

As shown in Figures 8.1 and 8.2, the most visible change in LULC of the basin during the 10 year period (1990 to 2000) was an increase in cropland and grassland and a decrease in savanna. Croplands increased by 14,623 km^2, representing a basin-wide coverage of 10% and grasslands by 8,815 km^2, representing an increase of 6% in basin coverage. Savanna woodland decreased by 20,246 km^2, a reduction from coverage of 56.9% to 42.5% (Table 8.1).

From 1990 to 2000, the average population growth rate in the Basin area occupied by Burkina Faso and Ghana was 2.38% and 2.5% respectively (Barry *et al*., 2005). In Burkina Faso about 78% of the total population lived in the Volta Basin in the year 2000 and the cropped area represented 82.5% of the total cropped land in Burkina Faso (ibid).The increase in cropland can thus be attributed to the increase in population in the basin within that period since expanding population demands more cultivation of crops for sustenance. In assessing the population and land use/land cover dynamics in the Volta River Basin of Ghana, Codjoe (2004), found a moderate to strong correlation between population size and agriculture land use, suggesting that population growth might have contributed to the increase in agriculture land use in 1992 and 2000. Agriculture (cultivation of crops and rearing of cattle) is the main land use type in the Volta Basin and plays a primary role in food security and poverty reduction by providing food and household incomes. Livestock (cattle, sheep and goats) production is

highly developed in the Burkinabe and Ghanaian (Northern part) sides of the basin, with the animals being kept mostly for prestige and security in times of economic crises (Codjoe, 2004).

Forest areas showed a slight decline (166 km^2) between 1990 and 2000. The decrease can be linked to the cutting down of vegetation for cultivation of grass to feed the livestock. The grazing method of the livestock in the basin, which is based on free mobility in all open forests, might have also contributed to the decline in vegetation. In addition, agricultural practices such as slash and burn technique which is widespread in the basin might have contributed to this decline.

Fuel wood is a cheap source of energy, and with rural population forming the dominant population (64-88%) of the Volta Basin (WDI, 2003 in Barry *et al*., 2005) as at the year 2000, dependence on savanna and forests for energy was commonplace. In big cities such as Ouagadougou (Burkina Faso) woodlands are the primary source of firewood and charcoal (Ouedraogo, 2006; Krämer, 2002). In Ghana, about 90% of households use charcoal or firewood for cooking (Derkyi *et al*, 2011). Therefore, in addition to clearing woodlands for cropping, the decline in savanna was most likely due to woodcutting for charcoal and firewood by the habitats of the basin. According to FAO (2001), the ascendency in cutting down trees for fuelwood and charcoal among others are responsible for deforestation in Africa.

Compared to all other land use/land cover types, shrublands showed the least changes (-0.15%). Figure 8.3 shows the net changes (%) of the different LULC classed during the 10 years. Despite all the changes however, savanna woodlands remained the dominant LULC during the 10 years (Figure 8.4). This was followed by grasslands and croplands in decreasing order of importance. As shown in Table 8.1, other minor changes included decreases in coverage of burned areas and herbaceous wetlands by 1,573 km^2 and 1,538 km^2 respectively. Infrastructure development led to an increase in area (108 km^2) of urban development. Shrublands, urban

areas, burned areas, herbaceous wetland and water body covered less than 2% of the total BVRB area in both datasets.

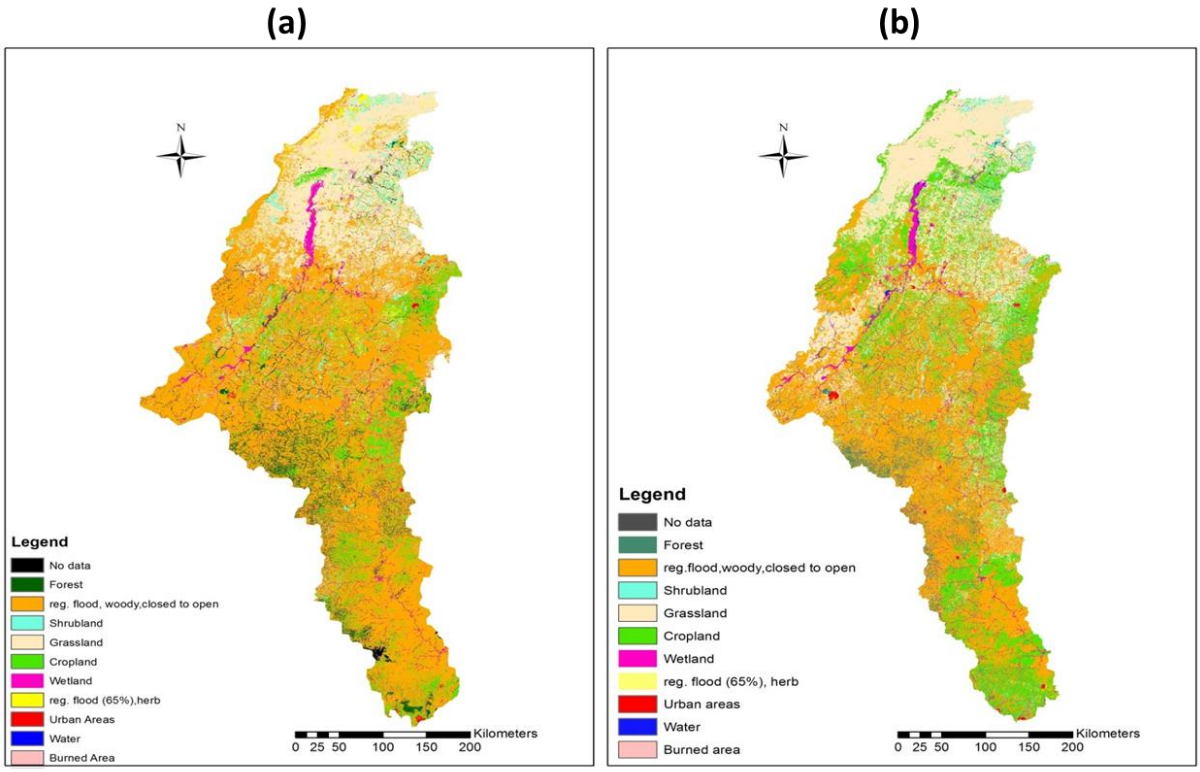

Note: reg. flood, woody, closed to open = savanna; reg. flood (65%), herb = herbaceous wetland

Figure 8.1: LULC maps for the Black Volta River Basin for the years (a) 1990 and (b) 2000 (source: Glowa Volta Portal)

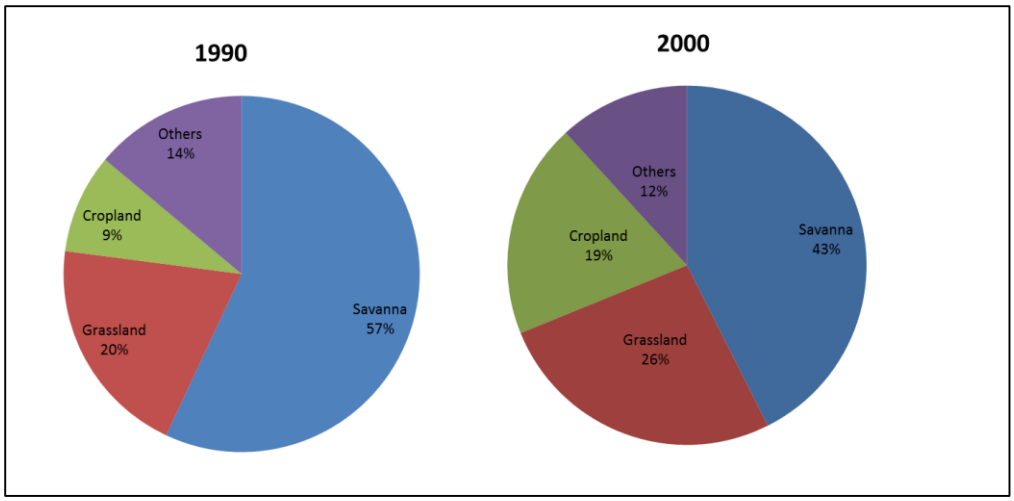

Figure 8.2: Most visible LULC changes in the Black Volta River Basin from 1990 to 2000

Table 8.1: Changes in in land use/land cover types in the Black Volta River Basin between 1990 and 2000

Land use types	1990		2000		Net Change	
	Area(km^2)	% Area	Area(km^2)	% Area	Area(km^2)	(%)
No data (unclassified)	280.86	0.20	40.26	0.03	-240.60	-85.67
Forest	7,629.48	5.39	7,463.52	5.27	-165.96	-2.18
Shrubland	2,553.84	1.80	2,549.94	1.80	-3.90	-0.15
Grassland	28,362.30	20.04	37,177.86	26.27	+8,815.56	+31.08
Cropland	12,763.08	9.02	27,386.40	19.35	+14,623.32	+114.58
Wetland	5,385.66	3.81	5,450.82	3.85	+65.16	+1.21
Urban areas	169.80	0.12	278.28	0.20	+108.48	+63.89
Water body	41.22	0.03	197.52	0.14	+156.30	+379.18
Burned area	2,187.18	1.55	613.26	0.43	-1,573.92	-71.96
Reg. flood (65%), herb (herbaceous wetland)	1,673.52	1.18	135.12	0.10	-1,538.40	-91.93
Reg. flood, woody,closed to open (savanna woodland)	80,461.62	56.86	60,215.58	42.55	-20,246.04	-25.16
Total	141,508.56	100.00	141,508.56	100.00		

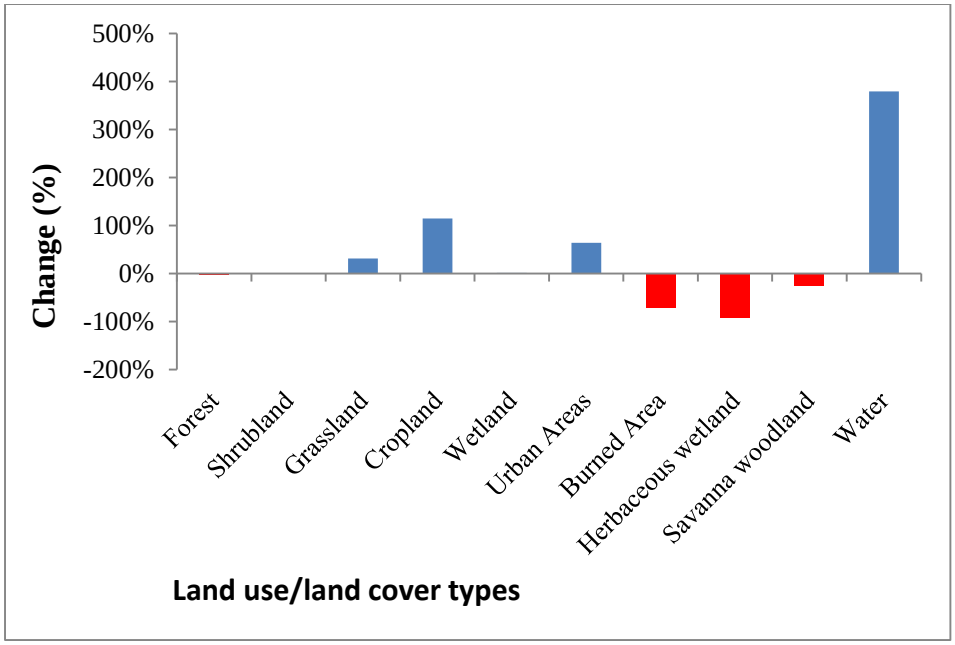

Figure 8.3: Net change per LULC class in the Black Volta River Basin between 1990 and 2000

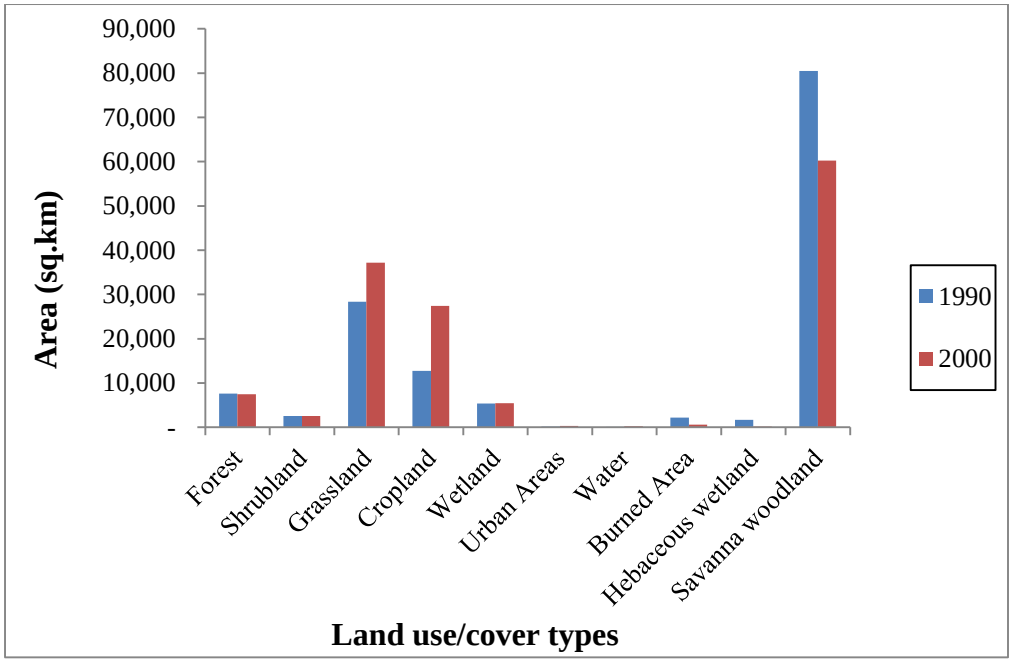

Figure 8.4: Land use/land cover coverage in the Black Volta River Basin from 1990 to 2000

8.1.2. Sensitivity of streamflow to land use/land cover change

The results of the annual and seasonal variability of streamflow in relation to changes in LULC in the BVRB are depicted in Figure8.5 and Table 8.2 respectively. The total annual flows based on the 1984-2010 simulation showed slight decreases in streamflow following the change in land use from 1990 to 2000. The decrease ranged between 0.5% in 1992 and 5.7% in 1984. For the seasonal analysis, whereas the change in land use resulted in a 1% increase in flow during the dry season (Jan-Mar), a decrease of 4% flow was recorded for the wet season (Jul-Sep). The analysis revealed no change in flow during the beginning of the rainfall season (Apr-Jun). The mean annual streamflow for the period of simulation using the LULC of the year 1990 was 319.12 m^3/s while that for the LULC of the year 2000 was 309.53 m^3/s, representing a slight reduction of -2% over the year 1990.This reduction is statistically insignificant. The coefficients of variation were 1.20 and 1.18 for the 1990- and 2000-LULC simulations, respectively (Table 8.3)

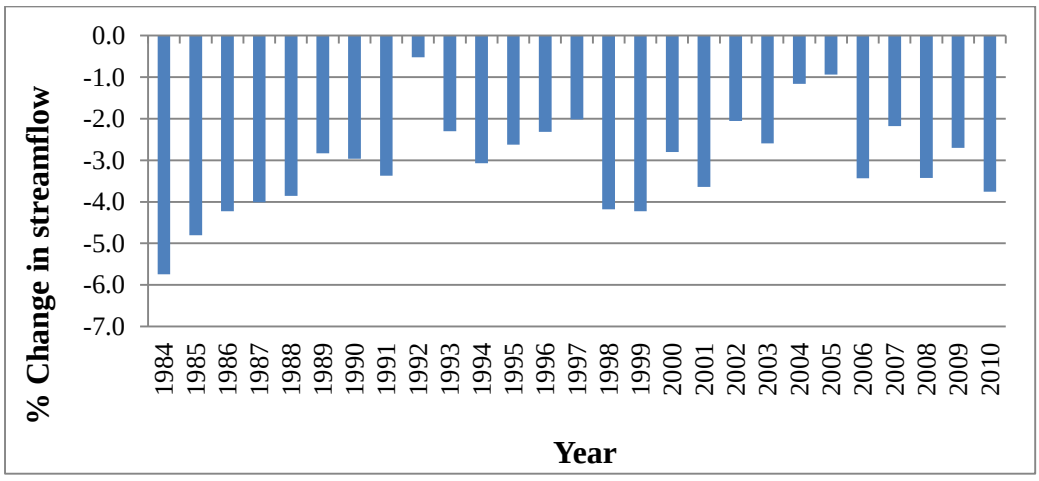

Figure 8.5: Simulated changes in total annual streamflow of the Black Volta River Basin using year 2000 land use map, relative to year 1990 land use map

Table 8.2: Change in seasonal streamflow of the Black Volta River Basin due to LULC change from 1990 to 2000

Seasons	LULC1990 (m^3/s)	LULC2000 (m^3/s)	% Change
Dry season (Jan-Mar)	2,324.535	2,337.934	+1
Beginning rainfall season (Apr-Jun)	2,314.123	2,312.178	0
Wet season (Jul-Sep)	3,758.848	3,619.221	-4
Wet dry season (Oct-Dec)	3,391.906	3,445.026	+2

Table 8.3: Statistics of streamflow simulation (1984-2010) for the Black Volta River Basin based on the LULC maps of the years 1990 and 2000

Statistical Parameter	**LULC1990**	**LULC2000**
Mean (m^3/s)	319.12	309.53
Maximum (m^3/s)	2,173.00	2,137.00
Minimum (m^3/s)	8.69	8.15
Standard Deviation (m^3/s)	383.10	363.96
Coefficient of Variation	1.20	1.18

9. GENERAL CONCLUSIONS AND PERSPECTIVES

9.1. Conclusions

The performance of the SWAT model in simulating the historical flow and sediment yield of the BVB, assessed through the quantitative statistics NSE, R^2, RSR and PBIAS, during monthly calibration and validation shows that the model reasonably simulates the two variables. The calibration results for flow were R^2 of 0.86; NSE of 0.85; RSR of 0.38; and PBIAS of 8.1. For sediment yield, the results were R^2 of 0.76; NSE of 0.68; RSR of 0.57, and PBIAS of 27.5. Both results show "good" model performance. The validation results were "satisfactory" for both flow and sediment yield, with R^2 of 0.62; NSE of 0.60; RSR of 0.64 and PBIAS of 20.1% for streamflow and R^2 of 0.74; NSE, 0.66; RSR of 0.59, and PBIAS of 39.1% for sediment yield. The PBIAS values show that the model has the tendency of underestimating flow and sediment yield in the basin. Results of the sensitivity analysis show that the most sensitive parameter to streamflow in basin is the curve number (CN2). The P-factor and R-factor values obtained during the model calibration shows that the uncertainties which exist in the model should not be ignored and must be taken into account when using the results for impact assessment.

The plots of mean monthly precipitation and temperature of the model-simulated uncorrected, model-simulated bias-corrected and observed data showed that the quantile-quantile downscaling and quantile-quantile transformation method performed well in reducing the RCM biases. The analysis of the data further showed that the corrected data fit much better to the observed data than the uncorrected data. Although the individual RCMs simulated quite well the historical precipitation of the basin, the ensemble mean of the three (3) RCMs were closer to the observation than any of the individual model simulations. With regards to temperature, all the models simulated well the historical temperature of the basin.

Relative to the baseline, annual precipitation amounts showed positive and negative signals across the models. Similar to the annual precipitation, the intra-annual and seasonal precipitation analysis also showed high uncertainty in the future rainfall amounts, with higher variability in the wet season compared to the dry season. Temperature projections by the models unanimously suggested warming of the basin during the 2060s and 2080s with increases ranging between 2.0^{o}C (2060s under RCP4.5) and 3.7^{o}C (2080s under RCP8.5). Trend analysis of annual future precipitation pointed in both positive and negative directions. The trends were however statistically insignificant at the 5% level of significance. Trends in the annual mean temperature however, showed mostly statistically significant (5% level of significance) increases in future temperature over the basin. A few of the model runs showed statistically insignificant decreasing trends. High temperatures may affect water availability and use in the basin. Since majority of the basin's population depend on agriculture for their livelihood, problems related to water scarcity in the basin may worsen the poverty situation in the basin. Measures to cope with the increasing temperature over the basin should therefore be explored and developed well ahead of time.

Seasonal analysis of streamflow and sediment yield showed statistically significant increases in flow and sediment during the dry and wet periods for the 2060s and 2080s under both RCP 4.5 and RCP 8.5 scenarios.

The land use/land cover change analysis of the Black Volta Basin showed that between the period 1990 and 2000, the coverage of cropland and grassland increased drastically, with corresponding reduction in savanna. These changes could be linked to population growth and the dependence on savanna for fuelwood in the basin. The sensitivity analysis of streamflow over the basin with respect to the 10 year change in land use also showed slight changes. The statistics of the flow simulation showed, however, that the changes were not significant. This

is an indication that the streamflow in the Black Volta Basin may be largely insensitive to changes in land use/land cover, especially changes in savanna and cropland, in the basin.

9.2. Perspectives

The impact of climate change on flow and sediment yield of the BVRB has been evaluated. This sensitivity of the basin's flow to changes in LULC changes has also been assessed. Future study on the other sub-basins of the Volta Basin on this theme will help to hasten the proper management of the Volt River Basin.

9.3. Recommendations

To reduce the vulnerability of the BVRB and indeed the entire VRB to the projected impacts of climate change, the following recommendations are proposed:

1. A comprehensive flood management plan should be developed for the entire VRB. This plan should include among other things the enhancement of existing reservoirs to take up extra water and the development of flood early warning systems.
2. A drought management plan which includes having irrigation facilities for supplemental irrigation in rainfed agriculture to offset the negative effect of drought on agriculture and food security should be developed.
3. Integrated watershed management approaches, aimed at reducing erosion and sedimentation in the basin should be explored and implemented.

REFERENCES

Abbas, I.I., Muazu, K.M. and Ukoje, J.A. (2010). Mapping Land Use-Land Cover and Change Detection in Kafur Local Government, Katsina, Nigeria (1995–2008) Using Remote Sensing and GIS. Res. J. Environ. Earth Sci., 2 (1), 6–12.

Abbaspour (2015). SWAT-CUP: SWAT Calibration and Uncertainty Programs - A User Manual. Department of Systems Analysis, Integrated Assessment and Modelling (SIAM), Eawag, Swiss Federal Institute of Aquatic Science and Technology, Duebendorf, Switzerland, 100pp.

Abbaspour, K.C., Johnson, A., van Genuchten, M.Th. (2004). Estimating uncertain flow and transport parameters using a sequential uncertainty fitting procedure. Vadose Zone Journal 3(4), 1340-1352.

Abbaspour, K.C., Yang, J., Maximov, I., Siber, R.. Bogner, K. K., Mieleitner, J., Zobrist, J. and Srinivasan, R. (2007). Modelling hydrology and water quality in the pre-alpine/alpine Thur watershed using SWAT. Journal of Hydrology, 333:413-430.

Abiodun, B.J., Abba, Omar. S., Lennard, C. and Jack, C. (2015). Using regional climate models to simulate extreme rainfall events in the Western Cape, South Africa. International Journal of Climatology. DOI: 10.1002/joc.4376.

Adams, W. M., Goudie A. S. and Orme A. R. (1996). The Physical Geography of Africa; Oxford University Press.

Agbenyega, E. (2014). "Ghana's power crisis: What about renewable energy?". graphic.com.gh. Retrieved 28- 12-2015.

Agyare, W. A. (2004). Soil characterization and modelling of spatial distribution of saturated hydraulic conductivity at two sites in the Volta Basin of Ghana; Ecology and Development Series No. 17; Cuvillier Verlag Gottingen.

Akpoti, K., Antwi, E.O., Karbo-bah, A.T. (2016). Impacts of Rainfall Variability, Land Use and Land Cover Change on Streamflow of the Black Volta Basin, West Africa. Hydrology, 3(3), 26; doi:10.3390/hydrology3030026.

Akrasi, S. A. (2005). The assessment of suspended sediment inputs to Volta Lake. Lakes & Reservoirs: Research and Management, 10:179–186.

Akrasi, S.A. (2011). West African Journal of Applied Ecology, volume 18.

Allwaters Consult (2012). Diagnostic Study of the Black Volta Basin in Ghana; Final Report; ALLWATERS Consult Limited: Kumasi, Ghana.

Amadou, A., Abdouramane, G., Seidou, O. and Seidou Sanda, I. (2015). Changes to flow regime on the Niger River at Koulikoro under a changing climate. Hydrological Sciences Journal, doi 10.1080/02626667.2014.916407.

Amisigo, B.A. (2005). Modelling riverflow in the Volta Basin of West Africa: A data-driven framework. PhD Thesis. Ecology and Development Series No. 34. ZEF Bonn. Cuvillier Verlag, Göttingen, http://www.glowa-golta.de/fileadmin/template/Glowa/downloads/Amisigo_doc_thesis_2006 .pdf.

Andah, W., van de Giesen, N., Huber-Lee, A. and Biney, C. (2004). Can we maintain food security without losing hydropower? The Volta Basin. Climate Change in Contrasting River Basins: Adaptation Strategies for Water, Food and Environment, J. Cayford, Ed., CABI Publishing,Wallingford, 181-194.

Annor, F. O. (2012). Diagnostic Study of the Black Volta Basin in Ghana. In-Service Training Centre, Upper West Region- Ghana.

Armah, F.A., Yawson, D.O., Yengoh, G.T., Odoi, J.O. and Afrifa. E.K.A. (2010). Impact of Floods on Livelihoods and Vulnerability of Natural Resource Dependent Communities in Northern Ghana. Water, 2, 120–139.

Arnold, J. G., Moriasi, D. N., Gassman, P. W., Abbaspour, K. C.,White, M. J., Srinivasan, R., Santhi, C., Harmel, R. D., van Griensven, A., Van Liew, M. W., Kannan, N., Jha, M. K. (2012b).

SWAT: Model use, calibration, and validation. Trans.ASABE, 55(4), 1494-1508. http://dx.doi.org/10.13031/2013.42256.

Arnold, J. G., Srinivasan, R., Muttiah, S., and Williams, J. R. (1998). "Large area hydrologic modelling and assessment: Part I. Model development." Journal of American Water Resource Association, 34(1), 73-89.

Arnold, J.G., Allen P.M. and Bernhardt, G. (1993). A comprehensive surface-groundwater flow model. Journal of Hydrology 142, p. 47-69.

Arnold, J.G., Kiniry, J.R., Srinivasan, R., Williams, J.R., Haney, E.B., Neitsch, S.L. (2012a). Soil and Water Assessment Tool. Input/Output Documentation, Version 2012. Texas Water Resources Institute. TR-439. Available at http://swat.tamu.edu/documentation/2012-io/. Accessed on 7/23/2015.

Awotwi, A., Yeboah, F. and Kumi M. (2015). Assessing the impact of land cover changes on water balance components of White Volta Basin in West Africa Water and Environment Journal 29, 259-267.

Babiński, Z. (2005) The relationship between suspended and bed load transport in river channels. In: Sediment Budgets 1 (Proc. Foz do Iguazu Symo., April 2005) (ed. by D. E. Walling & A. J. Horowitz), 182–188. IAHS Publ. 291. IAHS Press,Wallingford, UK.

Baldauf, M., Seifert, A., Foerstner, J., Majewski, D., Raschendorfer, M. and Reinhardt, T. (2011). Operational convective-scale numerical weather prediction with the cosmo model: Description and sensitivities. Monthly Weather Review, 139, 3887–3905, doi:10.1175/MWR-D-10-05013.1.

Barry B, Obuobie E, Andreini M, Andah W and Pluquet, M. (2005). The Volta river basin. Comprehensive assessment of water management in agriculture .Comparative study of river basin development and management.

Beven, K. and Binley, A. (1992). The Future of Distributed Models - Model Calibration and Uncertainty Prediction. Hydrological Processes, 6(3): 279-298.

Biney, C.A. (2010). Connectivities and linkages within the Volta Basin. Paper presented at the Conference of the Global Catchment Initiative (GCI), December 6-8, 2010, University Club, Bonn, Germany.

Boko, M., Niang, I., Nyong, A., Vogel, C., Githeko A, Medany, M., Osman-Elasha, B., Tabo, R., & Yanda, P. (2007). Africa Climate Change 2007: impacts, adaptation and vulnerability. In M. L. Parry, O. F. Canziani, J. P. Palutikof, P. J. van der Linden, & C. E. Hanson (Eds.), Contribution of Working Group II to the Fourth Assessment Report of the Intergovernmental Panel on Climate Change (pp. 433–467). Cambridge, UK: Cambridge University Press.

Boyer, C., Chaumont, D., Chartier, I. and Roy, A. G. (2010). Impact of climate change on the hydrology of St. Lawrence tributaries. Journal of Hydrology 384 65–83.

Braimoh, A.K. and Vlek, P.L.G. (2005). Land Cover Change Trajectories in Northern Ghana. Environ. Manage., 36 (3), 356–373.

Brath, A., Montanari, A., Moretti, G. (2006). Assessing the effect on flood frequency of land use change via hydrological simulation (with uncertainty). Journal of Hydrology 324 (1–4), 141–153.

Butt, B., and Olson, J. M. (2002). An approach to dual land use and land cover interpretation of 2001 satellite imagery of the eastern slopes of Mt. Kenya. Land use Change Impacts

and Dynamics (LUCID) Project Working Paper 16. International Livestock Research Institute (ILRI), Nairobi, Kenya.

CDKN (Climate and Development Knowledge Network) (2014). The IPCC's Fifth Assessment Report: What's in it for Africa? Available from http://cdkn.org/resource/highlights-africa-ar5/ [Accessed 14 August, 2015].

Chevallier, P. and Planchon, O. (1993). Hydrological processes in a small humid savanna basin (Ivory Coast); Journal of Hydrology; Vol. 151: pp. 173–191.

Chinowsky, Paul., Schweikert, Amy., Strzepek, Niko., Manahan, Kyle., Strzepek, Kenneth. and Schlosser, C. Adam (2011). "Adaptation Advantage to Climate Change Impacts on Road. Infrastructure in Africa through 2100," Working Paper 25, UNU-WIDER.

Christensen, H., Hewitson, B., Busuioc, A. et al. (2007). "Regional climate projections," in Climate Change (2007), Solomon, S., Qin, D., Manning, M., Eds., Cambridge University Press, New York, NY, USA.

Chylek, P., Li, J., Dubey, M.K., Wang, M., and Lesins, G. (2011). Observed and model simulated 20th century Arctic temperature variability : Canadian Earth System Model CanESM2 22893–22907. doi:10.5194/acpd-11-22893-2011.

Codjoe, S.N.A. (2004). Population and Land use/land cover dynamics in the Volta River Basin of Ghana, 1960-2010. Ecology and Development Series, No.15. Gottingen: Cuvillier Verlag. 184 pages.

Coffey, A.E., Workman, S.R., Taraba, J.L., Fogle, A.W. (2004). Statistical procedures for evaluating daily and monthly hydro- logic model predictions. Trans. ASAE 47 (1), 59–68.

Costa, M.H., Botta, A., Cardille, J.A. (2003). Effects of large-scale changes in land cover on the discharge of the Tocantins River, Southeastern Amazonia. Journal of Hydrology 283, 206–217.

Crooks, S., Davies, H. (2001). Assessment of land use change in the Thames catchment and its effect on the flood regime of the river. Physics and Chemistry of the Earth, Part B 26 (7–8), 583–591.

Derkyi, N.S.A., Sekyere, D., Okyere, P.Y., Darkwa, N.A. and Nketiah, S.K. (2011). Development of bioenergy conversion alternatives for climate change mitigation.International Journal of Energy and Environment, 2(3), pp 525-532.

Di Gregorio, A. and Jansen, L.J.M. (1998). Land cover classification system. Proceedings of the 1st Earth Observation and Environment Information 1997 Conference (EOET97), 13-16 October, 1997, Alexandria, Egypt.

Diallo, I., Sylla, M.B., Giorgi, F., Gaye, A.T., Camara, M. (2012). Multimodel GCM-RCM Ensemble-Based Projections of Temperature and Precipitation over West Africa for the Early 21st Century 2012. doi:10.1155/2012/972896.

Dosio, A., Panitz, H.-J., Schubert-Frisius, M., and Lüthi, D. (2015). Dynamical downscaling of CMIP5 global circulation models over CORDEX-Africa with COSMO-CLM: evaluation over the present climate and analysis of the added value. Climate Dynamics, 44:2637–2661.

Douville, H., Salas-M´elia, D. and Tyteca, S. (2006). "On the trop- ical origin of uncertainties in the global land precipitation response to global warming," Climate Dynamics, vol. 26, no. 4, pp. 367–385.

Duan, Z., Xianfeng, S. and Liu, J. (2009). Application of SWAT for sediment yield estimation in a mountainous agricultural basin. International Conference on Geoinformatics, Fairfax, 2009, pp. 1-5. Forkuo, E.K. (2011). Flood Hazard Mapping using Aster Image data with GIS. International Journal of Geomatics and Geosciences, 1, 932–950.

Duru, U. (2015). Modelling Sediment Yield And Deposition Using The Swat Model: A Case Study Of Cubuk I And Cubuk II Reservoirs, Turkey. PhD. Thesis. Colorado State University, Fort Collins.

Dwarakish, G.S. and Ganasri, B.P. (2015). Impact of land use change on hydrological systems:A review of current modelling approaches. Cogent Geoscience, 1: 1115691. http://dx.doi.org/10.1080/23312041.2015.1115691.

Eberhart, R. C. and Kennedy, J. (1995). A new optimizer using particle swarm theory. Proceedings of the sixth international symposium on micro machine and human science pp. 39-43. IEEE service center, Piscataway, NJ, Nagoya, Japan.

Edwards, K. (1993). Soil erosion and conservation in Australia. In: Pimentel, D. (Ed.). World Soil Erosion and Conservation, Cambridge, pp. 147–169.

Elfert, S., Bormann, H. (2010). Simulated impact of past and possible future land use changes on the hydrological response of the Northern German lowland 'Hunte' catchment. J HYDROL 383, 245 – 255, 2010.

Endris, H. S., Omondi, P., Jain, S., Lennard, C., Hewitson, B., Chang'a, L., Awange, J., Dosio, A., Ketiem, P., Nikulin, G., et al. (2013). Assessment of the Performance of CORDEX Regional Climate Models in Simulating East African Rainfall. Journal of Climate, 26(21):8453–8475.

Endris, H.S., Lennard, C., Hewitson, B., Dosio, A., Nikulin, G., Panitz, H. (2015). Teleconnection responses in multi-GCM driven CORDEX RCMs over Eastern Africa. Climate Dynamics. DOI 10.1007/s00382-015-2734-7

FAO (1997a). Africover land cover classification. Rome, Italy.

FAO (1997b). Irrigation potential in Africa: A basin approach. FAO Land and Water Bulletin 4

FAO (2001). Global forest resource assessment. Main report. (FAO Forest Paper 140. Food and Agriculture Organization of the United Nations,Rome, Italy.

FAO. 1995. Digital soil map of the World. Rome, Italy.

Fleming, M. and Neary, V. (2004). Continuous Hydrologic Modelling Study with the Hydrologic Modelling System, Journal of Hydrological Engineering, 9, 175–183.

Fohrer, N., Haverkamp, S., Eckhardt, K., Frede, H.G. (2001). Hydrologic Response to land use changes on the catchment scale. Physics and Chemistry of the Earth, Part B: Hydrology, Oceans and Atmosphere 26: 577-82.

Foley, J.A., DeFries, R., Asner, G.P., Barford, C., Bonan, G., Carpenter, S.R., Chapin, F.S., Coe, M.T., Daily, G.C., Gibbs, H.K., Helkowski, J.H., Holloway, T., Howard, E.A., Kucharik, C.J., Monfreda, C., Patz, J.A., Prentice, I.C., Ramankutty, N., Snyder, P.K. (2005). Global Consequences of Land Use. Science 309(5734), 570-574.

Frei, C., Christensen, J.H., De´que´, M., Jacob, D., Jones, R.G. and Vidale, P.L. (2003). Daily precipitation statistics in regional climate models:Evaluation and intercomparison for the European Alps, Journal of Geophysical Research,108 (D3):4124.

Gaetani, M., Fontaine, B., Roucou, P. and Baldi, M. (2010). Influence of the Mediterranean sea on the West African monsoon: Intraseasonal variability in numerical simulations. Journal of Geophysical Research 115: D24115, doi:JD014436.

Gassman P.W, Reyes M, Green, C.H. and Arnold, J.G. (2007). The Soil and Water Assessment Tool: Historical development, applications, and future directions. Trans. ASABE 50(4):1211-1250.

Gassman, P.W. (2015). The Soil and Water Assessment Tool (SWAT) Ecohydrological Model Circa 2015: Global Application Trends, Insights and Issues. Abstract H11k-01 presented at 2015 Fall meeting, AGU, San Francisco, California, 14-18 Dec.

Ghaffari, G., Keesstra, S., Ghodousi, J., Ahmadi, H. (2010). SWAT-simulated hydrological impact of land-use 10 change in the Zanjanrood Basin, Northwest Iran. Hydrological Processes 24(7), 892-903.

Ghana Energy Commission (2015). 2015 Energy (Supply and Demand) Outlook for Ghana. 50pp.

Giannini, A., Biasutti, M., Held, I.M. and Sobel, A.H. (2008). "A global perspective on African climate," Climatic Change, vol. 90, no. 4, pp. 359–383.

Giertz, S. (2004). Analyse der hydrologischen Prozesse in den sub-humiden Tropen Westafrikas unter besonderer Ber¨ucksichtigung der Landnutzung am Beispiel des AguimaEinzugsgebietes in Benin; PhD thesis; University Bonn.

Giorgi, F. (2010). "Uncertainties in climate change projections, from the global to the regional scale," EPJ Web of Conferences, vol. 9, pp. 115–129.

Giorgi, F., Diffenbaugh, N. S., Gao X. J., et al. (2008). "The regional climate change hyper-matrix framework," Eos, vol. 89, no. 45, pp. 445–446, 2008.

Giorgi, F., Jones, C., Asrar, G. (2009). Addressing climate information needs at the regional level: the CORDEX framework. World Meteorology Organ Bulletin Available online at http://wcrp.ipsl.jussieu.fr/RCD_Projects/CORDEX/CORDEX_giorgi_WMO.pdf., 58, 175-183.

Globalweather, (2012). NCEP Climate Forecast System Reanalysis (CFRS). http://globalweather.tamu.edu/.

Goodess, C.M., Anagnostopoulou, C., Bárdossy, A., Frei, C., Harpham, C., Haylock, M.R., Hundecha, Y., Maheras, P., Ribalaygua, J., Schmidli, J., Schmith, T., Tolika, K., Tomozeiu, R. and Wilby, R.L. (2005). An inter comparison of statistical downscaling methods for Europe and European regions – assessing their performance with respect to extreme temperature and precipitation events. Climatic Research Unit Research Publication 11.

Gordon, C. and Amatekpor, J. K. (1999). The Sustainable Integrated Development of the Volta Basin in Ghana. VBRP, University of Ghana-Legon 159 p.

Goula, B. T. A, Soro G. E., K. F. W. and S. B. (2010). Frequency analysis and new cartography of extremes daily rainfall events in Côte d'Ivoire. Journal of Applied Sciences, 10, 1684 – 1694.

Green Cross International (2001). Trans-boundary Basin Sub-Projects: The Volta River Basin. Website: www.gci.ch/Green- crossPrograms/ waterres/pdf/WFP_Volta.

Green, W. and Ampt, G. (1911). "Studies on soil physics, 1. The flow of air and water through soils." Journal of Agricultural Sciences 4: 11-24.

Gupta, H. V., Sorooshian, S. and Yapo, P. O. (1999). Status of automatic calibration for hydrologic models: Comparison with multilevel expert calibration. Journal of Hydrologic Engineering, 4(2): 135-143.

Guy, H.P. and Normann, V.W. (1970). Field Methods for Measurements of Fluvial Sediment. - Techniques of Water- Resources Investigations of the United States Geological Survey, Book 3, Chapter C2, 59 p.

Gyau-Boakye, P. and Tumbulto, J.W. (2006). Comparison of rainfall and runoff in the humid south-western and the semiarid northern savannah zone in Ghana. African Journal of Science and Technology. Science and Engineering Series Vol. 7, No.1, pp. 64-72.

Hargreaves, G. L., Hargreaves, G. H. and Riley, J. P. (1985). Agricultural benefits for Senegal River basin. Journal of Irrigation and Drainage Engineering. 108(3): 225-230.

Harmel, R.D., Cooper, R.J., Slade, R.M., Haney, R.L., and Arnold, J.G. (2006). Cumulative Uncertainty in Measured Streamflow and Water Quality Data for Small Watersheds. Transactions of theASABE 49(3), 689-701.

Hay, L.E., McCabe, G.J., Wolock, D.M. and Ayers, M.A. (1991). Simulation of precipitation by weather type analysis. Water Resources Research 27: 493–501.

Hayhoe, K. (2010). "A Standarized Framework for Evaluating the Skill of Regional Climate Downscaling Techniques," Doctoral Thesis, University of Illinois at Urbana-Champaign.

Hewitson, B. C. and Crane, R.G. (2006). Consensus between GCM climate change projections with empirical downscaling: Precipitation downscaling over South Africa, International Journal of Climatology 26: 1315–1337.

Hoerling, M., Hurrell, J., Eischeid, J. and Phillips, A. (2006). "Detection and attribution of twentieth-century northern and southern African rainfall change," Journal of Climate, vol. 19, no. 16, pp. 3989–4008.

Hong, S.Y. and Kanamitsu, M. (2014). Dynamical downscaling: fundamental issues from an NWP point of view and recommendations. Asia Pacific Journal of Atmospheric Science 50(1):83–104. doi:10.1007/ s13143-014-0029-2.

Houser, J.B., Hauck, L.M and Saleh, A. (2015). Modifying and Validating the SWAT Model to Determine Landuse Effects on Watershed Water Quality: Using a Dual Level of Model Performance Based on Subbasin Size. International Journal of Environmental Research 9(3):885-896. ISSN: 1735-6865.

http://srtm.csi.cgiar.org/index.asp

http://swat.tamu.edu/

Hulme, M., Doherty, R., Ngara, T., New, M. and Lister, D. (2001). "African climate change: 1900–2100," Climate Research, vol. 17, no. 2, pp. 145–168.

Huntingford, C., Jones, R.G., Prudhomme, C., Lamb, R., Gash, H.H.C. and Jones, D.A. (2003). Regional climate-model predictions of extreme rain- fall for a changing climate, Quarterly Journal of Royal Meteorological Society, 129:1607–1621.

Hurd, B. H., Callaway, M., Smith, J. and Kirshen, P. (2004). Climatic change and U.S. water resources: From modeled watershed impacts to national estimates. Journal of the American Water Resources Association, 40,129-148.

Intergovernmental Panel on Climate Change: IPCC (2007b) Climate Change 2007, Synthesis Report (AR4).

Intergovernmental Panel on Climate Change: IPCC Expert Meeting Report, (2007a). Towards New Scenarios For Analysis Of Emissions, Climate Change, Impacts, And Response Strategies, IPCC 2007.

Intergovernmental Panel on Climate Change: IPCC TAR WG3 (2001). Metz, B.; Davidson, O.; Swart, R.; and Pan, J., ed., Climate Change 2001: Mitigation, Contribution of Working Group III to the Third Assessment Report of the Intergovernmental Panel on Climate Change, Cambridge University Press, ISBN 0-521-80769-7 (pb: 0-521-01502-2).

IPCC - AR4 (2005). Available (https://esg.llnl.gov:8443/home/publicHomePage.do).

IPCC (2007). IPCC 4th Assessment Report - Climate Change 2007. Working Group II on "Impacts, Adaptation and Vulnerability". http://www.ipcc-wg2.org.

IPCC (2013). Climate Change 2013. The Physical Science Basis. Headline Statements from the Summary for Policymakers, 2pp.

IPCC (2014a). Climate Change 2014. Impacts, Adaptation, and Vulnerability. Chapter 12, Human Security (p2).

IPCC (2014b). Climate Change 2014. Impacts, Adaptation, and Vulnerability. Technical Summary (pp7, 27).

IPCC AR4 (2005). Available (https://esg.llnl.gov:8443/home/publicHomePage.do).

IPCC, Special Report of the IPCC (2012). Managing the risks of extreme events and disasters to advance climate Advance Climate Change Adaptation (SREX). Pp 115-117.

IPCC. (2013). Climate Change 2013: The Physical Science Basis. In T. F. Stocker, D. Qin, G. -K. Plattner, M. Tignor, S. K. Allen, J. Boschung, A. Nauels, Y. Xia, V. Bex & P. M. Midgley (Eds.), Contribution of Working Group I to the Fifth Assessment Report of the Intergovernmental Panel on Climate Change (p. 1535). Cambridge, United Kingdom and New York, NY, USA: Cambridge University Press. doi:10.1017/CBO9781107415324.

Jain, M. K. and Das, D. (2010). Estimation of sediment yield and areas of soil erosion and deposition for watershed prioritization using GIS and remote sensing. Water Resource Management, 24: 2091–2112.

Jansen, L.J.M. and Di Gregorio, A. (1998). The problem of current land cover classifications: Development of a new approach. Proceedings of the Eurostat Seminar on Land Cover and Land Use information Systems for European Union Policy Needs, 21-23 January, Luxembourg, Luxembourg.

Jones, C. G., Ullerstig, A., Willén, U. and Hansson, U. (2004). The Rossby Centre regional atmospheric climate model (RCA). Part I: model climatology and performance characteristics for present climate over Europe, AMBIO, 33, 199–210.

Jones, C., Giorgi, F. and Asrar, G. (2011). The Coordinated Regional Downscaling Experiment: CORDEX, An international downscaling link to CMIP5: CLIVAR Exchanges, No. 56, Vol 16, No.2 pages 34-40. Available from www.clivar.org/sites/default/files/imported/publications/exchanges/Exchanges_56.pdf (also see http://www.cordex.org/).

Julien, P.Y. (2010). Erosion and Sedimentation. 2nd ed. Cambridge University Press, Cambridge.

Jung, G. (2006). Regional Climate Change and the Impact on Hydrology in the Volta Basin of West Africa. PhD. Thesis Institut fur Meteorologie und Klimaforschung, Germany.

Kankam-Yeboah, K., Obuobie, E., Amisigo, B., and Opoku-Ankomah, Y. (2013). Impact of climate change on streamflow in selected river basins in Ghana. Hydrological Sciences Journal, 58(4), 773–788. doi:10.1080/02626667.2013.782101.

Kardel, I., Okruszko, T. (2013). Modelling of discharge , nitrate and phosphate loads from the Reda catchment to the Puck Lagoon using SWAT 45, 125–141.

Kasei, R. A. (2009). Modelling impacts of climate change on water resources in the Volta Basin, West Africa. PhD. Thesis Rheinischen Friedrich-Wilhelms-Universität Bonn. http://hss.ulb.uni-bonn.de/diss_online elektronisch publiziert.

Katz, R.W. (1996). Use of conditional stochastic models to generate climate change scenarios. Climatic Change 32: 237–55.

Kim, J., Waliser, D. E., Mattmann, C. A., Goodale, C. E., Hart, A. F., Zimdars, P. A., Crichton, D. J., Jones, C., Nikulin, G., Hewitson, B., et al. (2013). Evaluation of the CORDEX-Africa multi-RCM hindcast: systematic model errors. Climate Dynamics, pages 1–14.

Kjellström, E., Bärring, L., Gollvik, S., Hansson, U., Jones, C., Samuelsson, P., Rummukainen, M., Ullerstig, A., Willén, U. and Wyser, K. (2005). A 140-year simulation of European climate with the new version of the Rossby Centre regional atmospheric climate model (RCA3). In: Reports Meteorology and Climatology.Volume 108, SMHI, SE-60176 Norrköping, Sweden, 54.

Klutse, N.A.B., Sylla, M.B., Diallo, I., Sarr, A., Dosio, A., Diedhiou, A., Kamga, A., Lamptey, B., Ali, A., Gbobaniyi, E.O., Owusu, K., Lennard, C., Hewitson, B., Nikulin, G., Panitz, H-J., Bucher, M. (2014). Daily characteristics of West African summer monsoon precipitation in CORDEX simulations. Theoretical and Applied Climatology DOI 10.1007/s00704-014-1352-3.

Knisel, W. G. (1980). CREAMS, a field-scale model for chemicals, runoff, and erosion from agricultural management systems. USDA Conservation Research Report No. 26. Washington, D.C.: USDA.

Krämer, P. (2002). The fuel wood crisis in Burkina Faso, solar cooker as an alternative. Solar cooker archive. Ouagadougou, Burkina Faso.

Kupiainen, M., Samuelsson, P., Jones, C., Jansson, C., Willen, U., Hansson, U., Ullerstig, A., Wang, S. and Doscher, R. (2011). Rossby Centre regional atmospheric model, RCA4. Rossby Centre Newsletter, June

Lahmer, W., Pfutzner, B., Becker, A. (2001). Assessment of land use and climate change impacts on the mesoscale. Physics and Chemistry of the Earth Part B 26 (7–8), 565–575.

Lambin, F. E. and Geist, J. (2006). Land-use and land-cover Change, local processes and Global impacts.

Lane, L. J. (1982). Distributed model for small semi-arid watersheds. Journal of Hydraulic Engineering, ASCE, 108(HY10): 1114-1131.

Lane, L.J. (1983). Chapter 19: Transmission Losses. p.19-1–19-21. In Soil Conservation Service. National engineering handbook, section 4: hydrology. U.S. Government Printing Office, Washington, D.C.

Legates, D.R., McCabe, G. J. (1999). Evaluating the use of "goodness of fit" measures in hydrologic and hydroclimatic model validation. Water Resources Research 35(1): 233–241.

Lenderink, G., van den Hurk, B.J.J.M., van Meijgaard, E., van Ulden, A.P. and Cuijpers, H. (2003). Simulation of present-day climate in RACMO2: first results and model developments. KNMI Technical Report 252, 24 p.

Leonard, R. A., W. G. Knisel, and D. A. Still. 1987. GLEAMS: Groundwater loading effects of agricultural management systems. Trans. ASAE 30(5): 1403-1418.

Leopold, L.B., and Thomas, M. (1953). The Hydraulic Geometry of Stream Channels and Some Physiographic Implications. Pp 252. United States Geological Survey. http://pubs.er.usgs.gov/publication/pp252.

Li, K.Y., Coe, M.T., Ramankutty, N., de Jong, R. (2007). Modelling the hydrological impact of land-use change in West Africa. Journal of Hydrology. 337, 258-268, doi:10.1016/j.jhydrol.2007.01.038.

Li, Y., Chen, B.-M., Wang, Z.-G., and Peng, S.-L.(2011). Effects of temperature change on water discharge, and sediment and nutrient loading in the lower Pearl River basin based on SWAT modeling, Hydrological Science Journal., 56, 68–83.

Li, Z., Liu, W., Zhang, X., and Zheng, F. (2009). Impacts of land use change and climate variability on hydrology in an agricultural catchment on the Loess Plateau of China, J. Hydrol., 377, 35–42,2009.

Liang, X., Lettenmaier, D. P., Wood, E. F. and Burges, S. J. (1994). A Simple hydrologically Based Model of Land Surface Water and Energy Fluxes for GSMs, Journal of Geophys. Research., 99(D7), 14,415-14,428.

Liebe, J., Arntz, C., and Vlek P.L.G. (2010). GLOWA Volta Phase 111 completion report.

Lin, Y.P., Hong, N.M., Wu, P.J., Wu, C.F. and Verburg, P.H. (2007). Impacts of land use change scenarios on hydrology and land use patterns in the Wu-Tu watershed in Northern Taiwan. Landscape and Urban Planning, 80 (1–2), 111–126.

Maddock, T. (1975). Table 3.2 in Sediment Engineering, V.A. Vanoni (ed.). ASCE, New York.

Martin, N. (2006). Development of a water balance for the Atankwidi catchment, West Africa – A case study of groundwater recharge in a semi-arid climate. Ecology and Development Series, No. 41. Goettingen, Germany: Cuvillier Verlag. 168p.

Mbaye, M., Hagemann, S., Haensler, A., Stacke, T., Gaye, A. and Afouda, A. (2015) Assessment of Climate Change Impact on Water Resources in the Upper Senegal Basin (West Africa). American Journal of Climate Change, 4, 77-93. doi: 10.4236/ajcc.2015.41008.

McMahon, T.A., Brian, L.F., and Christopher, J.G. (2004). Stream Hydrology: An Introduction for Ecologists. John Wiley and Sons.

Meyer, W.B. and Turner, B.L. II (eds.) (1994). Changes in Land Use and Land Cover: A Global Perspective, 537pp. Cambridge: Cambridge University Press.

Monteith, J.L. (1965). Evaporation and the environment. p. 205-234. In The state and movement of water in living organisms, XIXth Symposium. Soc. For Exp. Biol., Swansea, Cambridge University Press.

Moriasi, D. N., Arnold, J. G., Van Liew, M. W., Bingner, R. L., Harmel, R.D. and Veith, T. L. (2007). Model evaluation guidelines for systematic quantification of accuracy in watershed simulations. Trans. ASABE 50(3): 885-900.

Moss, R. H., Babiker, M., Brinkman, S., Calvo, E., Carter, T., Edmonds, J., Elgizouli, I., Emori, S., Erda, L., Hibbard, K., Jones, R., Kainuma, M., Kelleher, J., Lamarque, J. F., Matthews, M. M. B., Meehl, J., Meyer, L., Mitchell, J., Nakicenovic, N., O'Neill, B., Pichs, R., Riahi, K., Rose, S., Runci, P., Stou_er, R., van Vuuren, D., Weyant, J., Wilbanks, T., van Ypersele, J. P. and Zurek, M. (2008). Towards New Scenarios for Analysis of Emissions, Climate Change, Impacts, and Response Strategies. IPCC Technical Summary, Geneva, Switzerland. Technical Summary, Intergovernmental Panel on Climate Change, WMO, Geneva, Switzerland.

Moss, R. H., Edmonds, J. A., Hibbard, K. A., Manning, M. R., Rose, S. K., van Vuuren, D. P., Carter, T. R., Emori, S., Kainuma, M., Kram, T., Meehl, G. A., Mitchell, J. F. B., Nakicenovic, N., Riahi, K., Smith, S. J., Stou_er, R. J., Thomson, A. M., Weyant, J. P. and Wilbanks, T. J. (2010). The next generation of scenarios for climate change research and assessment. Nature, 463, 747-756, doi:10.1038/nature08823.

Mul, M., Obuobie, E., Appoh, R., Kankam-Yeboah, K., Bekoe-Obeng, E., Amisigo, B., Logah, F.Y., Ghansah, B. and McCartney, M. (2015). Water Resources Assessment of the Volta River Basin (Vol. 166).

Mutchler, C. K., Murphree, C.E. and McGregor, K. C. (1988). Laboratory and field plots for soil erosion studies. In Soil erosion research methods, ed. R. Lal, 9-36. Soil and Water Conservation Society, Ia.

Nagle, G. (2000). Advanced Geography. Oxford University Press, Oxford, UK.

Nash, J.E. and Sutcliffe, J.V. (1970). River flow forecasting through conceptual models, I, A discussion of principles. Journal of Hydrology 10: 282–290.

Neitsch, S. L., Arnold, J. G. Kiniry, J. R. and Williams, J. R. (2005). Soil and Water Assessment Tool Theoretical Documentation, Version 2005. Temple, Tex.: USDA-ARS Grassland, Soil and Water Research Laboratory. Available at: www.brc.tamus.edu/swat/doc.html. Accessed 10/04/2015

Nikulin, G., Jones, C., Giorgi, F., Asrar, G., Büchner,M., Cerezo-Mota, R., Christensen, O. B., Déqué,M., Fernandez, J., Hänsler, A., et al. (2012). Precipitation climatology in an ensemble of CORDEX-Africa regional climate simulations. Journal of Climate, 25(18):6057–6078. doi:10.1175/JCLI-D-11-00375.1.

Obuobie E, Asante-Sasu, C. (2013). River flow under changing climate in Onchocerciasis-endemic Pru and Black Volta River Basins, West Africa. CSIR-Water Research Institute Technical Report No.367.

Obuobie, E. (2008). Estimation of groundwater recharge in the context of future climate change in the White Volta River Basin. Doctoral thesis, Rheinische Friedrich Wilhelms Universität, Bonn/ Germany.

Obuobie, E. and Barry, B. (2012). Burkina Faso. In: Chapter 2 of Groundwater availability and use in Sub-Saharan Africa:A review of 15 countries, eds., Pavelic, P.; Giordano, M.; Keraita, B.; Rao, T.; Ramesh, V. Colombo, Sri Lanka: International Water Management Institute (IWMI). Pp. 7-23p.

Obuobie, E., Barry, B. and Agyekum, W. (2016). Groundwater Resources of the Volta Basin. In: Timothy O. Williams , Marloes L. Mul , Charles A. Biney and Vladimir Smakhtin (eds). The Volta River Basin: Water for Food, Economic Growth and Environment, Routledge, September 2016.

Obuobie, E., Diekkrueger, B. and Reichert, B. (2010). Use of chloride mass balance method for estimating the groundwater recharge in northeastern Ghana, International Journal of River Basin Management, 8:3-4, 245-253, DOI:10.1080/15715124.2010.505895.

Obuobie, E., Kankam-Yeboah, K., Amisigo, B., Opoku-Ankomah, Y., Ofori, D. (2012). Assessment of vulnerability of river basins in Ghana to water stress conditions under climate change. Journal of Water and Climate Change (03.4), pp 276-286, doi: 10.2166/wcc.2012.030.

OCHA, (2007). "Special update on floods in West Africa". Available from http://reliefweb.int/report/ghana/special-update-floods-west-africa-04-oct-2007 [Accessed 4th October, 2007].

Odada, E.O. (2006). Freshwater resources of Africa: major issues and priorities. Global Water News, No. 3. Available at http://www.gwsp.org/downloads/GWSP_NL3_Internet.pdf.

Oguntunde, P. G. (2004) Evapotranspiration and complimentarity relations in the water balance of the Volta Basin: Field measurements and GIS-based regional estimates;. Ecology and Development Series No. 22 Cuvillier Verlag Göttingen, http://www.zef.de/fileadmin/webfiles/downloads/zefc_ecology_development/ecol_dev_22_text.pdf.

Opoku-Ankomah, Y. (2000). Impacts of Potential Climate Change on River Discharge in Climate Change Vulnerability and Adaptation Assessment on Water Resources of Ghana.Water Research Institute (CSIR), Accra. Ghana.

OTT Hydromet (2011). 'Operating instructions. Mobile River discharge measurement system OTT Qliner2'. Technical manual.

Ouedraogo, B. (2006). Household energy preferences for cooking in urban Ouagadougou, Burkina Faso. Energy Policy 34(18), 3787-3795.

Ouedraogo, I., Tigabu1, M., Savadogo, P., Compaore, P.C., Ode'N, H. and Ouadba, J.M. (2010). Land Cover Change and its Relation with Population Dynamics in Burkina Faso, West Africa. Land Degrad.Dev., 21 (5), 453–462.

Owusu, K., Klutse, N.A.B. (2013). Simulation of the rainfall regime over Ghana from CORDEX. International Journal of Geosciences, 4,785-791.

Oyebande, L. and Odunuga, S. (2010). Climate Change impact on water resources at the transboundary level in West Africa: The Cases of the Senegal, Niger and Volta Basins. The Open Hydrology Journal, 4,163-172.

Paeth, H., Hall, N.M.J., Gaertner, M.A., Alonso, M.D., Moumouni, S., Polcher, J., Ruti, P.M., Fink, A.H., Gosset, M., Lebel, T., Gaye, A.T., Rowell, D.P., Moufouma-Okia, W., Jacob, D., Rockel, B., Giorgi, F., Rummukainen, M. (2011). Progress in regional downscaling of West African precipitation. Atmospheric Science Letters doi:asl.306., 12, 75-82.

Panitz, H.J., Dosio, A., Büchner, M., Lüthi, D. and Keuler, K. (2014). COSMO-CLM (CCLM) climate simulations over CORDEXAfrica domain: analysis of the ERA-Interim driven simulations at 0.44 and 0.22 resolution. Climate Dynamics. doi:10.1007/ s00382-013-1834-5.

Parry, M.L. et al. (2007). Climate change 2007: Impacts, adaptation and vulnerability. Contribution of Working Group II to the Fourth Assessment Report of the Intergovernmental Panel on Climate Change (IPCC). Cambridge, Cambridge University Press.

Parsons, A.J. and Stromberg, S.G.L. (1998). Experimental analysis of size and distance of travel of unconstrained particles in interrill flow. Water Resources Research, 34, pp. 2377–2381.

Patra, K.C. (2001). Hydrology and water resources engineering. Pangbourne, UK: Alpha Science International.

Persson, G., Bärring, L., Kjellström, E., Strandberg, G. and Rummukainen, M. (2007). Climate indices for vulnerability assessments. Meteorology and Climatology 111. SMHI, SE-601 76 Norrköping, Sweden, 64 pp.

Phan, D. B.,Wu, C. C., and Hsieh, S. C.(2011). Impact of climate change on stream discharge and sediment yield in Northern Viet Nam, Water Research., 38, 827–836.

Priestley, C.H.B and Taylor, R.J. (1972). On the assessment of surface heat flux and evaporation using large scale parameters. Mon. Weather Rev. 100, p. 82 – 92.

Prowse, T.D. et al. (2006). Climate change, flow regulation and land-use effects on the hydrology of the Peace-Athabasca-Slave system; findings from the northern rivers ecosystem initiative. Environmental Monitoring and Assessment 113,167–197.

Qi, S., Sun, G., Wang, Y., McNulty, S. G. and Myers, J. A. M. (2009). Streamflow response to climate and landuse changes in a coastal watershed in North Carolina. Transactions of the ASABE, 52, 739-749.

Räisänen, J., Hansson, U., Ullerstig, A., Döscher, R., Graham, L.P., Jones, C., Meier, M., Samuelsson, P. and Willén, U. (2003). GCM driven simulations of recent and future climate with the Rossby Centre coupled atmosphere – Baltic Sea regional climate model RCAO. Reports Meteorology and Climatology 101, SMHI, SE 60176 Norrköping, Sweden, 61 pp.

Räisänen, J., Hansson, U., Ullerstig, A., Döscher, R., Graham, L.P., Jones, C., Meier, H.E.M., Samuelsson, P. and Willén, U. (2004). European climate in the late 21st century: regional simulations with two driving global models and two forcing scenarios. Climate Dynamics, 22, 13-31.

Rantz, S.E., et al. (1982). Measurement and computation of streamflow: Volume 1. Measurement of stage and discharge and Volume 2. Computation of discharge: U.S. Geological Survey Water-Supply Paper 2175, 631 p.

Refsgaard, J. C. (1997). Parameterisation, calibration, andvalidation of distributed hydrological models. J. Hydrol., 198(1),69-97. http://dx.doi.org/10.1016/S0022-1694(96)03329-X.

Riahi, K., Rao, S., Krey, V., Cho, C., Chirkov, V., Fischer, G., Kindermann, G., kicenovic, N. and Rafaj, P. (2011). RCP8.5—A scenario of comparatively high greenhouse gas emissions, Climate Change, 109, 33–57. doi:10.1007/s10584-011-0149-y.

Riebsame, W. E., Meyer, W. B., and Turner II, B. L. (1994). Modelling Land Use and Cover as Part of Global Environmental Change. Climate Change 28, 45–64.

Rockel, B., Will, A., and Hense, A. (2008). The Regional Climate Model COSMO-CLM (CCLM),Meteorologische Zeitschrift, 17, 347–348.

Rodgers, C, van de Giesen N, Laube W, Vlek P.L.G, Youkhana, E. (2007). The GLOWA Volta project: A framework for water resources decision-making and scientific capacity building in a transnational West African Basin. In: E. Craswell, M. Bonell, D. Bossio, S. Demuth, and N. van de Giesen (Editors), Intergrated assessment of water resources and global change (A north-south analysis). Springer, p.295-313.

Rogelji, J., Meinshausen, M., and Knutti, R., (2012). Global Warming Under Old and New Scenarios Using IPCC Climate Sensitivity Range Estimates. Nature Climate Change, 2:248. http://dx.doi.org/10.1038/nclimate1385.

Rosenzweig, C.E., Tubiello, F., Goldberg, R. and Bloomfield, J. (2002). Increased crop damage in the US from excess precipitation under climate change. Global Environmental Change, 12, 197-202.

Rummukainen, M., Räisänen, J., Bringfelt, B., Ullerstig, A., Omstedt, A., Willén, U., Hansson, U. and Jones, C. (2001). A regional climate model for northern Europe: model description and results from the downscaling of two GCM control simulations. Climate Dynamics, 17, 339-359.

Rummukainen, M., Räisänen, J., Ullerstig, A., Bringfelt, B., Hansson, U., Graham, P. and Willén, U. (1998). RCA – Rossby Centre regional Atmospheric climate model: model description and results from the first multi-year simulation, Reports Meteorology and Climatology 83, SMHI, SE-601 76 Norrköping, Sweden, 76 pp.

Ruti, P. M. and Dell'Aquila, A. (2010). The twentieth century African easterly waves in reanalysis systems and IPCC simulations, from intra-seasonal to inter-annual variability. Climate Dynamics , 35, 1099-1117.

Salathe, E. P. (2003). Comparison of various precipitation downscaling methods for the simulation of streamflow in a rainshadow river basin. International Journal of Climatology 23: 887–901.

Samuelsson, P., Jones, C.G., Willen, U., Ullerstig, A., Gollvik, S., Hansson, U., Jansson, C., Kjellstrom, E., Nikulin, G. and Wyser, K. (2011). The Rossby Centre Regional Climate model RCA3: model description and performance. Tellus Series A – Dynamic Meteorology and, 63, 1, 4-23, doi: 10.1111/j.1600-0870.2010.00478.x.

Santhi, C., Arnold, J.G., Williams, J.R., Dugas, W.A., Srinivasan, R. Hauck, L.M. (2001). Validation of the SWAT Model on a Large River Basin with Point and Nonpoint Sources, Journal of the American Water Resources Association, 37(5), pp 1169-1188.

Sarr, A.M., Seidou, O. and Tramblay, Y. (2015). Comparison of downscaling methods for mean and extreme precipitation in Senegal. Journal of Hydrology: Regional Studies (4): 369-385.

Sawai, N., Kobayashi, K., Apip, Takara, K., Ishikawa, H., Yokomatsu, M., Samaddar, S., Juati, A-N., Kranjac-Berisavljevic, G. (2014). Impact of Climate Change on River flows in the Black Volta River. Journal of Disaster Research, 9,4, p 432-442.

Schoul, J and Abbaspour, K. C. (2006). "Calibration and uncertainty issues of a hydrological model (SWAT) applied to West Africa," Advances in Geosciences,pp. 137-143.

Schulla, J. (1997). Hydrologische Modellierung von Flussgebieten zur Absch¨atzung der Folgen von Klima¨anderungen., Z¨uricher Geographische Schriften, Z¨urich.

Shrestha, B., Babel, M. S., Maskey, S., van Griensven, A., Uhlenbrook, S., Green, A., and Akkharath, I. (2013). Impact of climate change on sediment yield in the Mekong River basin: a case study of the Nam Ou basin, Lao PDR, Hydrol. Earth Syst. Sci., 17, 1-20, doi:10.5194/hess-17-1-2013.

Singh, J., Knapp, H. V. and Demissie. M. (2004). Hydrologic modeling of the Iroquois River watershed using HSPF and SWAT. ISWS CR 2004-08. Champaign, Ill.: Illinois State Water Survey. Availableat: www.sws.uiuc.edu/pubdoc/CR/ISWSCR2004-08.pdf. Accessed 8 September 2005.

Sloan, P.G. and Moore, I.D. (1984). Modelling subsurface stormflow on steeply sloping forested watersheds. Water Resources Research. 20(12), p. 1815-1822.

Sloan, P.G., Morre, I.D., Coltharp, G.B. and Eigel, J.D. (1983). Modelling surface and subsurface stormflow on steeply-sloping forested watersheds. Water Resources Inst. Report 142. Univ. Kentucky, Lexington.

Soil Conservation Service (1972). Section 4: Hydrology. In: National Engineering Handbook. SCS.

Sood, A., Muthuwatta, L. and McCartney, M. (2013). A SWAT evaluation of the effect of climate change on the hydrology of the Volta River basin, Water International, 38:3, 297-311, DOI: 10.1080/02508060.2013.792404.

Steppeler, J., Doms, G., Sch¨attler, U., Bitzer, H., Gassmann, A., Damrath, U., and Gregoric, G.(2003). Meso-gamma scale forecasts using the nonhydrostatic model LM, Meteorology and Atmospheric Physics, 82, 75–96, doi:10.1007/s00703-001-0592-9.

Stonestrom, D. A., Scanlon, B. R., and Zhang, L. (2009). Introduction to special section on Impacts of Land Use Change on Water Resources, Water Resources Research, 45, W00A00,doi:10.1029/2009WR007937.

Strandberg, G., B¨arring, L., Hansson, U., Jansson, C., Jones, C., Kjellstr ¨om, K., Kolax, M., Kupiainen, M., Nikulin, G., Samuelsson, P., Ullerstig, A. and Wang, S. (2014). CORDEX scenarios for Europe from the Rossby Centre regional climate model RCA4. Reports Meteorology and Climatology 999, SMHI, SE-601 76 Norrk¨oping, Sweden.

Sylla MB, Elguindi N, Giorgi F and Wisser D (2015a). Projected Robust Shift in Climatic Zones over West Africa in Response to Anthropogenic Climate Change for the Late 21st Century. Climatic Change (under review).

Sylla MB, Giorgi F, Pal JS, Gibba P, Kebe I and Nikiema M (2015b). Projected Changes in the Annual Cycle of High Intensity Precipitation Events over West Africa for the Late 21st Century. Journal of Climate, 28(16), 6475–6488.

Sylla, M. B., Dell'Aquila, A., Ruti, P.M. and Giorgi, F. (2010). Simulation of the Intraseasonal and the Interannual Variability of Rainfall over West Africa with a Regional Climate Model (RegCM3) during the Monsoon Period. International Journal of Climatology doi:joc.2029., 30, 1865-1883.

Sylla, M. B., Giorgi, F., Ruti, P. M., Calmanti, S. and Dell'Aquila. A. (2011). The impact of deep convection on the West African summer monsoon climate: a regional climate model sensitivity study. Quarterly Journal of Royal Meteorological Society doi:qj. 853., 137, 1417-1430.

Sylla, M.B., Nikiema, P.M., Gibba, P., Kebe, I., and Klutse, N.A.B. (2016). Climate Change over West Africa : Recent Trends and Future Projections Climate Change over West Africa : Recent Trends and Future Projections. doi:10.1007/978-3-319-31499-0.

Tebaldi C. and Knutti, R. (2007). "The use of the multi-model ensemble in probabilistic climate projections," Philosophical Transactions of the Royal Society A, vol. 365, no. 1857, pp. 2053–2075.

Themeßl, M., Gobiet, A. and Leuprecht, A., 2011. Empirical-statistical downscaling and error correction of daily precipitation from regional climate models. *International Journal of Climatology*, 31, 1531–1544.

Tilrem, A.O. (1979). Sediment transport in streams sampling, analysis and computation. Manual on procedures in operational hydrology. Volume 5, 110p.

Tu, T. (2009). Combined impact of climate and land use changes on streamflow and water quality in eastern Massachusetts, USA, J. Hydrol., Vol. 379, pp.268-283.

UNESCO World Water Assesssment Programme (UNESCO-WWAP), (2006). Water: A Shared Responsibility. United Nations, New York.

United Nations (2012). The Millennium Development Goals Report, United Nations, New York. http://www.un.org/.

United Nations Committee on Economic Social and Cultural Rights, (2003). General Comment No. 15 (2002). The Right to Water. E/C.12/2002/11, United Nations Social and Economic Council, 18 pp.

USDA US Department of Agriculture, Agricultural Research Service Texas (2012). SWAT - Soil and Water Assessment Tool. URL: http://swat.tamu.edu/software/arcswat/.

van de Giesen, N.C, Andreini M, van Edig A, Vlek, P.L.G. (2001). Competition for water resources of the Volta basin. Regional Management of Water Resources. Proceedings of a symposium held during the Sixth IAHS. Scientific Assembly atMaastricht, the Netherlands, July 2001. IAHS Publ. no. 268.

Van Griensven, A. and Meixner, T. (2006). Methods to quantify and identify the sources of uncertainty for river basin water quality models. Water Science and Technology, 53(1): 51-59.

van Meijgaard, E., van Ulft, L. H., van de Berg, W. J., Bosveld, F. C., van den Hurk, B., Lenderink, G. and Siebesma A. P. (2008). The KNMI regional atmospheric climate model RACMO version 2.1, Technical Report 302.

van Vuuren, D. P., et al. (2011b). RCP2.6: Exploring the possibility to keep global mean temperature increase below 2 °C, Climate Change., 109,95–116. Doi:10.1007/s10584-011-0152-3.

van Vuuren, D. P., et al. (2011c): The representative concentration pathways: An overview. Climatic Change, 109, 5-31.

van Vuuren, D.P., Edmonds, J., Kainuma, M., Riahi, K., Thomson, A., Hibbard, K., Hurtt, G.C., Kram, T., Krey, V., Lamarque, J.-F., Masue, T., Meinshausen, M., Nakicenovic, N., Smith, S. and Rose, S.K. (2011a). The Representative Concentration Pathways: An Overview. Climatic Change, 109:1-2:5. http://dx.doi.org/10.1007/s10584-011-0148-z.

VBA Geoportal (2015). 131.220.109.2/geonetwork. Accessed 4th August, 2015.

Vizy, E. and Cook, K. (2002). Development and application of a mesoscale climate model for the tropics: influence of sea surface temperature anomalies on the West African monsoon. Journal of Geophysical Research 107(D3):4023, doi:JD000686

Volta Basin Profile (2005). Baseline Report No. 8. Volta River Basin: Enhancing agriculture water productivity through strategic research.

von Storch, H., Zorita, E., Cubasch, U. (1993). Downscaling of global climate change estimates to regional scales: an application to Iberian rainfall in wintertime. Journal of Climate 6 (6), 1161–1171.

Vrugt, J. A., Gupta, H. V. Bouten, W. and Sorooshian, S. (2003). A shuffled Complex Evolution Metropolis Algorithm for Estimating Posterior Distribution of Watershed Model Parameters, in Calibration of Watershed Models , ed. Q. Duan, S. Sorooshian, H. V. Gupta, A. N. Rousseau, and R. Turcotte, AGU Washington DC, DOI: 10.1029/006WS07.

Walling, D. E. (1977). Assessing the Accuracy of Suspended Sediment Rating Curves for a Small Basin. Water Resources Research 13 (3): 531–38. doi:10.1029/WR013i003p00531.

Walling, D. E. (2008) The changing sediment load of the Mekong River, Ambio, 37, 150–157.

Walling, D.E. (1994). Measuring sediment yield from river basins in Lal, R. ed., Soil Erosion Research Methods. Soil and Water Conservation Society, Ankeny, IA.

Ward, P.J.,van Balen, R.T., Verstraeten, G., Renssen, H., Vandenberghe, J. (2009).The impact of land use and climate change on late Holocene and future suspended sediment yield of the Meuse catchment. Geomorphology.103, 389–400.

Wasson, R.J., L.J. Olive, Rosewell, C.J. (1996). Rates of erosion and sediment transport in Australia. D.E. Walling, R. Webb (Eds.), Erosion and Sediment Yield: Global and Regional Perspectives, pp. 139–148 (IAHS Publication No. 236).

Water Resource Commission (2016). Rain Water Harvesting Strategy, Final Report 2011. 45pp. www.wrc-gh.org/dmsdocument/25.

Wilby, R.L., Charles, S.P., Zorita, E. and Timbal, B., Whetton, P., Mearns, L.O. (2004). The guidelines for use of climate scenarios developed from statistical downscaling methods. http://ipcc-ddc.Cru.Uea.ac.uk/guidelines/Stat- Down_Guide.pdf.

Wilby, R.L., Conway, D. and Jones, P.D. (2002). Prospects for downscaling seasonal precipitation variability using conditioned weather generator parameters. Hydrological Processes, 16, 1215-1234.

Wilk, J. and Hughes, D. A. (2002). Simulating the impacts of land-use and climate change on water resource availability for a large south Indian catchment. Hydrological Science Journal, 47(1), 19–30.

Williams, J. R. (1975). Sediment-Yield Prediction with Universal Equation Using Runoff Energy Factor.In Present and Prospective Technology for Predicting Sediment Yields and Sources, Agricultural Research Service, ARS-S-40, 244-252. Washington, DC: U.S. government Printing Office.

Williams, J.R. (1995). Chapter 25. The EPIC Model. In Computer Models of Watershed Hydrology. Water Resources Publications. Highlands Ranch, CO. p. 909-1000.

Winchell, M., Srinivasan, R., Di Luzio, M., Arnold, J. (2010). ArcSWAT Interface for SWAT2009. User's Guide. Blackland Research Center, Texas Agricultural Experiment Station and Grassland, Soil and Water Research Laboratory, USDA Agricultural Research Service, Temple, Texas.

Wischmeier, W. H. and Smith, D. D. (1978). Predicting rainfall erosion losses - A guide to conservation planning. Agricultural Handbook 537. USDA. Washington (DC): 58pp.

Wischmeier, W.H. and Smith, D.D. (1965). Predicting rainfall-erosion losses from cropland east of the Rocky Mountains. Agriculture Handbook 282. USDA-ARS.

World Resources Institute (2003). Watersheds of Africa: Water Resources eAtlas Land Cover and Use Variables: A19 Volta.

Xu C.Y. (1999). Review Paper, Climate change and hydrologic models: A review of existing gaps and recent research developments. Water Resources Management, 13: 369–382.

Yang, J., Reichert, P., Abbaspour, K.C., Xia, J. and Yang, H. (2008). Comparing uncertainty analysis techniques for a SWAT application to Chaohe Basin in China. Journal of Hydrology., 358: 1-23.

Yves Tramblay, Andre St-Hilaire and Taha B. M. J. Ouarda (2008). Frequency analysis of maximum annual suspended sediment concentrations in North America / Analyse fréquentielle des maximums annuels de concentration en sédiments en suspension en Amérique du Nord, Hydrological Sciences Journal, 53:1, 236-252, DOI: 10.1623/hysj.53.1.236.

Zhang, W., Wei, X., Jinhai, Z. Yuliang, Z. and Zhang, Y. (2012). Estimating Suspended Sediment Loads in the Pearl River Delta Region Using Sediment Rating Curves. Continental Shelf Research 38 (April): 35–46. doi:10.1016/j.csr.2012.02.017.

Zhu, Y.-M., Lu, X. X., and Zhou, Y. (2008). Sediment flux sensitivity to climate change: a case study in the Longchuanjiang catchment of the upper Yangtze River, China, Global Planet. Change, 60, 429–442.

ANNEX 1 (Research Article in International Journal of Current Engineering and Technology)

Trend analysis in observed and projected precipitation and mean temperature over the Black Volta Basin, West Africa

Fati Aziz[†*] and Emmanuel Obuobie[‡]

[†]Laboratoire d'Hydrologie Appliquée, Universite D'Abomey-Calavi, Benin Republic
[‡]Water Research Institute, Council for Scientific and Industrial Research (CSIR), Ghana

Received 02 May 2017, Accepted 01 July 2017, Available online 02 July 2017, **Vol.7, No.4 (Aug 2017)**

Abstract

The study analyzed the trends in observed (1981-2010) and future projected annual precipitation and mean temperature over the Black Volta River Basin using the Mann-Kendall test and the Sen's slope estimator. Projected changes in precipitation and temperature by multi-model ensemble runs over the Black Volta basin for the late (2051-2075) and end of the 21st century (2076-2100) horizons under two IPCC Representative Concentration Pathways (RCP4.5 and RCP8.5) scenarios was also analyzed. The results showed statistically significant (at the 5% significance level) increase of 111mm in the annual rainfall over the observed period. The future direction of this trend is uncertain as some ensemble members projected positive trends while others gave negative trends. However, both the positive and negative future trends in the rainfall were statistically non-significant. The results also showed that the studied basin has warmed over the observed period, with significant increase of 0.9°C in the mean annual temperature. Similarly, significant increasing trend in the mean annual temperature are projected by the ensemble runs under both RCPs for the late and end of the 21st century. Analyses of the average annual, intra-annual and seasonal precipitation indicated high uncertainty regarding the direction of the future rainfall. Mean annual precipitation change for the late 21st century ranged between -16% and +6% under the RCP4.5 scenario and between -27% and +14% under the RCP8.5 scenario. The end of the 21st century projections showed changes in mean precipitation amounts ranging between -23% and +2% and between -33% and +13% under the RCP4.5 and RCP8.5 scenarios, respectively. With regards to temperature, average annual projections by the ensemble runs showed increases over the basin under both RCP scenarios and for both time periods. Warming over the basin is projected to be higher under the RCP8.5 scenario than under the RCP4.5 scenario, with the end of 21st century period being warmer than the late 21st century. Average annual mean temperature increase across the model run ranged between 2.2^{o}C and 2.6^{o}C under the RCP4.5 scenario and between 3.5^{o}C and 3.7^{o}C under the RCP8.5 scenario for the end of the 21st century.

Keywords: *Climate change, precipitation, temperature, CORDEX West Africa, Black Volta Basin*

1. Introduction

The IPCC highlighted in their Fifth Assessment Report that each of the last three decades has been successively warmer at the Earth's surface than any preceding decade since 1850 (IPCC, 2014a). Indeed, the effects of rising temperatures are being felt globally and there is increasing pressure to put in effective and practicable adaptation measures at the regional and local levels. In West Africa, for example, temperatures are projected to increase by between 3°C and 6°C by the end of the 21st century under a range of scenarios. Whereas rainfall projections for the region are less certain many global models project a wetter main rainfall season with a slight delay in the start of the rainfall season towards the end of the 21st century (CDKN, 2014). Changes in climate are expected to increase the pressure on water availability, affect food security and impact on human health in the region (IPCC 2013, IPCC 2014b).

The Black Volta River Basin in West Africa supports economic activities such as agriculture, hydro-power generation and domestic water supply in Burkina Faso, Cote D'lvoire and Ghana. These hydrological benefits are threatened by global change (Kasei, 2009). Therefore, information on the current climate as well as the projected changes in the future can be useful for the sustainable development and management of water and other natural resources in the region.

In the past, climate projections over West Africa were limited in part by the coarse resolution of GCMs (normally 100–400 km resolution) as well as the large spread among GCM projections (Hoerling *et. al.*, 2006; Giannini *et al*., 2008). More recently, however, the Coordinated Regional Downscaling EXperiment (CORDEX), an initiative founded by the World Climate Research Program of the World Meteorological Organization produced an ensemble of high-resolution historical and future climate projections at regional scales (Giorgi *et al*. 2009; Jones *et al*. 2011). For the Africa domain, the RCM simulations are at a grid resolution of 0.44°x 0.44° (approximately 50 km), which is an improvement over previous simulations for Africa. Studies conducted over the entire African continent (e.g. Nikulin *et al*., 2012; Panitz *et al*., 2014; Kim *et al*., 2014 and Dosio *et al*., 2015) and at the regional level (e.g. Klutse *et al*., 2014; Abiodun *et al*., 2015 and Endris *et al*., 2015) have shown that CORDEX RCMs simulate well the spatial and temporal distributions of the West African precipitation, with some seasonal and sub-regional biases.

In this study we analyzed the trends in historical (1981-2010) annual precipitation and mean temperature over the Black Volta River Basin using the Mann-Kendall test and Sen's slope estimator. The study also analyzed 12 ensemble runs together with 4 ensemble means of the runs generated from the combination of 2 RCMs driven by 3 GCMs for the IPCC medium-low (RCP4.5) and high (RCP8.5) emission scenarios for the late 21st century (2051-2075) and end of the 21st century (2076-2100). The trends in the projected annual precipitation and mean temperature were also evaluated.

2. Materials and Methods

2.1 Study area

The Black Volta River Basin (BVRB) is a major sub-basin of the Volta River Basin in West Africa. It is located between Latitude 7.0°N and 14.0°N and Longitude 5.3°W and 1.3°W

(Annor, 2012). The basin is shared by Ghana, Burkina Faso, Cote D'Ivoire and Mali (Figure 1) and has a total area of about 142,056 km^2. The annual climate in the basin is characterized by two distinct periods of wet or rainy season and the dry season. Rainfall pattern in the northern half of the basin is mono-modal with peak in August/September while the South has a bi-modal pattern with peaks in May/June and August/September. The mean annual rainfall varies from less than 500mm in the extreme north of the basin in Mali to about 1,350 mm in the forested areas in south-eastern Ghana (MWH, 1998). About three-quarters of the annual rainfall occur between May and September (Obuobie *et al*., 2017). Studies in the evolution of rainfall in West Africa where the BVRB is located revealed that the region suffered strong rainfall deficit in the 1970's following wet periods in the 1950s and 1960s (Hubert and Carbonnel, 1987; Mahe *et al*., 2001; Nicholson and Palao, 1993; Nicholson, 2000). According to recent studies (Druyan, 2011; Ibrahim *et al*., 2014; Sylla *et al*., 2016) precipitation over some parts of West Africa has seen some recovery since the 1980s.

Average monthly minimum temperature in the basin ranges between 18^{o}C to 25^{o}C while average maximum temperatures range from 30^{o}C to 37^{o}C. Agriculture represents the main economic activity of the basin, with the most commonly cultivated crops (usually under rain-fed conditions) being millet, sorghum, maize, groundnuts and yams (Barry et. al., 2005). The Basin's population was approximately 4.5 million in 2000 and projected to reach 8 million by 2025 (Annor, 2012). The population density ranges between 8 and 123 people/km2 (Allwaters Consult, 2012), and the population growth rate, around 3% per annum (Green Cross International, 2001).

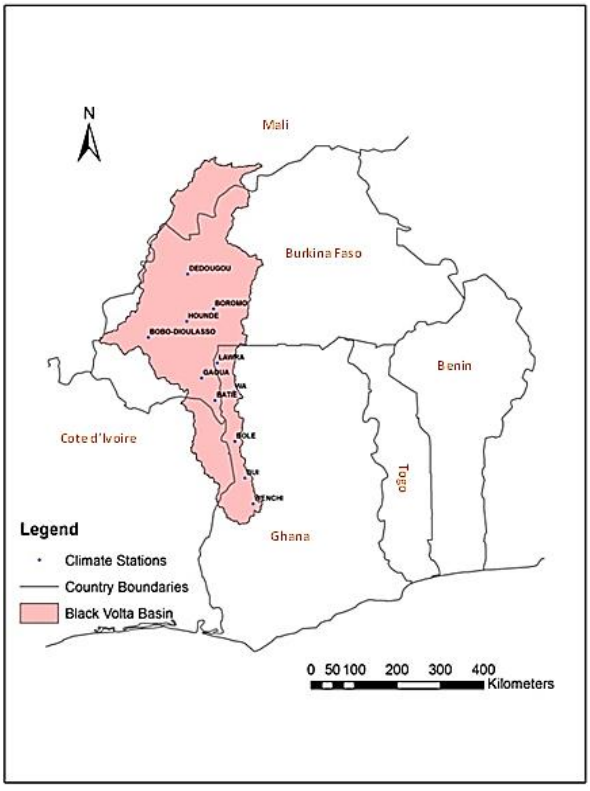

Fig.1 Map of Black Volta Basin with Meteorological stations used in the study

2.2 Data set and model description

The data used in this study included observed (1981-2010) precipitation and mean temperature series for eleven climate stations (Table 1) in the BVRB obtained from the Meteorological Agencies in Ghana and Burkina Faso. Model simulation data covering 1981-2005 (control period) and 2051-2100 (future period) for RCP 4.5 and RCP 8.5 were obtained from the CORDEX West African project. As mentioned earlier, the simulation data consisted of projections from 2 RCMs driven by 3 GCMs for a total of 3RCM/GCM pairs (Table 2). The 2 RCMs, were the Rossby Centre of the Swedish Meteorological and Hydrological Institute (SMHI) regional climate model - fourth generation (RCA4) and the Regional Atmospheric Climate Model (RACMO). Simulations from these models were used as they were the only data available to us at the time of the study. The RCA4 is based on HIRLAM, a numerical weather prediction model and is an improvement of the RCA3 (Samuelsson *et al*. 2011). It has undergone physical and technical changes to make it applicable for any domain worldwide (Strandberg *et al*., 2014). Within the CORDEX project framework, the SMHI applied the RCA4 model to (Strandberg *et al*., 2014) downscale the ERA-Interim Reanalysis (1980-2010) and eight (8) different GCMs from the Coupled Model Intercomparison Project 5 (CMIP5) archives over the African domain (Jones *et al*., 2011, Nikulin *et al*., 2012). The data are available for RCP 2.6, RCP4.5 and 8.5 and cover the period 1951-2100. The Regional Atmospheric Climate Model (RACMO) is on the other hand a hydrostatic limited-area model developed and maintained by the modeling group at the Royal Netherlands Meteorological Institute (KNMI) (van Meijgaard *et al*., 2008). The first version of the model, RACMO1 combines the HIRLAM model with the physics of ECHAM4. The second version, RACMO2, was developed based on the ECMWF-NWP release cy23r4 and the Numerical Weather Prediction (NWP) model HIRLAM version 5.0.6 (Lenderink *et al*., 2003). Climate change simulations generated with RACMO22T model, driven by the EC-EARTH for RCP 4.5 and 8.5 within the CORDEX project are used in this study.

Table 1 Climate stations used in this study

No.	Station Name	Latitude (°)	Longitude (°)
1	Batie (BF)	9.86	-2.9
2	Bobo-Dioulasso (BF)	11.17	-4.3
3	Bole (GH)	9.03	-2.48
4	Boromo (BF)	11.73	-2.92
5	Bui (GH)	8.28	-2.27
6	Dedougou (BF)	12.46	-3.48
7	Gaoua (BF)	10.33	-3.18
8	Hounde (BF)	11.48	-3.5
9	Lawra (GH)	10.63	-2.85
10	Wa (GH)	10.05	-2.5
11	Wenchi (GH)	7.75	-2.1

*BF=Burkina Faso; GH=Ghana

Table 2 RCMs with driving GCMs from CORDEX used in this study

Regional Climate Model (RCM)	Global Climate Model (GCM)	GCM/RCM Combination
RCA4 (SMHI) (Samuelsson *et al*. 2011; Kupiainen *et al*. 2011; Strandberg *et al*. 2014)	MPI-ESM-LR (MPI-M)(Stevens *et al*. 2013)	RCA4/ MPI-ESM-LR
RCA4 (SMHI) (Samuelsson *et al*. 2011; Kupiainen *et al*. 2011; Strandberg *et al*. 2014)	CCCma-CanESM2 (Chylek *et al*., 2011)	RCA4/CCCma-CanESM2
KNMI Regional Climate Model, (RACMO22T) (van Meijgaard *et al*. 2008)	ICHEC-EC-EARTH (Hazeleger *et al*. 2010)	RACMO22T/ ICHEC-EC-EARTH

2.3 Trend analysis of observed and projected annual precipitation and mean temperature

Assessment of trends in observed (1981-2010) and projected (2051-2075 and 2076-2100) annual precipitation and mean temperature over the basin was carried out using the non-parametric Mann-Kendall (MK) test (Mann, 1945; Kendall 1975; Gilbert 1987). The MK test has been widely applied in analyzing trends in climatologic and hydrologic time series (Mavromatis and Santhis, 2011; Karpouzos *et al*., 2010; Yue and Wang 2004). According to the test, a null hypothesis H_0, which assumes that there is no trend in the series (the data is independent and randomly ordered), is tested against an alternative hypothesis, H_1, which assumes otherwise (Onoz and Bayazit, 2012). For this study, the null hypothesis was tested at the significance level $\alpha=0.05$ for both annual precipitation and mean temperature. P-values less than 0.05 indicated the existence of statistically significant trends while P-values greater than 0.05 indicated that trends in the series were statistically insignificant. The magnitude (slope) of the trends were estimated using the Sen's slope estimator (Sen, 1968). A brief explanation of the procedure for the MK test and the Sen's estimator are presented in Annex 1A and 1B respectively. The trend analysis was performed at the basin scale. The basin data on rainfall and temperature were obtained as averages of data from the 11 climate stations used in the study.

2.4 Statistical downscaling/bias correction and generation of ensemble runs

The statistical downscaling/bias-correction of the future precipitation and temperature data obtained from the RCMs for the eleven (11) climate stations were done with the Quantile-Quantile (Q-Q) transformation technique (Maraun *et al*., 2010; Themeßl *et al*., 2011). Prior to its use on the future climate data, the Q-Q technique was adapted to each station using the statistics of the observed climate at the stations. The Q-Q transformation procedure is described in detail by Amadou *et al*., (2015) and Sarr *et al*., (2015). A brief description is given in Annex 1C. Twelve ensemble runs consisting of RCM/GCM outputs for the RCP 4.5 and RCP 8.5 were generated for the two 25-year periods: 2051-2075 (referred to as the late 21st century or 2060s) and 2076-2100 (the end of the 21st century or 2080s). Four additional scenarios based on the ensemble mean of the RCM/GCM pairs were also generated. In total, sixteen ensemble runs were formed (Table 3) and used in the analysis.

Table 3 Model scenarios used in this study

Scenario Number	Model Scenarios
1	RACMO22T/ICHEC-EC-EARTH (RCP4.5/2060s)
2	RACMO22T/ICHEC-EC-EARTH (RCP4.5/2080s)
3	RACMO22T/ICHEC-EC-EARTH (RCP8.5/2060s)
4	RACMO22T/ICHEC-EC-EARTH (RCP8.5/2080s)
5	RCA4/CanESM2 (RCP4.5/2060s)
6	RCA4/CanESM2 (RCP4.5/2080s)
7	RCA4/CanESM2 (RCP8.5/2060s)
8	RCA4/CanESM2 (RCP8.5/2080s)
9	RCA4/MPI-ESM-LR (RCP4.5/2060s)
10	RCA4/MPI-ESM-LR (RCP4.5/2080s)
11	RCA4/MPI-ESM-LR (RCP8.5/2060s)
12	RCA4/MPI-ESM-LR (RCP8.5/2080s)
13	Ensemble of RCMs (RCP4.5/2060s)
14	Ensemble of RCMs (RCP4.5/2080s)
15	Ensemble of RCMs (RCP8.5/2060s)
16	Ensemble of RCMs (RCP8.5/2080s)

2.5 Assessment of model-uncorrected-simulation and model-corrected –simulation against observed climate

Plots of average monthly precipitation and temperature of the model- uncorrected and -corrected data were made at one of the stations of the Basin (Bobo-Dioulasso) and compared with plots of the observed data to assess the superiority of the corrected data over the uncorrected. The comparison was also to establish the importance of bias correction in climate change assessment study. The assessment was done by comparing the annual mean values, and standard deviations of the model-uncorrected and –corrected data to the observed data. In addition, plots of monthly precipitation, monthly mean temperature, and probability of

exceedence of defined precipitation classes were made to assess the accuracy with which the model-uncorrected and –corrected data mimic the observed.

2.6 Estimation of changes in precipitation and temperature

Projected changes in precipitation and mean temperature over the basin were assessed under the RCP 4.5 and RCP 8.5 scenarios using the downscaled and bias-corrected RCM runs for the late- and end of the 21st century. Relative changes (%) were calculated for precipitation while absolute changes (^{o}C) were computed for the mean temperature. The changes were determined and discussed at the annual, intra-annual and seasonal time steps. Prior to analysis, the bias-corrected data from the 11 climate stations were averaged to obtain basin average data.

3. Results and discussion

3.1 Trends in observed annual precipitation and temperature

Trend analysis of annual precipitation over the basin revealed a statistically significant increase (Sen's slope = 3.7 mm/year, p-value = 0.02;) of 111mm over the 30-year period (1981-2010). The lowest annual precipitation in the observed period was 744mm (1981) and highest, 1188mm (1991) as shown in Figure 2. Our findings of increasing precipitation in the Black Volta is in agreement with findings of Sylla *et al*. (2016), which observed statistically significant positive trends in precipitation over West Africa. The aforementioned study noted that Burkina Faso, located in the northern half of our study area, is one of the countries which experienced an increase in precipitation during the 1983-2010 period. In a similar study, Maidement *et al*. (2015) reported statistically significant increases in annual rainfall across the Sahel between 1983 and 2010. Other studies in the Sahel by Nicholson (2005), Mahé and Paturel (2009) and more recently Ibrahim *et al*. (2014) for example also revealed that annual precipitation in the region has increased since the end of the 1990s.

Consistent with the IPCC report (IPCC, 2013) the analysis of observed mean temperature over the BVRB indicated a statistically significant increase (5% level of significance; p-value = 0.00; Sen's slope = 0.03) of 0.9°C over the 30-year period (0.3°C per decade). According to Sylla *et al*. (2016), countries such as Ghana and la Cote d'lvoire, both located in the BVRB, experienced the most significant warming signals during the 1983-2010 period. Figure 3 shows the increase in mean temperature over the basin for the period of analysis.

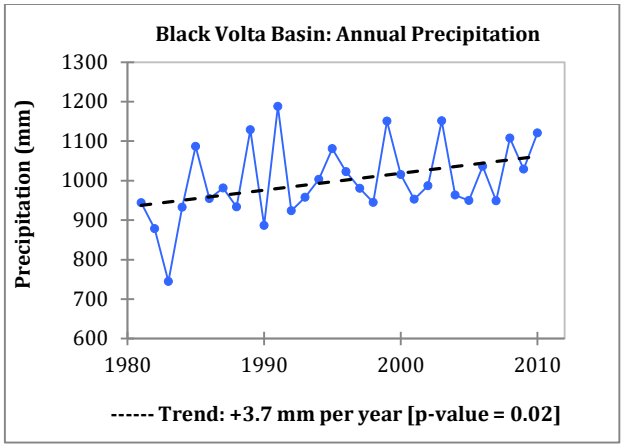

Fig.2 Trend analysis of annual precipitation over the Black Volta River Basin (1981-2010)

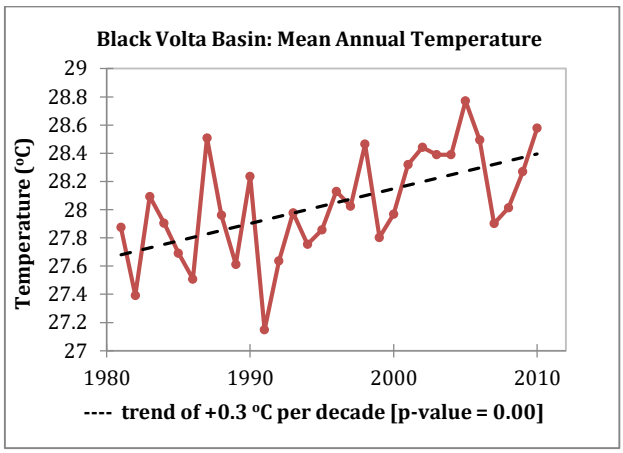

Fig.3 Trend analysis of mean temperature over the Black Volta River Basin (1981-2010)

Table 4 Basic statistics of uncorrected and bias- corrected RCA4/ CanESM2 model simulations of historical (1981-2005) temperature and precipitation at Bobo-Dioulasso

Variables	Mean			Standard Deviation		
	Observed	Corrected	Uncorrected	Observed	Corrected	Uncorrected
Temperature	27.56	27.58	27.12	2.01	1.99	1.87
Precipitation	83.03	79.40	80.38	90.25	91.14	81.57

3.2 Assessment of the model- corrected and –uncorrected simulations of the observed climate

Figures 4, 5 and 6 present the trends in monthly precipitation, the probability of exceedance of precipitation events and the trends in mean monthly temperature, respectively, at the Bobo-Dioulasso station in the north of the basin in Burkina Faso. The plots were based on station observed data as well as the RCA4/CanESM2 model-corrected and –uncorrected data for the precipitation and mean temperatures. As shown in Figure 4, both the model-corrected and–

uncorrected simulations show a double peak in the precipitation while the observed data has a single peak. However, the double peak in the corrected simulation is weak while the uncorrected exhibits a strong double peak. In addition, the corrected simulation fairly reproduces the monthly amounts though it shows a slight over estimation of the May and August rainfall and underestimates that of March, June, July and September through November. The uncorrected simulation, on the other hand, heavily over-estimated the precipitation in April and May and underestimated the amounts for July through to November. As Figure 5 shows, the model corrected data overestimated the probability of precipitation events less than 1mm while the uncorrected data showed an underestimation. In addition, the uncorrected data overestimated highly the probability of precipitation exceedance between 1mm and 10mm. Results of the mean monthly temperature (Figure 6) shows that the corrected model data represents well the observed monthly temperature at the Bobo-Dioulasso station, with slight under- and over-estimations. The uncorrected output, on the other hand, underestimates the monthly temperature values in January through April and overestimates them from June through September. The mean and standard deviation of the precipitation and temperature at the station (Table 4) also confirms the closeness of the corrected data to the observed data, relative to the uncorrected data. As rightly pointed out by Ehret *et. al*. (2012), climate simulations often exhibit systemic deviations from the observed climate. Our results show that bias correction is without doubt important for climate change impact assessment.

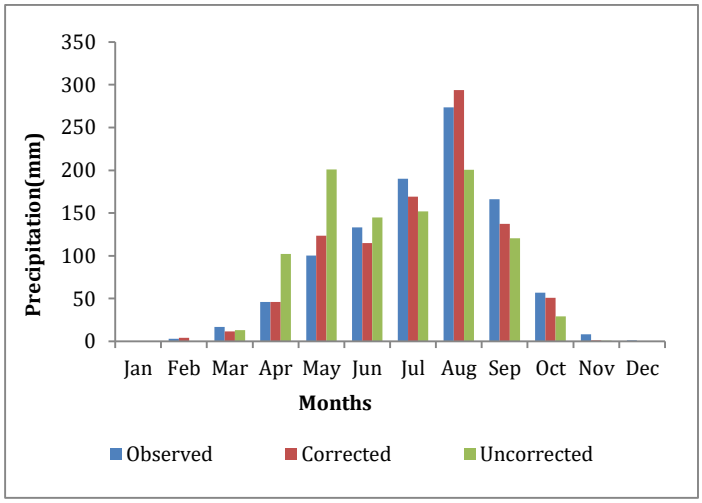

Fig.4 RCA4/ CanESM2 bias-corrected and –uncorrected precipitation and observed data at the Bobo-Dioulasso station (1981-2005)

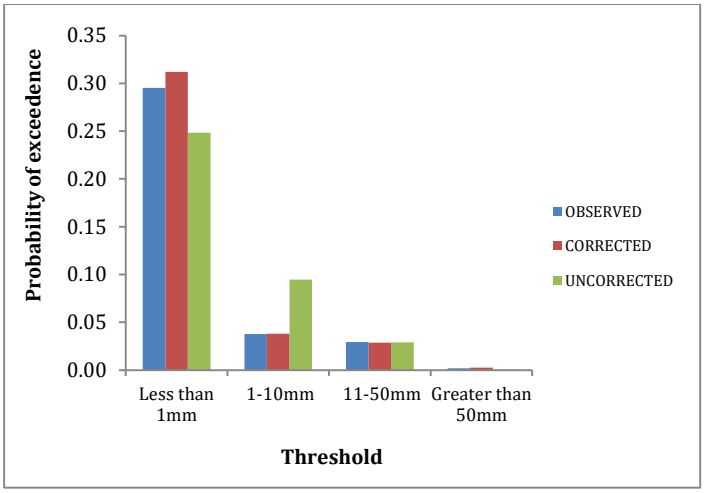

Fig.5 Probability of exceedance of precipitation thresholds for the bias-corrected and uncorrected RCA4/ CanESM2 model simulates of historical precipitation at the Bobo-Dioulasso station (1981-2005)

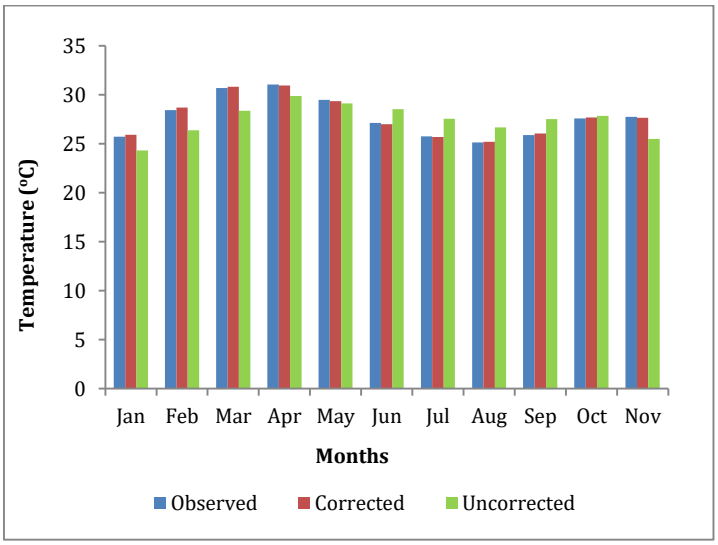

Fig.6 Uncorrected and bias-corrected RCA4/ CanESM2 model simulated data and historical mean temperature at the Bobo-Dioulasso station (1981-2005)

3.3 Projected changes in precipitation

The analysis of average annual precipitation over the basin for the late- and end of the 21st century showed high level of uncertainties, with mixed signals of increases and decreases in precipitation amounts across the models (Table 5). Relative to the baseline, mean annual precipitation for the late 21st century ranged between -16% and +6%, with a mean of -2% under the RCP4.5 scenario and between -27% and +14%, with a mean of -1% under the RCP8.5

scenario. The end of the 21st century projection showed precipitation changes of between -23% and +2%, with a mean of -7% under the RCP4.5 scenario. The high emission RCP8.5 scenario projects changes ranging between -33% and +13%, with a mean of -4%. From the results, it is established that the uncertainty in the projections increases with increasing RCP forcing and increasing time frames. Similar observations were made by Sylla *et al*. (2016).

Figure 7 and 8 show the projected changes in intra-annual precipitation over the BVRB for the late and end of 21st century, respectively. As shown in both graphs (7a and 7b), future rainfall projections by the models show high variability consistent with findings for the West African region reported in the IPCC 5th Assessment report (IPCC, 2013). The variability is mostly pronounced during the wet season. Precipitation amount for the month of July for example is projected to range between +51mm and -16mm under the RCP 4.5 scenario and between +81mm and -30mm under the RCP8.5 scenario in the 2060s. From the months of October through December however, the variability is highly reduced, especially under the RCP4.5 scenario. The end of the 21st century rainfall projections also shows substantial variability, in this case especially in the months of February through September, which reduces from October through December.

Changes in precipitation for the dry (January-March) and wet (August-October) seasons are presented in Figures 9 and 10. In the late 21st century, the ensemble runs project a change in the range of +6% to -35% in the dry season precipitation, with a mean change of 11% for the RCP4.5 scenario. The change in wet season precipitation is projected to range from +4% to -10%, with a mean of -3%. Under the RCP8.5 scenario, the change in dry and wet season precipitations are projected to range from +22% to -67%, with a mean of -26%, and +9% to -16%, with a mean of -1%. Similarly, the dry and wet season precipitations over the basin for the end of the 21st century are projected to range between +20% and -48%, with a mean of -11% and from -2% to -16%, with a mean of -8% for the RCP4.5 scenario. The high emission RCP8.5 scenario projections show a rate of change in dry season precipitation ranging from +48% and -68%, with a mean of -18% while for the wet season the projected changes are between +16% and -23%. The high variability in the projections across the models and the opposing change in signals are indications of uncertainty surrounding precipitation projections in the basin. Whereas a decrease in precipitation over the region may cause droughts, affect agriculture development and cause a decline in hydropower generation, increases in precipitation may cause floods in the basin.

Table 5 Projected changes in precipitation for the late and end of 21st century in the Black Volta River Basin under RCPs 4.5 and 8.5

RCMs	Baseline (1981-2010) observed	Late-Century (2051-2075)				End-of-Century (2076-2100)			
		RCP4.5		RCP8.5		RCP4.5		RCP8.5	
		Ave (mm)	% change	Ave (mm)	% change	Ave (mm)	% change	Ave (mm)	% change
RACMO22T/ ICHEC-EC-EARTH	999.48	1064.12	6.47	1091.52	9.21	999.37	-0.01	1126.88	12.75
RCA4/MPI-ESM-LR		1050.77	5. 13	1136.19	13.68	1021.95	2.25	1094.23	9.48
RCA4/ CCCma-CanESM2		836.55	-16.30	728.64	-27.10	767.69	-23.19	665.25	-33.44
ENSEMBLE		983.81	-1.57	985.45	-1.40	929.67	-6.98	926.12	-3.74

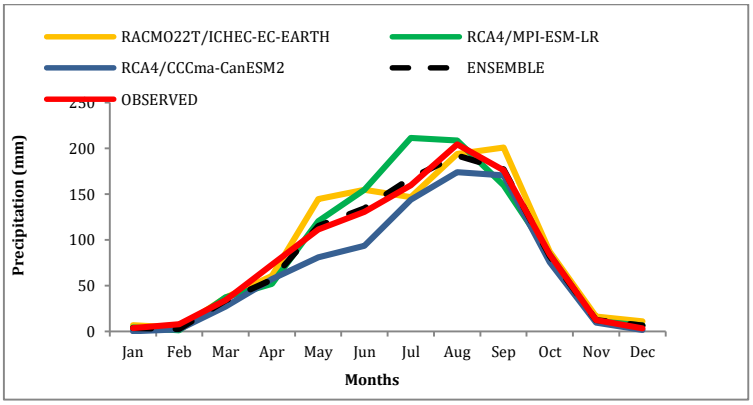

(a)

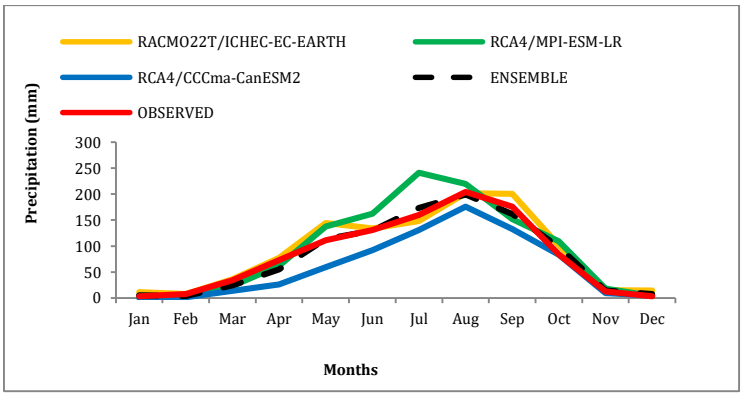

(b)

Fig.7 Observed and projected intra-annual precipitation under (a) RCP4.5 and (b) RCP8.5 for the 2060s (2051-2075)

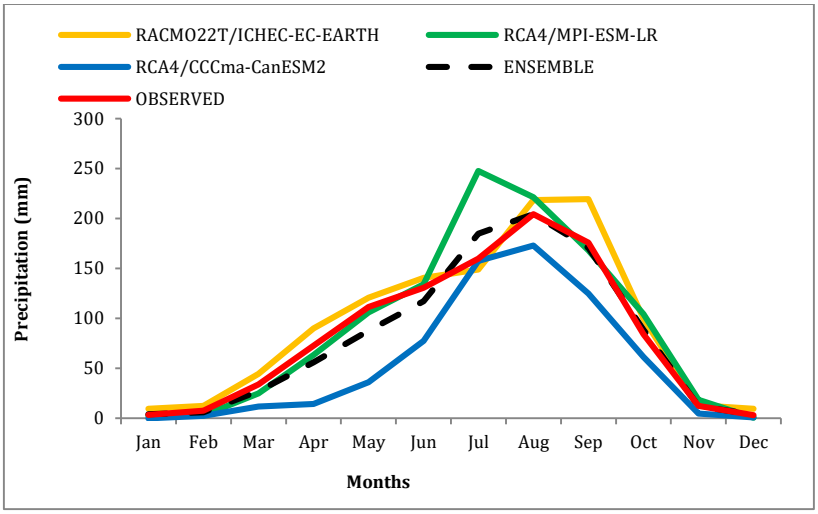

(a)

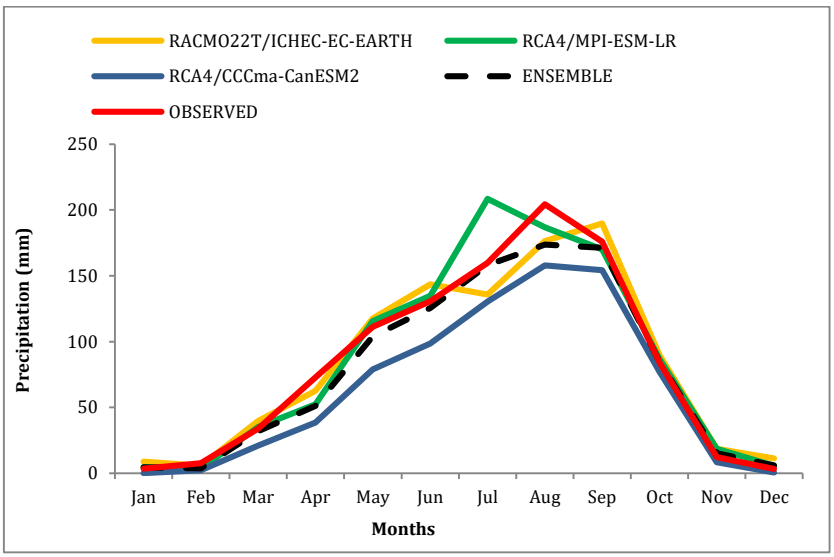

(b)

Fig. 8 Observed and projected intra-annual precipitation under (a) RCP4.5 and (b) RCP8.5 for the 2080s (2076-2100)

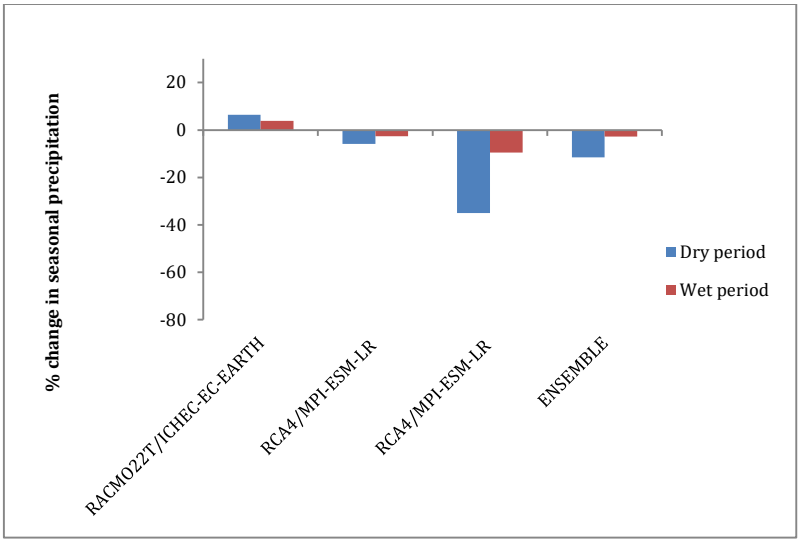

(a)

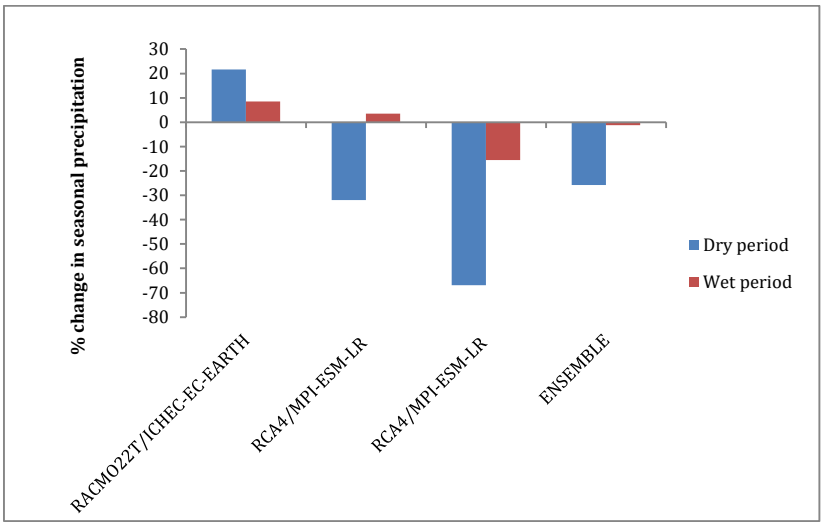

(b)

Fig. 9 Changes in mean seasonal precipitation for the 2060s (2051-2071) under (a) RCP4.5 and (b) RCP8.5 scenarios, relative to the baseline (1981-2010)

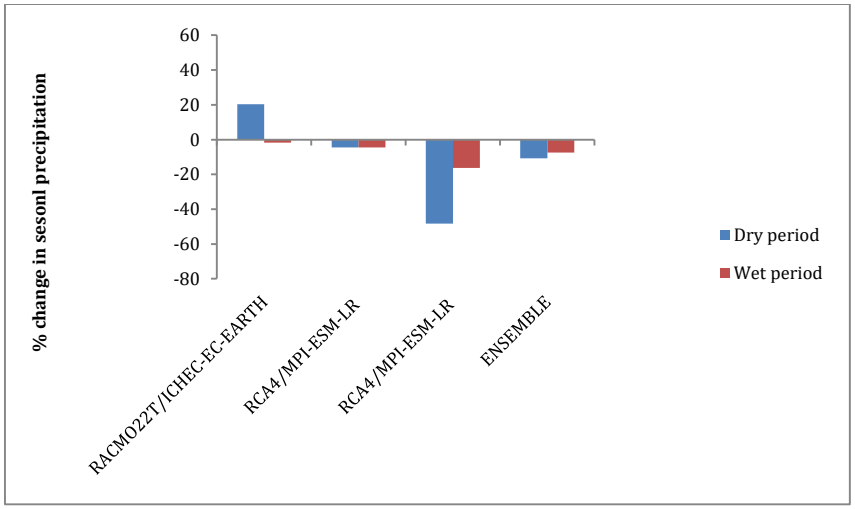

(a)

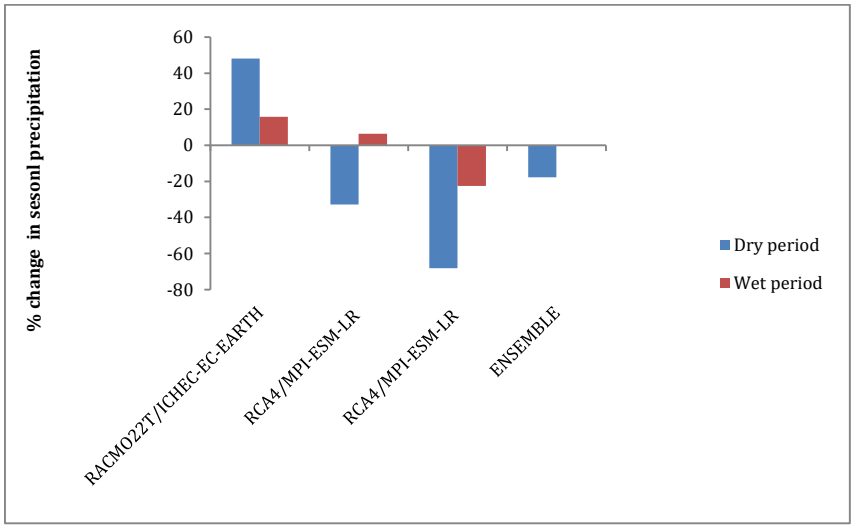

(b)

Fig. 10 Changes in mean seasonal precipitation for the 2080s under (a) RCP4.5 and (b) RCP8.5 scenarios, relative to the baseline (1981-2010)

3.4 Projected changes in temperature

In agreement with the IPCC (2013) report, results of the temperature projections for the basin (Table 6) point towards a warmer climate in the late- and end of the 21st century under both RCP scenarios, relative to the baseline (1981-2005). The projected increases in temperature by the ensemble runs are significant. The magnitude of the projected increase in mean temperature over the basin is greater in the 2080s compared to the 2060s. As expected, the increase in temperature is higher in the RCP8.5 scenario than in the RCP4.5 scenario. The mean annual temperature for 2060s is projected to rise by between 2.0°C and 2.3°C for the RCP4.5 scenario and 2.7 °C and 3.0°C for the RCP8.5 scenario. By the end of the 21st century, larger temperature increases between 2.2°C and 2.6°C is projected for the RCP4.5 scenario and from 3.5°C to 3.7°C for the RCP8.5 scenario. These projected changes in temperature for the basin are in line with the projected range for West Africa (Sylla *et al*., 2016).

Table 6 Projected changes in temperature (°C) for the late and end of 21st century in the Black Volta River Basin under RCPs 4.5 and 8.5

RCM/GCM pairs	Baseline (1981-2010) Observed mean values	2051-2075				2076-2100			
		RCP4.5		RCP8.5		RCP4.5		RCP8.5	
	Tmean (°C)	Tmean (°C)		Tmean (°C)		Tmean (°C)		Tmean (°C)	
		Ave	Change	Ave	Change	Ave	Change	Ave	Change
RACMO22T/ICHEC-EC-EARTH	27.9	30.0	2.1	30.7	2.8	30.2	2.3	31.4	3.5
RCA4/MPI-ESM-LR		29.9	2.0	30.6	2.7	30.1	2.2	31.4	3.5
RCA4/CCCma-CanESM2		30.2	2.3	30.9	3.0	30.5	2.6	31.6	3.7
ENSEMBLE		30.0	2.1	30.7	2.8	30.2	2.3	31.4	3.5

3.5 Trends in projected annual precipitation and mean temperature

The Man-Kendall trend test showed increases and decreases in future precipitation over the basin (Table 7) with majority of the trends (about 67%) being in the positive direction. The projected trend ranges from a decrease of 5.5mm/year to an increase of 3.6mm/year for the RCP4.5 scenario in the late century period. For the RCP8.5 scenario, the trend ranges from a decrease of 2.7mm/year to an increase of 8.6mm/year. The end of the century projected trend ranges from a decline of 3mm/year to an increase of 4.9mm/year under the RCP4.5 and from a decline of 2.7mm/year to an increase of 8.6mm/year under the RCP8.5 scenario. All the trends were however statistically insignificant at the 5% level of significance. Unlike temperature,

precipitation projection in the West African Region is in general associated with higher uncertainties (Rowell 2012; Orlowsky and Seneviratne 2012). Trend analysis of temperature, revealed statistically significant (5% level of significance) increases in agreement with the IPCC (2013) report. For the late century increase in trends up to 0.03^{o}C/year is projected by both RCP4.5 and RCP8.5 scenarios. The projected trend for the end of the century ranges from a decrease 0f 0.01^{o}C/year to an increase of 0.02^{o}C/year for the RCP4.5 scenario and from 0.02^{o}C/year to 0.06 ^{o}C/year for the RCP8.5 scenario. The decreasing trends are however not significant at the 5% level as shown in Table 8.

Table 7 Results of the Mann-Kendall test for annual precipitation (mm) for the late and end of 21st century in the Black Volta River Basin under RCPs 4.5 and 8.5

Model runs	Mann-Kendall Statistic (S)	Sen's slope	p-value	Trend
RACMO22T/ICHEC-EC-EARTH (RCP4.5/2060s)	-50.00	-5.53	0.26	Not significant
RACMO22T/ICHEC-EC-EARTH (RCP4.5/2080s)	-46.00	-2.96	0.30	Not significant
RACMO22T/ICHEC-EC-EARTH (RCP8.5/2060s)	18.00	2.53	0.70	Not significant
RACMO22T/ICHEC-EC-EARTH (RCP8.5/2080s)	18.00	2.54	0.70	Not significant
RCA4/CanESM2 (RCP4.5/2060s)	18.00	1.54	0.70	Not significant
RCA4/CanESM2 (RCP4.5/2080s)	42.00	4.90	0.34	Not significant
RCA4/CanESM2 (RCP8.5/2060s)	74.00	8.56	0.09	Not significant
RCA4/CanESM2 (RCP8.5/2080s)	74.00	8.56	0.09	Not significant
RCA4/MPI-ESM-LR (RCP4.5/2060s)	28.00	3.55	0.53	Not significant
RCA4/MPI-ESM-LR (RCP4.5/2080s)	12.00	1.86	0.80	Not significant
RCA4/MPI-ESM-LR (RCP8.5/2060s)	-28.00	-2.67	0.53	Not significant
RCA4/MPI-ESM-LR (RCP8.5/2080s)	-26.00	-2.67	0.56	Not significant

Table 8 Results of the Mann-Kendall test for mean annual temperature (°C) for the late and end of 21st century in the Black Volta River Basin under RCPs 4.5 and 8.5

Model runs	Mann-Kendall Statistic (S)	Sen's slope	P-value	Trend
RACMO22T/ICHEC-EC-EARTH (RCP4.5/2060s)	104.00	0.03	0.02	Significant increase
RACMO22T/ICHEC-EC-EARTH (RCP4.5/2080s)	108.00	0.02	0.01	Significant increase
RACMO22T/ICHEC-EC-EARTH (RCP8.5/2060s)	152.00	0.03	0.00	Significant increase
RACMO22T/ICHEC-EC-EARTH (RCP8.5/2080s)	190.00	0.06	< 0.00	Significant increase
RCA4/CanESM2 (RCP4.5/2060s)	-4.00	-0.00	0.94	Not significant
RCA4/CanESM2 (RCP4.5/2080s)	-44.00	-0.01	0.32	Not significant
RCA4/CanESM2 (RCP8.5/2060s)	130.00	0.02	0.00	Significant increase
RCA4/CanESM2 (RCP8.5/2080s)	132.00	0.02	0.00	Significant increase
RCA4/MPI-ESM-LR (RCP4.5/2060s)	26.00	0.00	0.56	Not significant
RCA4/MPI-ESM-LR (RCP4.5/2080s)	-28.00	-0.01	0.53	Not significant
RCA4/MPI-ESM-LR (RCP8.5/2060s)	164.00	0.02	0.00	Significant increase
RCA4/MPI-ESM-LR (RCP8.5/2080s)	148.00	0.03	0.00	Significant increase

Conclusion

In this study, we first analyzed the trends in observed (1981-2010) annual precipitation and mean temperature over the Black Volta River Basin using the Man-Kendall test and the Sen's slope estimator. We also analyzed projected changes in precipitation and mean temperature over the basin using simulation data set by 2 Regional Climate Models for the late (2051-2075) and end of the 21st century (2076-2100) periods under two IPCC Representative Concentration Pathways (RCP4.5 and RCP8.5). Lastly, we assessed the trends in the future annual precipitation and temperature.

The trend analysis of the observed annual precipitation and mean temperature showed statistically significant increases, indicating that the basin was wetter and warmer in the 1981-2010 period. Relative to the baseline, annual precipitation amounts showed positive and negative signals across the models. Similar to the annual precipitation, the intra-annual and seasonal precipitation analysis also showed high uncertainty in the future rainfall amounts, with higher variability in the wet season compared to the dry season. Temperature projections by the models unanimously suggested warming of the basin during the 2060s and 2080s with increases ranging between 2.0^{o}C (2060s under RCP4.5) and 3.7^{o}C (2080s under RCP8.5).

Trend analysis of annual future precipitation pointed in both positive and negative directions. The trends were however statistically insignificant at the 5% level of significance. Trends in the annual mean temperature however, showed mostly statistically significant (5% level of significance) increases in future temperature over the basin. A few of the model runs showed statistically insignificant decreasing trends. High temperatures may affect water availability and use in the basin. Since a good number of the basin's population depend on agriculture for their livelihood, problems related to water scarcity in the basin may worsen the poverty situation in the basin. Measures to cope with the increasing temperature over the basin should therefore be explored and developed well ahead of time.

Acknowledgement

The authors would like to thank the German Federal Ministry of Education and Research (BMBF) for providing the funds for this research through the West African Science Service Centre on Climate Change and Adapted Land Use (WASCAL; www.wascal.org). We thank Dr. Osumane Seidou of the University of Ottawa, Canada for providing the CORDEX data used in this study. Our thanks also go to the Meteorological Agencies in Ghana and Burkina Faso for the observed meteorological data for the Black Volta Basin.

Conflicts of Interest

The authors declare no conflict of interest.

Annex 1A

The Mann-Kendall trend test

The Mann-Kendall test statistic (S), is calculated according to:

$$S = \sum_{i=1}^{n-1} \sum_{j=i+1}^{n} sgn(xj - xi) \quad (1)$$

Where, $x_{1,}x_{2,}x_{3\ldots,}x_n$ represent n data points and x_j represents the data point at time j.

with

$$sgn\left(x_{j-}x_i\right) = \begin{pmatrix} +1\ if\ \left(x_j - x_k\right) > 0 \\ 0\ if\ \left(x_j - x_k\right) = \ \ 0 \\ -1\ if\ \left(x_j - x_k\right) < 0 \end{pmatrix} \quad (2)$$

The test statistic (S) is assumed to be approximately normal, with E(S) = 0 for sample size n ≥ 8 and variance as follows:

$$Var\ (S) = \frac{[n(n-1)(2n+5) - \sum_t t(t-1)(2t+5)}{18} \quad (3)$$

Where t represents the number of ties up to sample i. The standardized MK test statistics (Zmk) is estimated as follows:

$$Z_{mk} = \begin{matrix} \frac{S-1}{\sqrt{V(S)}}\ if\ S > 0 \\ 0\ is\ S + \ 0 \\ \frac{S+1}{\sqrt{V(S)}}\ if\ S < 0 \end{matrix} \quad (4)$$

The standardized MK test statistics (Zmk) follows the standard normal distribution with a mean of zero and variance of one. A positive (negative) value of Zmk indicates an 'upward trend' (downward) trend.

Annex 1B

The non-parametric Sen's slope estimator

In this test, the slope Qi estimates N pairs of data values which are computed using

$$Qi = \frac{xj - xk}{j - k} \quad (5)$$

where xj and xk are data values at time j and k respectively, and j>k. The Sen's estimator of the slope is the median of these N values of Qi. The N values of Qi are ranked from the smallest to the largest and the Sen's estimator is computed by:

$$Q_{med} = Q\left[\frac{(n+1)}{2}\right], if\ N\ is\ odd \quad (6)$$

or

$$Q_{med} = \frac{1}{2}\left(Q\frac{n}{2} + Q\left[\left(\frac{n+2}{2}\right)\right]\right), if\ N\ is\ even \quad (7)$$

Q_{med} is then tested with a two-sided test which is carried out at 100(1 – α)% confidence interval to obtain the true slope for the non-parametric test in the series. The positive slope Qi is obtained as an increasing trend and the negative slope Qi as a decreasing trend.

Annex 1C

The Q-Q transformation procedure

The observed data covering the present horizon (1981-2010) was split into two, one half for calibration and the other half for validation. The calibration period consisted of every odd year starting from the beginning of the present horizon (i.e. years 1, 3, 5, etc.) while the validation was done on even years (i.e. years 2, 4, etc.). The daily time series of the month were extracted for both calibration and validation periods from both observation and RCA4 projection data.

Two empirical cumulative distribution functions, F_{obs} and F_{RCM}, were then developed. F_{obs} was generated using observed data covering the calibration period while the F_{RCM} was generated using the RCA4 projections for the calibration period.

The probability mass function (PMF) of precipitation occurrence (i.e intensity greater than 1mm/day) and probability density function (PDF) of precipitation intensity on wet/rainy days, maximum and minimum temperatures were built. The quantile-quantile transformation was applied to produce improved (corrected) future RCM simulations of a variable if it was noticed that the PDF (or (PMF) of a corrected variable was closer to the PDF of the observations than the PDF (or PMF) of the raw non-corrected variable.

Thus, the bias-corrected RCA4 projections ,X_{CORR}, were generated for the entire period of the uncorrected projection data using the transformation: $X_{CORR} = F_{obs}^{-1}\left(F_{RCM}(X_{RCM})\right)$, where X_{RCM} refers to the uncorrected RCA4 projection data.

References

Abiodun, B.J., Abba, Omar. S., Lennard, C. and Jack, C. (2015). Using regional climate models to simulate extreme rainfall events in the Western Cape, South Africa. International Journal of Climatology, DOI: 10.1002/joc.4376.

Allwaters Consult (2012). Diagnostic Study of the Black Volta Basin in Ghana; Final Report; ALLWATERS Consult Limited: Kumasi, Ghana.

Amadou, A., Abdouramane, G., Seidou, O. and Seidou Sanda, I. (2015). Changes to flow regime on the Niger River at Koulikoro under a changing climate. *Hydrological Sciences Journal*, doi 10.1080/02626667.2014.916407.

Annor, F. O. (2012). Diagnostic Study of the Black Volta Basin in Ghana. In-Service Training Centre, Upper West Region- Ghana.

Barry B, Obuobie E, Andreini M, Andah W and Pluquet, M. (2005). The Volta river basin. Comprehensive assessment of water management in agriculture .Comparative study of river basin development and management.

CDKN (Climate and Development Knowledge Network) (2014). The IPCC's Fifth Assessment Report: What's in it for Africa? Available from http://cdkn.org/resource/highlights-africa-ar5/ [Accessed 14 August, 2015].

Chylek, P., Li, J., Dubey, M.K., Wang, M., and Lesins, G. (2011). Observed and model simulated 20th century Arctic temperature variability: Canadian Earth System Model CanESM2 22893–22907. doi:10.5194/acpd-11-22893-2011.

Diallo, I., Sylla, M.B., Giorgi, F., Gaye, A.T., Camara, M. (2012). Multimodel GCM-RCM Ensemble-Based Projections of Temperature and Precipitation over West Africa for the Early 21st Century 2012. doi:10.1155/2012/972896.

Dosio, A., Panitz, H.-J., Schubert-Frisius, M., and Lüthi, D. (2015). Dynamical downscaling of CMIP5 global circulation models over CORDEX-Africa with COSMO-CLM: evaluation over the present climate and analysis of the added value. *Climate Dynamics*, 44:2637–2661.

Druyan, L. M. (2011). Studies of 21st-century precipitation trends over West Africa. International Journal of Climatology, 31(10), 1415–1424. http://doi.org/10.1002/joc.2180

Ehret, U., Zehe, E., Wulfmeyer, V., Warrach-Sagi, K., and Liebert, J. (2012). HESS Opinions Should we apply bias correction to global and regional climate model data?. *Hydrology and Earth System Sciences*,16, 3391-3404.

Endris, H.S., Lennard, C., Hewitson, B., Dosio, A., Nikulin, G., Panitz, H. (2015). Teleconnection responses in multi-GCM driven CORDEX RCMs over Eastern Africa. *Climate Dynamics*, DOI 10.1007/s00382-015-2734-7.

Giannini, A., Biasutti, M., Held, I.M. and Sobel, A.H. (2008). A global perspective on African climate, *Climatic Change*, vol. 90, no. 4, pp. 359–383.

Gilbert, R.O. (1987). Statistical Methods for Environmental Pollution Monitoring, Wiley, NY.

Giorgi, F., Jones, C., Asrar, G. (2009). Addressing climate information needs at the regional level: the CORDEX framework. *World Meteorology Organ Bulletin* Available online at http://wcrp.ipsl.jussieu.fr/RCD_Projects/CORDEX/CORDEX_giorgi_WMO.pdf., 58, 175-183.

Green Cross International (2001). Trans-boundary Basin Sub-Projects: The Volta River Basin. Website: www.gci.ch/Green- crossPrograms/ waterres/pdf/WFP_Volta.

Hazeleger W, Severijns C, Semmler T, Stefanescu S, Yang S, Wang X, Wyser K, Dutra E, Baldasano JM, Bintanja R, Bougeault P, Caballero R, Ekman AML, Christensen JH, van den Hurk B, Jimenez P, Jones C, Kallberg P, Koenigk T, McGrath R, Miranda P, van Noije T, Parodi JA, Schmith T, Selten F, Storelvmo T, Sterl A, Tapamo H, Vancoppenolle M,Viterbo P, Willen U (2010) EC-earth: a seamless earth-system prediction approach in action. *Bulletin of American Meteorological Soc*iety, 91:1357–1363.

Hoerling, M., Hurrell, J., Eischeid, J. and Phillips, A. (2006). Detection and attribution of twentieth-century northern and southern African rainfall change, *Journal of Climate*, vol. 19, no. 16, pp. 3989–4008.

Hong, S.Y. and Kanamitsu, M. (2014). Dynamical downscaling: fundamental issues from an NWP point of view and recommendations. *Asia Pacific Journal of Atmospheric Science*, 50(1):83–104. doi:10.1007/s13143-014-0029-2.

Hubert P., Carbonnel, J. P. (1987). Approche statistique de l'aridification de l'Afrique de l'Ouest. Journal of Hydrology, 95, 165–183.

Ibrahim, B., Karambiri, H., Polcher, J., Yacouba, H., & Ribstein, P. (2014). Changes in rainfall regime over Burkina Faso under the climate change conditions simulated by 5 regional climate models. Climate Dynamics, 42, 1363–1381. doi:10.1007/s00382-013-1837-2.

IPCC (2014a). Climate Change 2014. Impacts, Adaptation, and Vulnerability. Chapter 12, Human Security (p2).

IPCC (2014b). Climate Change 2014. Impacts, Adaptation, and Vulnerability. Technical Summary (pp7, 27).

IPCC. (2013). Climate Change 2013: The Physical Science Basis. In T. F. Stocker, D. Qin, G. -K. Plattner, M. Tignor, S. K. Allen, J. Boschung, A. Nauels, Y. Xia, V. Bex & P. M. Midgley (Eds.), Contribution of Working Group I to the Fifth Assessment Report of the Intergovernmental Panel on Climate Change (p. 1535). Cambridge, United Kingdom and New York, NY, USA: Cambridge University Press. doi:10.1017/CBO9781107415324.

Jones, C., Giorgi, F. and Asrar, G. (2011). The Coordinated Regional Downscaling Experiment: CORDEX, An international downscaling link to CMIP5: *CLIVAR Exchanges*, No. 56, Vol 16, No.2 pages 34-40. Available from www.clivar.org/sites/default/files/imported/publications/exchanges/Exchanges_56.pdf (also see http://www.cordex.org/).

Karpouzos, D.K., Kavalieratou, S., Babajimopoulos, C. (2010) Trend analysis of precipitation data in Pieria Region (Greece). Euro Water 30:31–40.

Kasei, R. A. (2009). Modelling impacts of climate change on water resources in the Volta Basin, West Africa. PhD. Thesis Rheinischen Friedrich-Wilhelms-Universität Bonn. http://hss.ulb.uni-bonn.de/diss_online elektronisch publiziert.

Kendall, M.G. (1975). Rank Correlation Methods, 4th edition, Charles Griffin, London.

Kim, J., Waliser, D. E., Mattmann, C. A., Goodale, C. E., Hart, A. F., Zimdars, P. A., Crichton, D. J., Jones, C., Nikulin, G., Hewitson, B., *et al*. (2013). Evaluation of the CORDEX-Africa multi-RCM hindcast: systematic model errors. *Climate Dynamics*, pages 1–14.

Klutse, N.A.B., Sylla, M.B., Diallo, I., Sarr, A., Dosio, A., Diedhiou, A., Kamga, A., Lamptey, B., Ali, A., Gbobaniyi, E.O., Owusu, K., Lennard, C., Hewitson, B., Nikulin, G., Panitz, H-J., Bucher, M. (2014). Daily characteristics of West African summer monsoon precipitation in CORDEX simulations. *Theoretical and Applied Climatology*, DOI 10.1007/s00704-014-1352-3.

Kupiainen, M., Samuelsson, P., Jones, C., Jansson, C., Willen, U., Hansson, U., Ullerstig, A., Wang, S. and Doscher, R. (2011). Rossby Centre regional atmospheric model, RCA4. Rossby Centre Newsletter, June.

Lenderink, G., van den Hurk, B.J.J.M., van Meijgaard, E., van Ulden, A.P. and Cuijpers, H. (2003). Simulation of present-day climate in RACMO2: first results and model developments. *KNMI Technical Report*, 252, 24 p.

Mahé G, Paturel, J. (2009). 1896–2006 Sahelian annual rainfall variability and runoff increase of Sahelian Rivers. Comptes Rendus Geosci 341(7):538–546. doi:10.1016/j.crte.2009.05.002

Mahe, L'Hote, Y., Olivry, J. C., & Wotling, G. (2001). Trends and discontinuities in regional rainfall of West and Central Africa: 1951–1989. Hydrological Sciences Journal, 46(March 2015), 211–226. http://doi.org/10.1080/02626660109492817

Maidment, R. I., R. P. Allan, and E. Black (2015), Recent observed and simulated changes in precipitation over Africa, Geophys. Res. Lett., 42, 8155–8164, doi:10.1002/2015GL065765.
Mann, H.B. (1945). Non-parametric tests against trend, Econometrica 13:163-171.
Maraun, D, Wetterhall F, Ireson AM., Chandler RE, Kendon EJ, Widmann M, Brienen S, Rust, HW, Sauter T, Themeßl M, Venema VKC, Chun KP, Goodess CM, Jones RG, Onof C, Vrac M and Thiele-Eich I (2010). Precipitation downscaling under climate change: Recent developments to bridge the gap between dynamical models and the end user. *Reviews of Geophysics*, 48, RG3003.
Mavromatis T., Stathis D. (2011). Response of the Water Balance in Greece to Temperature and Precipitation Trends. Theoretical and Applied Climatology 104:13-24, DOI 10.1007/s00704-010-0320-9.
Ministry of Works and Housing (1998). Water Resources Management Study, Information Building Block study. Part II, Volta Basin System, Groundwater Resources. Ministry of Works and Housing, Accra.
Nicholson, S. (2005). On the question of the recovery of the rains in the West African Sahel. Journal of Arid Environment 63(3):615–641. doi:10.1016/j.jaridenv.2005.03.004.
Nicholson, S. E. (2000). Land Surface Processes and Land Use Change Land. Reviews of Geophysics, 38, 1 / February 2000, 38(1999), 117–139. Retrieved from http://www.peer.eu/ fileadmin/user_upload/opportunities/metier/course3/c3_lan d_surface_processes.pdf.
Nicholson, S. E., & Palao, I. M. (1993). A RE-Evaluation of rainfall variability in the sahel. Part I. Characteristics of rainfall fluctuations. International Journal of Climatology, Vol.13, 371389, 371–389. http://doi.org/0899-8418/93/040337119$14.50.
Nikulin, G., Jones, C., Giorgi, F., Asrar, G., Büchner,M., Cerezo-Mota, R., Christensen, O. B., Déqué,M., Fernandez, J., Hänsler, A., *et al*. (2012). Precipitation climatology in an ensemble of CORDEX-Africa regional climate simulations. *Journal of Climate*, 25(18):6057–6078. doi:10.1175/JCLI-D-11-00375.1.
Obuobie, E. (2008). Estimation of groundwater recharge in the context of future climate change in the White Volta River Basin. Doctoral thesis, Rheinische Friedrich Wilhelms Universität, Bonn/ Germany.
Obuobie, E., Logah, F., Asante-Sasu, C. (2017). Analysis of historical climate trends and future climate change projections over the White Volta, Black Volta and Oti Basins. A technical report of the CSIR-Water Research Institute, Accra, 89pp.
Onoz, B., Bayazit, M., 2012. The Power of Statistical Tests for Trend Detection.
Orlowsky, B., & Seneviratne, S. (2012). Global changes in extreme events: Regional and seasonal dimension. Climatic Change, 110, 669–696.
Paeth, H., Hall, N.M.J., Gaertner, M.A., Alonso, M.D., Moumouni, S., Polcher, J., Ruti, P.M., Fink, A.H., Gosset, M., Lebel, T., Gaye, A.T., Rowell, D.P., Moufouma-Okia, W., Jacob, D., Rockel, B., Giorgi, F., Rummukainen, M. (2011). Progress in regional downscaling of West African precipitation. Atmospheric Science Letters, doi:asl.306., 12, 75-82.
Panitz, H.J., Dosio, A., Büchner, M., Lüthi, D. and Keuler, K. (2014). COSMO-CLM (CCLM) climate simulations over CORDEXAfrica domain: analysis of the ERA-Interim driven simulations at 0.44 and 0.22 resolution. Climate Dynamics, doi:10.1007/ s00382-013-1834-5.
Rowell, D. (2012). Sources of uncertainty in future changes in local precipitation. Climate Dynamics, 39, 1929–1950.
Samuelsson, P., Jones, C.G., Willen, U., Ullerstig, A., Gollvik, S., Hansson, U., Jansson, C., Kjellstrom, E., Nikulin, G. and Wyser, K. (2011). The Rossby Centre Regional Climate model RCA3: model description and performance. Tellus Series A. Dynamic Meteorology, 63, 1, 4-23, doi: 10.1111/j.1600-0870.2010.00478.x.
Sarr, A.M., Seidou, O. and Tramblay, Y. (2015). Comparison of downscaling methods for mean and extreme precipitation in Senegal. Journal of Hydrology, Regional Studies (4): 369-385.
Sen, P. K. (1968). Estimates of the Regression Coefficient Based on Kendall's Tau. Journal of the American Statistical Association, 63(324), 1379-1389. DOI: 10.1080/01621459.1968.10480934.

Stevens, B., M. Giorgetta, M. Esch, T. Mauritsen, T. Crueger, S. Rast, M. Salzmann, H. Schmidt, J. Bader, K. Block, R. Brokopf, I. Fast, S. Kinne, L. Kornblueh, U. Lohmann, R. Pincus, T. Reichler, E. Roeckner, 2013: Atmospheric component of the MPI-M Earth System Model: ECHAM6. ournal of Advances in Modelling Earth Systems, 5, 146–172.

Strandberg, G., B¨arring, L., Hansson, U., Jansson, C., Jones, C., Kjellstr ¨om, K., Kolax, M., Kupiainen, M., Nikulin, G., Samuelsson, P., Ullerstig, A. and Wang, S. (2014). CORDEX scenarios for Europe from the Rossby Centre regional climate model RCA4. Reports Meteorology and Climatology, 999, SMHI, SE-601 76 Norrk¨oping, Sweden.

Sylla, M.B., Nikiema, P.M., Gibba, P., Kebe, I., and Klutse, N.A.B. (2016). Climate Change over West Africa : Recent Trends and Future Projections Climate Change over West Africa : Recent Trends and Future Projections. doi:10.1007/978-3-319-31499-0.

Themeßl M.J, Gobiet A and Leuprecht A (2011). Empirical-statistical downscaling and error correction of daily precipitation from regional climate models. International Journal of Climatology, 31, 1531–1544.

Turkish Journal of Engineering & Environmental Sciences 27 (2003), 247 – 251.

van Meijgaard, E., van Ulft, L. H., van de Berg, W. J., Bosveld, F. C., van den Hurk, B., Lenderink, G. and Siebesma A. P. (2008). The KNMI regional atmospheric climate model RACMO version 2.1, Technical Report 302.

van Meijgaard, E., van Ulft, L. H., van de Berg, W. J., Bosveld, F. C., van den Hurk, B., Lenderink, G. and Siebesma A. P. (2008). The KNMI regional atmospheric climate model RACMO version 2.1, Technical Report 302.

Yue S., Wang, C. (2004). The Mann-Kendall Test Modified by Effective Sample Size to Detect Trend in Serially Correlated Hydrological Series. Water Resources Management 18, 201–218.

ANNEX 2

Table 2A: Weather generated input files for SWAT

STATION	BOLE	DEDOUGOU	BOBO-DIOULASSO
WLATITUDE	9.03	12.46	11.16
WLONGITUDE	-2.48	-3.48	-4.31
WELEV	-	-	-
RAIN_YRS	30	30	30
TMPMX1	35.21	33.35	32.60
TMPMX2	36.92	36.52	35.45
TMPMX3	36.83	38.99	37.18
TMPMX4	34.80	40.07	37.03
TMPMX5	33.11	38.65	35.00
TMPMX6	31.02	35.13	32.12
TMPMX7	29.56	32.47	30.13
TMPMX8	29.11	31.13	29.38
TMPMX9	30.17	32.80	30.61
TMPMX10	32.25	36.45	33.29
TMPMX11	34.13	36.85	34.48
TMPMX12	34.64	34.43	33.05
TMPMN1	17.73	17.47	18.83
TMPMN2	20.83	20.64	21.80
TMPMN3	23.28	24.34	24.49
TMPMN4	23.82	26.86	25.14
TMPMN5	23.07	26.59	24.04
TMPMN6	22.05	24.34	22.35
TMPMN7	21.47	22.87	21.54
TMPMN8	21.31	22.14	21.23
TMPMN9	21.20	22.10	21.19
TMPMN10	21.24	22.45	21.85
TMPMN11	19.18	20.19	20.93
TMPMN12	16.84	17.90	19.15
TMPSTDMX1	1.93	2.88	2.61
TMPSTDMX2	1.75	2.79	2.39
TMPSTDMX3	2.16	2.39	2.15
TMPSTDMX4	2.44	2.31	2.42
TMPSTDMX5	2.08	2.69	2.45
TMPSTDMX6	1.81	2.83	2.31
TMPSTDMX7	1.65	2.35	2.01

TMPSTDMX8	1.61	2.04	1.87
TMPSTDMX9	1.78	2.28	2.06
TMPSTDMX10	1.78	1.93	1.86
TMPSTDMX11	1.27	1.58	1.42
TMPSTDMX12	1.54	2.47	2.15
TMPSTDMN1	2.66	2.50	2.20
TMPSTDMN2	3.41	2.65	2.30
TMPSTDMN3	2.25	2.59	1.86
TMPSTDMN4	1.59	2.08	1.82
TMPSTDMN5	1.38	2.27	1.98
TMPSTDMN6	1.20	2.20	1.76
TMPSTDMN7	1.01	1.60	1.34
TMPSTDMN8	0.94	1.28	1.13
TMPSTDMN9	1.01	1.21	1.20
TMPSTDMN10	0.95	1.34	1.07
TMPSTDMN11	2.35	2.14	1.53
TMPSTDMN12	2.89	2.19	1.82
PCPMM1	2.46	0.05	0.22
PCPMM2	8.40	1.22	2.39
PCPMM3	49.53	6.32	15.08
PCPMM4	104.19	16.48	44.45
PCPMM5	131.18	68.60	99.11
PCPMM6	141.97	98.94	131.18
PCPMM7	143.73	172.30	195.08
PCPMM8	159.17	231.62	271.51
PCPMM9	207.30	134.25	175.35
PCPMM10	95.78	38.65	61.41
PCPMM11	18.07	1.89	7.49
PCPMM12	6.02	0.01	0.98
PCPSTD1	1.37	0.04	0.12
PCPSTD2	2.89	1.07	1.47
PCPSTD3	7.69	2.08	3.00
PCPSTD4	9.98	3.06	5.83
PCPSTD5	10.84	7.74	9.01
PCPSTD6	10.27	8.51	10.01
PCPSTD7	11.43	11.27	11.55
PCPSTD8	12.67	13.38	14.63
PCPSTD9	13.90	9.78	11.12
PCPSTD10	8.38	4.64	5.82
PCPSTD11	4.18	0.93	2.92

PCPSTD12	2.19	0.01	0.62
PCPSKW1	22.99	26.52	18.30
PCPSKW2	14.69	27.87	24.47
PCPSKW3	8.31	13.61	9.27
PCPSKW4	4.14	7.62	6.20
PCPSKW5	3.54	5.35	4.31
PCPSKW6	2.92	3.64	3.19
PCPSKW7	4.10	2.75	2.42
PCPSKW8	3.85	2.59	2.37
PCPSKW9	3.91	3.78	3.12
PCPSKW10	3.97	5.20	4.11
PCPSKW11	10.54	18.47	17.65
PCPSKW12	15.00	30.50	23.00
PR_W1_1	0.01	0.00	0.01
PR_W1_2	0.04	0.00	0.02
PR_W1_3	0.13	0.03	0.06
PR_W1_4	0.28	0.08	0.20
PR_W1_5	0.34	0.21	0.34
PR_W1_6	0.41	0.32	0.42
PR_W1_7	0.38	0.44	0.54
PR_W1_8	0.43	0.55	0.68
PR_W1_9	0.57	0.37	0.53
PR_W1_10	0.27	0.13	0.21
PR_W1_11	0.05	0.01	0.02
PR_W1_12	0.02	0.00	0.00
PR_W2_1	0.00	0.00	0.25
PR_W2_2	0.12	0.33	0.40
PR_W2_3	0.16	0.27	0.31
PR_W2_4	0.21	0.22	0.30
PR_W2_5	0.33	0.25	0.35
PR_W2_6	0.32	0.29	0.37
PR_W2_7	0.45	0.43	0.52
PR_W2_8	0.52	0.49	0.64
PR_W2_9	0.50	0.43	0.55
PR_W2_10	0.34	0.30	0.36
PR_W2_11	0.20	0.23	0.24
PR_W2_12	0.10	0.00	0.00
PCPD1	0.23	0.07	0.27
PCPD2	0.87	0.10	0.67
PCPD3	4.00	1.00	2.60

PCPD4	7.97	2.57	6.63
PCPD5	9.90	6.17	10.40
PCPD6	11.00	9.03	12.07
PCPD7	11.93	13.50	16.23
PCPD8	14.07	15.93	20.30
PCPD9	15.67	11.90	16.27
PCPD10	9.07	5.03	8.03
PCPD11	2.00	0.43	1.10
PCPD12	0.67	0.03	0.10
RAINHHMX1	12.4	0.37	0.83
RAINHHMX2	19.9	10.23	13.37
RAINHHMX3	36.8	12.03	16.5
RAINHHMX4	27.1	12.07	26.87
RAINHHMX5	30.9	29.87	24.83
RAINHHMX6	27.2	26.87	25.67
RAINHHMX7	43.4	26.03	23.7
RAINHHMX8	40.7	31.83	31.43
RAINHHMX9	46.4	37.73	34.67
RAINHHMX10	26.2	13.43	16.67
RAINHHMX11	24.7	6.3	22.1
RAINHHMX12	15.1	0.07	5.57
SOLARAV1	21.75193548	21.11031183	21.88035484
SOLARAV2	21.82035419	23.25414404	23.13768595
SOLARAV3	21.58137634	24.24336559	22.42603226
SOLARAV4	20.91045556	23.52022222	20.33536667
SOLARAV5	20.51666667	22.25516685	20.4888172
SOLARAV6	19.30751111	22.62063404	21.22778889
SOLARAV7	16.93456989	20.98801075	18.80260215
SOLARAV8	17.0021828	19.90676344	18.86547312
SOLARAV9	19.12341111	20.76876667	20.17678889
SOLARAV10	19.72076344	20.30930108	19.29926882
SOLARAV11	19.92984444	21.4456	20.98394444
SOLARAV12	20.96318478	20.50864425	20.85556522
DEWPT1	0.25916129	0.130096774	0.129978495
DEWPT2	0.366257379	0.113801653	0.16231405
DEWPT3	0.452483871	0.14027957	0.257741935
DEWPT4	0.527166667	0.220866667	0.371211111
DEWPT5	0.608741935	0.31467169	0.457096774
DEWPT6	0.675444444	0.37868743	0.516
DEWPT7	0.746075269	0.501354839	0.664010753

DEWPT8	0.792623656	0.622935484	0.74
DEWPT9	0.761444444	0.557188889	0.650033333
DEWPT10	0.642215054	0.381752688	0.476913978
DEWPT11	0.454777778	0.187088889	0.232544444
DEWPT12	0.254537634	0.140629067	0.143608696
WNDAV1	1.976010753	2.699204301	2.66455914
WNDAV2	2.100330579	2.612916175	2.398807556
WNDAV3	2.474645161	2.331677419	2.26983871
WNDAV4	2.8106	2.166355556	2.586944444
WNDAV5	2.764763441	2.531776103	2.855290323
WNDAV6	2.740822222	2.742825362	2.915588889
WNDAV7	2.584043011	2.655784946	2.678645161
WNDAV8	2.26244086	2.372537634	2.313354839
WNDAV9	2.012155556	2.19	2.181944444
WNDAV10	1.96183871	1.918397849	1.934150538
WNDAV11	1.7754	2.097022222	2.008322222
WNDAV12	1.821021739	2.539414317	2.559793478

ANNEX 3

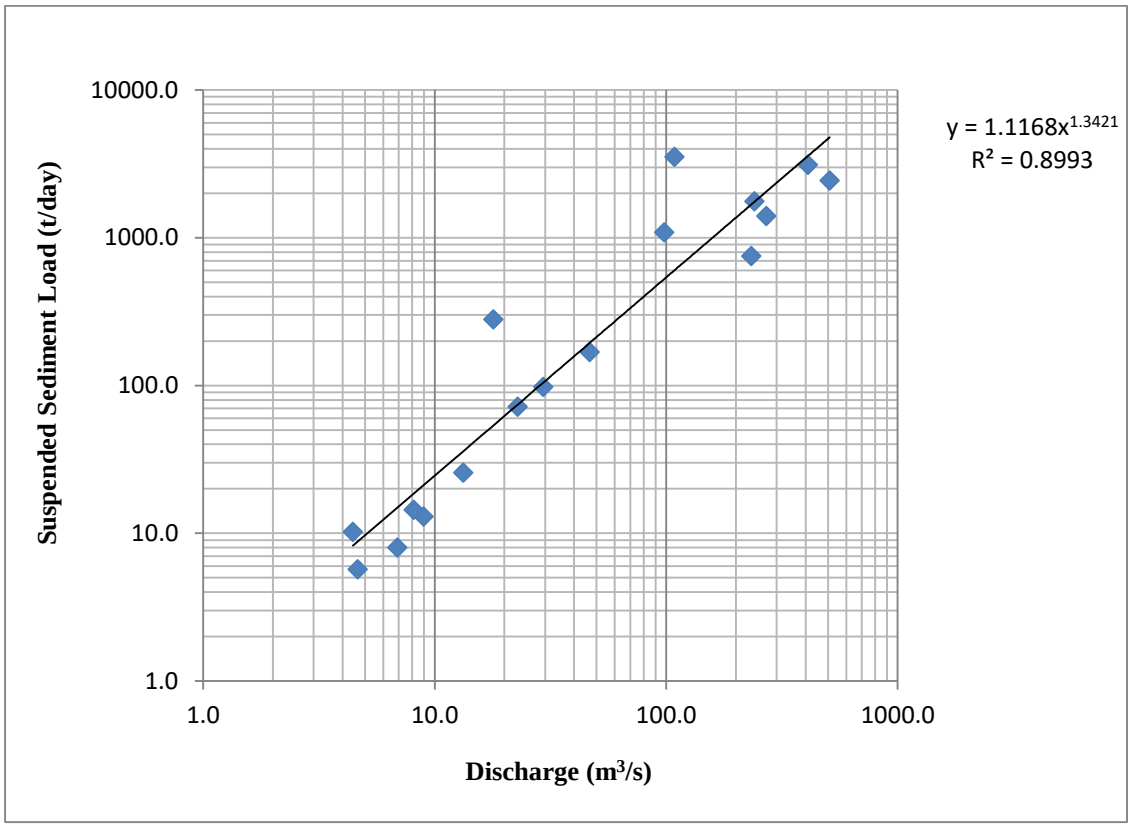

Figure A3: Sediment rating curve for the Black Volta Basin at Chache

ANNEX 4

Table A4: Maddock's classification for estimation of the bedload (Maddock, 1975)

Concentration of Suspended Load (ppm)	Type of Material forming the Stream Channel	Texture of Suspended Material	% of Measured Suspended Load that could be taken as Bed Load
Less than 1000	Sand	Similar to bed material	25 to 150
Less than 1000	Gravel, rock or consolidate clay	Small amount of sand	5 to 12
1000 to 7500	Sand	Similar to bed material	10 to 35
1000 to 7500	Gravel, rock or consolidate clay	25% sand or less	5 to 15
Over 7500	Sand	Similar to bed material	5 to 15
Over 7500	Gravel, rock or consolidate clay	25% sand or less	2 to 8

(Source: http://www.fao.org/docrep/t0848e/t0848e-10.htm)

ANNEX 5

Table A5: Estimated monthly total sediment load for Chache

Date	Mean monthly suspended load (tonnes)	25% of suspended load	Total sediment load (tonnes)
Jan-00	2111.0	527.8	2638.8
Feb-00	876.5	219.1	1095.6
Mar-00	323.1	80.8	403.9
Apr-00	207.9	52.0	259.9
May-00	211.4	52.9	264.3
Jun-00	3816.4	954.1	4770.5
Jul-00	10248.5	2562.1	12810.7
Aug-00	59532.5	14883.1	74415.7
Sep-00	124933.7	31233.4	156167.1
Oct-00	81428.7	20357.2	101785.8
Nov-00	8424.0	2106.0	10530.0
Dec-00	1985.7	496.4	2482.1
Jan-01	405.6	101.4	507.1
Feb-01	75.4	18.8	94.2
Mar-01	47.4	11.8	59.2
Apr-01	98.8	24.7	123.5
May-01	1534.1	383.5	1917.6
Jun-01	6872.2	1718.0	8590.2
Jul-01	13996.9	3499.2	17496.1
Aug-01	32400.7	8100.2	40500.9
Sep-01	99393.9	24848.5	124242.4
Oct-01	26602.3	6650.6	33252.9
Nov-01	1786.1	446.5	2232.6
Dec-01	252.2	63.1	315.3
Jan-02	-99.9	-99.9	-99.9
Feb-02	12.5	3.1	15.6
Mar-02	41.6	10.4	52.0
Apr-02	152.6	38.2	190.8
May-02	1460.6	365.1	1825.7
Jun-02	2569.4	642.4	3211.8
Jul-02	9129.3	2282.3	11411.7
Aug-02	54971.7	13742.9	68714.6
Sep-02	69159.9	17290.0	86449.8
Oct-02	22304.1	5576.0	27880.1

Nov-02	842.9	210.7	1053.7
Dec-02	148.1	37.0	185.2
Jan-03	70.4	17.6	88.1
Feb-03	53.1	13.3	66.4
Mar-03	51.7	12.9	64.6
Apr-03	140.7	35.2	175.8
May-03	1134.7	283.7	1418.4
Jun-03	9670.5	2417.6	12088.1
Jul-03	31521.7	7880.4	39402.2
Aug-03	-99.9	-99.9	-99.9
Sep-03	-99.9	-99.9	-99.9
Oct-03	-99.9	-99.9	-99.9
Nov-03	7396.9	1849.2	9246.2
Dec-03	2499.5	624.9	3124.4
Jan-04	929.7	232.4	1162.2
Feb-04	237.5	59.4	296.9
Mar-04	213.4	53.3	266.7
Apr-04	571.2	142.8	714.1
May-04	1938.0	484.5	2422.5
Jun-04	1978.6	494.6	2473.2
Jul-04	12596.8	3149.2	15746.0
Aug-04	103547.3	25886.8	129434.2
Sep-04	132493.5	33123.4	165616.8
Oct-04	10344.2	2586.1	12930.3
Nov-04	2101.9	525.5	2627.3
Dec-04	395.3	98.8	494.1
Jan-05	206.3	51.6	257.9
Feb-05	114.2	28.6	142.8
Mar-05	62.7	15.7	78.3
Apr-05	186.5	46.6	233.1
May-05	-99.9	-99.9	-99.9
Jun-05	2451.2	612.8	3064.0
Jul-05	8920.5	2230.1	11150.6
Aug-05	13992.1	3498.0	17490.1
Sep-05	76261.8	19065.5	95327.3
Oct-05	31439.6	7859.9	39299.5
Nov-05	2044.4	511.1	2555.5
Dec-05	166.0	41.5	207.5
Jan-06	72.4	18.1	90.5

Feb-06	48.9	12.2	61.1
Mar-06	57.3	14.3	71.6
Apr-06	41.2	10.3	51.5
May-06	495.2	123.8	619.0
Jun-06	9340.6	2335.2	11675.8
Jul-06	7810.6	1952.6	9763.2
Aug-06	15997.8	3999.5	19997.3
Sep-06	225778.5	56444.6	282223.1
Oct-06	161361.3	40340.3	201701.6
Nov-06	7807.3	1951.8	9759.1
Dec-06	1163.3	290.8	1454.1
Jan-07	709.7	177.4	887.2
Feb-07	329.8	82.5	412.3
Mar-07	295.2	73.8	369.1
Apr-07	1799.4	449.8	2249.2
May-07	3628.3	907.1	4535.3
Jun-07	566.4	141.6	708.0
Jul-07	9081.0	2270.2	11351.2
Aug-07	79846.2	19961.5	99807.7
Sep-07	341221.4	85305.3	426526.7
Oct-07	37136.1	9284.0	46420.2
Nov-07	3974.4	993.6	4967.9
Dec-07	1457.4	364.4	1821.8

ANNEX 6

Table A6: Distribution of BVRB soil in the SWAT model

Watershed	Area [ha]	Area[acres]	%Wat.Area

		13500318	33359960.88	
		Area [ha]	Area[acres]	
SOILS:	Qc1-1598	217000.946	536220.1885	1.61
	Ql1-1a-1614	1087540.85	2687367.819	8.06
	Re35-1a-1684	131711.628	325466.0189	0.98
	I-Re-b-1294	248117.525	613110.8111	1.84
	Re24-1665	9265.1669	22894.6908	0.07
	Re34-1a-1680	369320.956	912610.548	2.74
	Re35-1a-1685	11819.0526	29205.4699	0.09
	Re36-1a-1687	115620.819	285704.8238	0.86
	Re33-1674	365365.156	902835.5675	2.71
	Vc8-1729	67540.672	166896.3776	0.5
	Re33-1a-1677	1143927.81	2826702.812	8.47
	Lg5-2a-1515	729801.882	1803376.94	5.41
	Lg1-1495	67491.0817	166773.8374	0.5
	Vc1-3a-954	169574.344	419026.6814	1.26
	Je1-1359	55674.012	137573.2675	0.41
	Vc9-1730	65610.7041	162127.3305	0.49
	Lf18-1434	162087.09	400525.3038	1.2
	Vp9-1960	29241.9174	72258.24	0.22
	Lg3-2a-786	450080.162	1112170.585	3.33
	Lg1-3a-1496	426913.301	1054924.113	3.16
	I-Lf-1255	33689.3193	83247.9924	0.25
	Re33-1a-1676	33711.7079	83303.3158	0.25
	Lf30-1a-1450	341530.784	843939.6436	2.53
	Lf37-1463	536260.01	1325125.297	3.97
	Lp4-1532	299777.365	740764.8575	2.22
	Lp7-1541	501403.865	1238994.02	3.71
	Lg12-1501	142863.997	353024.0797	1.06
	Bv6-1145	69194.6528	170983.4469	0.51
	Lp5-1a-1536	191432.844	473040.1291	1.42
	Lp6-1a-1540	493122.552	1218530.481	3.65
	Lp8-1542	543159.067	1342173.212	4.02
	Nd1-1544	144817.64	357851.6294	1.07
	Vc11-1718	39975.6052	98781.7193	0.3
	Be25-1083	670887.617	1657796.845	4.97
	I-Rd-79	24285.7662	60011.3425	0.18
	Lf31-a-1453	1570695.52	3881267.161	11.63
	Lg11-1500	2734.1508	6756.2232	0.02

	Lg8-1520	156160.112	385879.4459	1.16
	Lf30-132	85295.0389	210768.3059	0.63
	I-Lp-1274	18989.4628	46923.912	0.14
	Lf32-1a-1457	89666.9571	221571.5343	0.66
	Lp9-1543	194098.814	479627.8745	1.44
	Lf38-1464	16177.9967	39976.6388	0.12
	Lp10-1a-1527	11860.1009	29306.9024	0.09
	Lg28-1a-1513	735697.44	1817945.159	5.45
	Lp5-1534	42881.9623	105963.4729	0.32
	Nd3-1565	41056.102	101451.6807	0.3
	Lf26-a-1442	5745.6396	14197.7627	0.04
	Ap22-2a-1074	93970.6552	232206.1876	0.7
	Be42-2-3b-1093	3210.8951	7934.2823	0.02
	Lf12-b-1431	95813.9524	236761.0671	0.71
	Ao46-a-1058	146311.616	361543.3178	1.08
	Bf5-2-3ab-1102	57658.4234	142476.8472	0.43
	Af18-1a-1024	22944.9135	56698.0286	0.17
	Be7-1b-1096	1819.834	4496.9009	0.01
	Ao59-a-1063	117710.586	290868.7425	0.87

Candidate biography

Fati Aziz (Mrs) is a Ghanaian Environmental Scientist. She received her Master's degree in Environmental Science (2011) and her Bchelor's degree in Biological Science (2007) at the Kwame Nkrumah University of Science and Technology, Ghana.

Abstract:

This study investigated the impacts of climate change and the sensitivity of land use/land cover (LULC) changes on river flow and sediment yield in the Black Volta River Basin (BVRB) using the Soil and Water Assessment Tool (SWAT) model, with the aim of providing water resources and basin managers with science-based evidence of impacts of global change at basin level to inform sustainable planning and management of water resources in the basin. The results of the study showed that climate change will cause changes in flow and sediment yield in the basin. Sensitivity analysis of streamflow in the basin based on a 10-year land use/land cover change showed statistically insignificant changes.

Key words: Climate Change, Land use/land cover change, streamflow, sediment yield.